FIC-MEDIATED AMPYLATION IN BACTERIAL INFECTION AND ENDOPLASMIC RETICULUM STRESS

APPROVED BY SUPERVISORY COMMITTEE

Kim Orth, PhD

Qinghua Liu, PhD

Melanie Cobb, PhD

Paul Sternweis, PhD

ACKNOWLEDGEMENTS

There are many people to which I owe thanks for making this work possible. First, I would like to thank my mentor Kim Orth for invaluable advice and guidance throughout my dissertation work. She brings a unique type of energy to the lab that makes it truly dynamic. My thesis committee, Qinghua Liu, Melanie Cobb, and Paul Sternweis were also invaluable by providing great advice and numerous reagents that I begged from their labs. I also thank Melanie for including me in the Molecular and Cellular Biology Training grant, as the science and career based discussions were always excellent.

The members of the Orth lab always made it an enjoyable place to work, especially TJ and Anju who joined the lab with me. I have to give special thanks to Phi Luong for training me in many essential aspects of Biochemistry, and thank Dor Salomon for showing how to work intelligently and efficiently in science. I know that these skills will be invaluable as I continue in academia or in other careers.

I am also very grateful for the numerous essential collaborations I have enjoyed here in my time at UT Southwestern. Xiaobo Yu and Joshua LaBaer at Arizona State were a joy to work with, and their incredible expertise in NAPPA screening made for a great collaboration. The UT Southwestern Proteomics core, especially Hamid Mirzaei and David Trudgian, always provided an excellent, personal and professional level of care with all our mass

spectrometry needs. Helmut Kramer and his lab provided essential help not only with Drosophila but also in critical thinking about numerous Fic-related experiments.

Of course, the most important dedication goes to my fiancée, Beth Frances Asbury, who has brought so much happiness into my life this past year. I can't wait to begin our life together, from Dallas to Chicago and beyond.

However, none of this work would have been possible without the lifelong and unwavering support from my family. I can't overstate the importance of the hard work my mother Paula, my father Keith, and my grandparents Terry and Sue put in raising me. My mom always put me first, and supported me in anything and everything I ever wanted to do. My dad always pushed me to work hard in athletics and academics, and those lessons led to my strong competiveness and self-pride that leads to me naively believing I can do anything, and sometimes it's even true. My cousins Misty and Krista and my aunt Connie provided the big family that most sibling-less children don't get to enjoy, for which I am very thankful. My grandfather in particular will always serve as the perfect example for me on how to live life: love your family, work hard, and treat everyone with respect. He is missed every day.

FIC-MEDIATED AMPYLATION IN BACTERIAL INFECTION AND ENDOPLASMIC RETICULUM STRESS

by

ANDREW RYAN WOOLERY

DISSERTATION

Presented to the Faculty of the Graduate School of Biomedical Sciences

The University of Texas Southwestern Medical Center at Dallas

In Partial Fulfillment of the Requirements

For the Degree of

DOCTOR OF PHILOSOPHY

The University of Texas Southwestern Medical Center at Dallas

Dallas, Texas

May, 2015

FIC-MEDIATED AMPYLATION IN BACTERIAL INFECTION AND ENDOPLASMIC RETICULUM STRESS

ANDREW RYAN WOOLERY, Ph.D.

The University of Texas Southwestern Medical Center at Dallas, 2015

Supervising Professor: KIM ORTH, Ph.D.

The post-translational modification AMPylation is emerging as a significant regulatory mechanism in both prokaryotic and eukaryotic biology. This process involves the covalent addition of an adenosine monophosphate to a protein resulting in a modified protein with altered activity. Proteins capable of catalyzing AMPylation, termed AMPylators, are comparable to kinases in that they both hydrolyze ATP and reversibly transfer a part of this primary metabolite to a hydroxyl side chain of the protein substrate. To date, all AMPylators discovered contain one of two domains: the Fic domain or the adenylyl transferase domain.

All currently characterized AMPylators are bacterial in origin and are primarily Type III or Type IV secreted effector proteins, which are injected into a host cell to manipulate host signaling to the microbe's advantage. Examples of these are VopS (*Vibrio parahaemolyticus*), IbpA (*Histophilus somni*) and DrrA (*Legionella pneumophila*). The discovery of SidD, a deAMPylator also from *L. pneumophila*, shows that this modification is dynamic and could likely have a regulatory role in eukaryotic biology. Supporting this idea is the presence of a single copy of the Fic domain in most metazoans, including humans. The substrates, localization, and function of Fic proteins and other AMPylators in eukaryotic biology are perhaps the largest open questions in this rapidly expanding field.

The goal of my dissertation work was to expand the understanding of the effects of AMPylation in eukaryotic signaling. I approached this goal in three ways: by examining the effects of an AMPylator (VopS) with known targets (Rho GTPases) on different aspects of cell signaling, developing screening tools for AMPylation and attempting to elucidate some of the functions of the human AMPylator, FicD, in which the targets are unclear. I found that VopS, in addition to collapsing the host actin cytoskeleton, also inhibits many aspects of host defense signaling including NFκB, MAP kinases and the phagocytic NADPH oxidase system. I explored the possibility of other potential substrates of VopS by collaborating on an extensive protein microarray screen for AMPylation, determining that the entire Rho GTPase family is AMPylated. I also discovered that the human AMPylator FicD is induced during the unfolded protein response, is localized to the endoplasmic reticulum and is capable of AMPylating the ER chaperone BiP/GRP78. The progress made in these studies will

contribute to understanding the role of this enigmatic modification in mammalian cell signaling.

TABLE OF CONTENTS

PUBLICATIONS

Ham H, **Woolery AR**, Tracy C, Stenesen D, Kramer H, Orth K. (2014) Unfolded Protein Response-Regulated dFic Reversibly AMPylates BiP during Endoplasmic Reticulum Homeostasis. *Journal of Biological Chemistry*, 289(52):36059-69.

Woolery AR, Yu X, LaBaer J, Orth K. (2014) AMPylation of Rho GTPases Subverts Multiple Host Signaling Processes. *Journal of Biological Chemistry*. 289(47):32977-88

Yu X*, **Woolery AR***, Luong P, Hao YH, Grammel M, Westcott N, Park J, Wang J, Bian X, Demirkan G, Hang HC, Orth K, LaBaer J. (2014) Copper-catalyzed azide-alkyne cycloaddition (click)-based Detection of Global Pathogen-host AMPylation on Self-assembled Human Protein Microarrays. *Molecular and Cellular Proteomics*. (11):3164-76

Krachler AM, **Woolery AR**, Orth K. (2011) Manipulation of kinase signaling by bacterial pathogens. *Journal of Cell Biology*. 195(7):1083-92. REVIEW

Woolery AR, Luong P, Broberg CA, Orth K. (2010) AMPylation: Something Old is New Again. *Frontiers in Microbiology*. 1:113. REVIEW

* INDICATES CO-AUTHORSHIP

LIST OF FIGURES

LIST OF TABLES

LIST OF DEFINITIONS

AMP	Adenosine monophosphate
Amp	Ampicillin
ATP	Adenosine triphosphate
DA-Rac	Dominant active Rac
DMEM	Dulbecco's modified eagle medium
DTT	Dithiothreitol
EDTA	Ethylenediaminetetraacetic acid
ER	Endoplasmic reticulum
FBS	Fetal Bovine Serum
Fic	Filamentation induced by cAMP
FPLC	Fast protein liquid chromatography
GAP	GTPase activating protein
GDI	Guanine nucleotide dissociation inhibitor
GDP	Guanosine diphosphate
GEF	Guanine nucleotide exchange factor
GFP	Green fluorescent protein
GS	Glutamine synthetase
GST	Glutathione S-transferase
GTP	Guanosine triphosphate
GTPases	Guanosine triphosphatases
tpi	time post-infection

HPLC	High pressure liquid chromatography
HRP	Horseradish peroxidase
IPTG	Isopropyl-beta-D-thiogalactopyranoside
kDa	Kilodaltons
LB	Luria Bertani
LC	Liquid chromatography
m/z	mass to charge
MAPK	Mitogen-activated protein kinase
Mg^{2+}	Magnesium
MLB	Marine LB
MOI	Multiplicity of infection
MS	Mass spectrometry
NFκB	Nuclear factor kappa B
Ni-NTA	Nickel-nitriloacetic acid matrix
O.D.	Optical density
OD600	Optical Density 600 nm wavelength
PAK-PBD	p21-activated kinase protein binding domain
PBS	Phosphate-buffered saline
PMSF	Phenylmethylsulfonylfluoride
SD	Standard deviation
SDS-PAGE	Sodium dodecyl sulfate-polyacrylamide gel electrophoresis
T3SS	Type III secretion system

T3SS1	T3SS on chromosome 1
T3SS2	T3SS on chromosome 2
TDH	Thermostable direct hemolysin
Tet	Tetracycline
Thr	Threonine
TM	Transmembrane
TPR	Tetratricopeptide repeat
TRH	Thermostable related hemolysin
Tyr	Tyrosine
UPR	Unfolded Protein Response
Vop	Vibrio outer protein

CHAPTER ONE

Introduction and Literature Review

INTRODUCTION

AMPylation: an emerging post-translational modification

Post-translational modifications are an essential molecular mechanism for regulation of proteins in the cell. The variety of modifications that a translated protein can undergo is ever expanding, with the most well-known being phosphorylation, ubiquitination and glycosylation. The possible effects of a modification are complicated, and dependent on many variables including the type of modification, the partners of the modified protein, subcellular localization and the quantity of modifications. The focus of my dissertation work has been on one particular modification: AMPylation. This modification, also known as adenylylation, is defined as the stable and reversible covalent addition of an adenosine monophosphate (AMP) to a hydroxyl side chain of a protein (**Figure 1**) [1]. This modification has been most commonly associated with the *Escherichia coli* protein glutamine synthetase adenylyl transferase but more recently has been seen to be mediated by several different bacterial toxins [2-5].

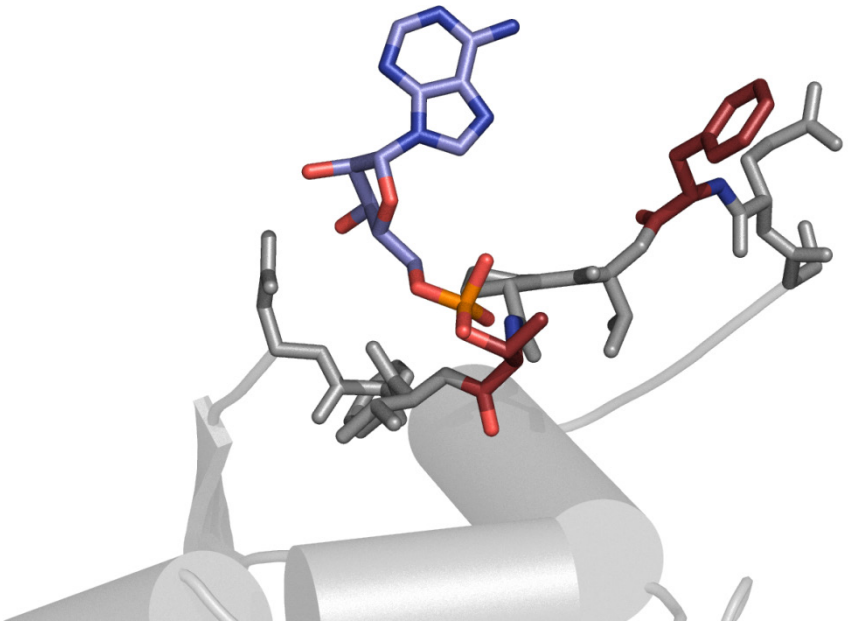

Figure 1. AMPylation is the transfer of an AMP molecule from ATP to a hydroxyl side chain. Shown is an AMPylated threonine residue from the switch-1 loop of CDC42, a Rho family GTPase. Maroon: hydroxyl-containing side chains (Thr or Tyr) than can be AMPylated. Orange and red: phosphate of AMP. Blue, light blue and red: ribose and nitrogen base of AMP.

AMPylation is a bulky modification and thus far has been implicated in inhibitory processes. Like phosphorylation, the cofactor used for the modification is ATP and its covalent attachment is mediated through a phosphate molecule. Phosphorylation, however, oftentimes causes activating conformational changes or binding moieties for other proteins, but as a larger modification AMPylation appears to primarily work to sterically hinder downstream protein:protein interactions [3]. However, it is conceivable that AMPylation binding domains analogous to the phosphorylation binding SH2 domains exist. While AMPylation has only been observed to modify threonine and tyrosine residues, it is likely

that serine can function as a target as well. AMPylation is a stable modification and distinct from transient adenylylation events that involve the addition of AMP to the protein targets and use the energy of ATP to drive a reaction such as activation of amino acid-tRNAs complexes or E1 ubiquitination enzymes [6].

Discovery of AMPylation/adenylylation

Until 2009, only one AMPylator had been discovered: the adenylyl transferase of glutamine synthetase (GS-ATase). In the 1960s, Earl Stadtman and colleagues discovered that tyrosine residues of the *E. coli* protein glutamine synthetase were modified with AMP under certain conditions [2, 7, 8]. Later studies went on to discover that this AMPylation (adenylylation) was mediated by the GS-ATase, and that modification with AMP was used to control the activity of glutamine synthetase to regulate nitrogen metabolism. GS-ATase is actually a dual function enzyme that catalyzes both AMPylation and deAMPylation through two separate adenylyl transferase domains [9]. While it was first characterized in *E. coli*, GS-ATase is conserved across many bacterial species and solved structures exist for both the *E. coli* (PDB ID IV4A and 3K7D) and *Mycobacterium tuberculosis* homologues (PDB ID 2WHI and 2WGS).

GS-ATase plays a role in nitrogen metabolism by controlling the AMP modified state of glutamine synthetase and thus its ability to synthesize glutamine (**Figure 2, [10]**). This modification is controlled by a complex regulatory system, in which the PII protein controls the activity of GS-ATase, which in turn controls the activity of glutamine synthetase via the

addition or removal of AMP. PII activity is dependent on the intracellular concentrations of the metabolites α-ketoglutarate and glutamine, which reflect the current state of nitrogen metabolism in the cell. When levels of intracellular glutamine are low during nitrogen starvation, the PII protein exists primarily as PII-UMP. In the presence of PII-UMP and high α-ketoglutarate, GS-ATase is stimulated to remove AMP from glutamine synthetase, allowing the synthesis of glutamine. When glutamine levels are high, PII is unmodified allowing GS-ATase to inhibit glutamine metabolism by transferring AMP to Y397 on glutamine synthetase. It has become clear, more than 40 years after its discovery, that GS-ATase catalyzes the same reaction that has since been termed AMPylation. Thus, the GS-ATase and related proteins are the first and only confirmed example of an endogenous signaling system that is regulated by AMPylation, a reversible post-translational modification.

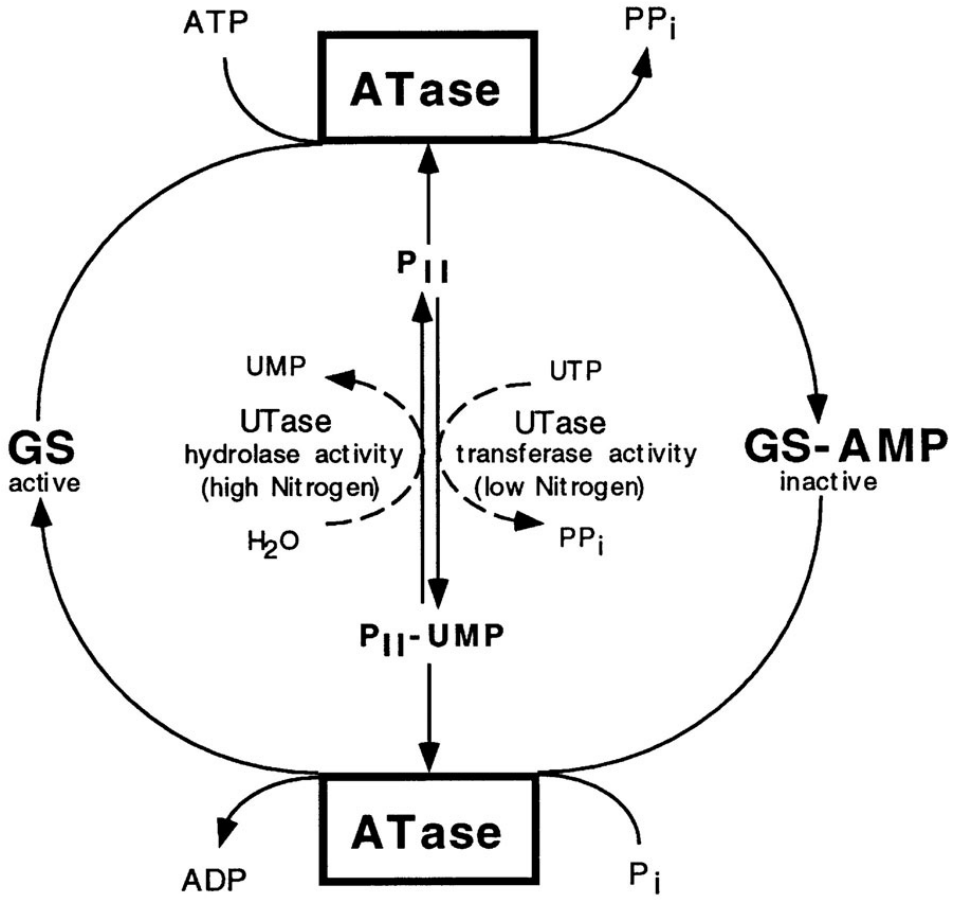

Figure 2. Metabolic regulation by the glutamine synthetase adenylyl transferase. The activity of GS is regulated by nitrogen levels through the AMPylation activity of its AT-ase, which is controlled by the protein UMP-modified state of PII, which is in turn regulated by its UTase. When nitrogen levels are low in the cell, the PII UTase UMPylates PII, which causes the ATase to remove AMP from GS, making it active. When nitrogen levels are high, the PII UTase removes UMP from PII, which causes ATase to AMPylate GS and inhibit its activity. Source: [10] (The EMBO Journal(1997)16,5562-5571)

The adenylyl transferase domain (GlnE family) is part of the larger nucleotidyl transferase protein family and is characterized by a conserved G-X11-D-X-D motif, of which the aspartate residues have been shown to be essential for the AMPylation activity. This domain has been identified in more than 1,400 bacterial proteins among 685 bacterial

species, of which the large majority are proteobacteria [11]. While studies of glutamine synthetase and its adenylyl transferase have been subjects of considerable interest in the intervening decades, the question of whether this type of modification might be catalyzed by other proteins remained open until recent studies on the Fic domain from the bacterial pathogen *Vibrio parahaemolyticus*.

Discovery of Fic domain function through the type three secreted effector VopS

The filamentation induced by cAMP (Fic) domain, as its name indicates, was first detailed in a protein (*fic1*) that was necessary for the filamentation of *E. coli* induced by cAMP [12]. While the function of this and other cell division-related bacterial Fic-domain containing proteins remained unclear, studies on a study on another Fic domain-containing protein, VopS from *V. parahaemolyticus,* allowed for the discovery that the Fic domain is an AMPylation domain [3]. *V. parahaemolyticus* is an extracellular Gram negative bacterium that causes gastroenteritis from eating undercooked seafood [13, 14]. An essential virulence factor for many Gram-negative pathogens, including *V. parahaemolyticus*, is the type three secretion system (T3SS), a needle–like structure that extends from the bacterium and penetrates a host cell to inject effectors [15, 16]. All strains of *V. parahaemolyticus* contain a cytotoxic but non-disease causing T3SS (T3SS1) that secretes a variety of effectors, each of which individually are responsible for a broad range of phenotypes in the infected cell . Some pathogenic *V. parahaemolyticus* strains also contain a second T3SS (T3SS2) that is responsible for gastroenteritis and cellular invasion [17].

VopS, an effector of the ubiquitous and non-disease causing T3SS of *V. parahaemolyticus*, was the first example of a Fic domain functioning as an AMPylator. VopS modifies a conserved threonine 35 on the switch-1 region of the Rho family GTPases, resulting in their inability to bind to downstream effectors like p21 activated kinase 1 protein (PAK) (**Figure 3**). The loss of this interaction disables the host cell's control of the actin cytoskeleton, which leads to cell rounding (**Figure 4**). Loss of actin cytoskeletal control has obvious drastic consequences for an infected cell, as it would likely disrupt the epithelium of the gut, as well as prevent phagocytosis by professional immune cells .

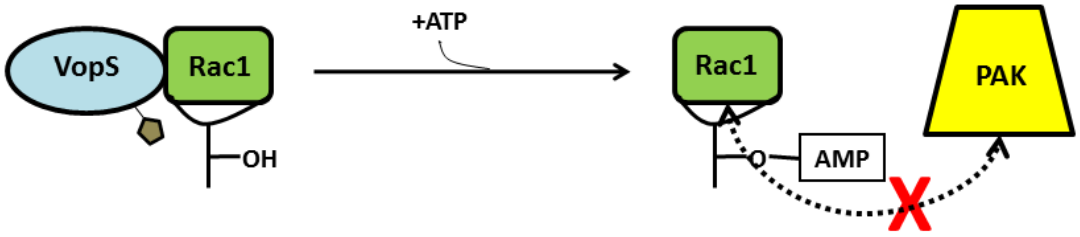

Figure 3. AMPylation of Rac1 prevents binding of downstream effectors. AMPylation on the switch-1 loop of GTPases like Rac1 sterically blocks their interaction with their binding partner, for example PAK.

The discovery of this function for the Fic domain led to a rush of papers on Fic domains and AMPylation and other novel mechanisms [4, 18-29]. One of these new discoveries is an adenylyl transferase domain AMPylator, DrrA/SidM from *Legionella pneumophila* [5, 30]. This type four secreted (T4SS) protein AMPylates Rab GTPases, blocking their interaction with GTPase activating proteins and locking them into an active

state. Interestingly, *L. pneumophila* also secretes a deAMPylator that removes the AMP from Rab proteins, reminiscent of the reversibility GS-ATase AMPylation [26, 31]. The pathogen tightly controls the activation state of Rab at different stages of infection, preferring AMPylated Rab in the first few hours but removing it at later times. Despite the rush of discoveries in this field, little time has been devoted to understanding the full potential breadth of AMPylation on its targets or the overall effect of AMPylation on host cell signaling. These aspects are more fully explored in this work.

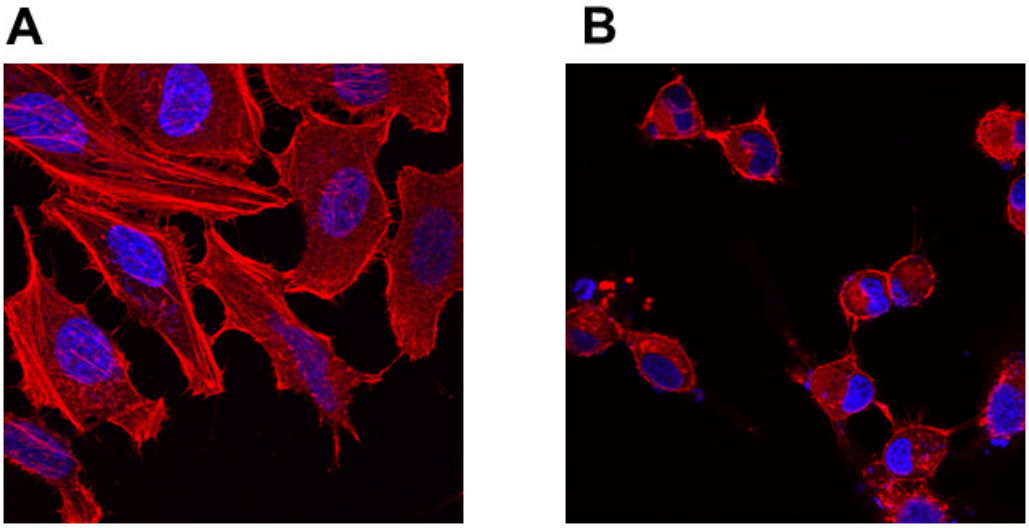

Figure 4. VopS causes collapse of the actin cell cytoskeleton by targeting Rho GTPases. A. Mock infected HeLa cells. B. HeLa cells infected with *V. parahaemolyticus* containing VopS show cell rounding due to actin cytoskeleton collapse. Blue: DAPI (nucleus). Red: Rhodamine-phalloidin (actin).

Features of Fic/Doc superfamily

The Fic and adenylyl transferase domains each have distinct primary sequence and structural features. AMPylation by these domains has been demonstrated to have roles in

both the pathogenicity of bacterial species and in endogenous metabolic regulation. Based on strong similarity, the Fic domain was merged with the Doc family of toxins which are used by the bacteriophage P1 of *E. coli [11]*. This merged family has been termed Fido (Fic/doc) and is widely conserved across most non-plant species. Fic and doc domains share the conserved HPFx[D/E]GN[G/K]R motif, in which the invariant histidine residue has proven to be essential for catalytic activity in Fic proteins and their cytotoxicity. While the adenylyl transferase domain has thus far been limited to AMPylation, the Fido superfamily appears to have much more diversity in the modifications it can catalyze. Surprisingly, Doc itself has recently been shown to be a kinase rather than an AMPylator [32]. Doc phosphorylates the translation elongation factor Ef-Tu to drastically reduce global translation in infected bacteria and cause senescence[32].

Perhaps one of the most surprising findings in studies of the Fido super family is that this flexibility extends even beyond the choice of ATP as a cofactor (**Table 1**). The pathogen *Legionella pneumophila* uses the Fic-domain protein AnkX in its large repertoire of effectors, although its activity remained a mystery for some time. AnkX was known to subvert vesicular trafficking to the advantage of the pathogen by targeting Rab family GTPases, but no AMPylation activity could be observed. After much study, it was discovered that instead of AMPylation, AnkX catalyzes the phosphocholination of Rab proteins using CDP-choline as a cofactor [33]. Utilization of CDP-choline in the nucleotide binding pocket is achieved by inverting the orientation of the nucleotide, presenting the phosphocholine moiety for transfer to the target hydroxyl [34]. Phosphocholination of AnkX, like AMPylation by DrrA, is reversed by another *L. pneumophila* effector, Lem3 [35, 36]. The

plant pathogen *Xanthomonas campestris* encodes a Fic-domain protein, AvrAC, that catalyzes the transfer of UMP from UTP to the immune regulators BIK1 and RIPK to suppress the host response to infection, demonstrating that other triphosphonucleotides are potential cofactors [37, 38]. Perhaps the most surprising activity is that of the *E. coli* P1 bacteriophage doc protein, which was discovered to be a kinase [32, 39]. Kinase activity by Doc is also achieved by inverting the orientation of ATP in the Fic pocket. The Doc protein is half of a toxin:antitoxin module and phosphorylates the translation elongation factor Ef-Tu to inhibit translation of *E. coli* [40]. The Fic and doc domains are an excellent example of the diversity of chemistry that can be achieved through evolution of a protein family.

Table 1. Examples of Fic protein targets and cofactors

Fic protein	Species	Target	Cofactor	Modification	Source
VopS	*Vibrio parahaemolyticus*	Rho GTPases	ATP	AMPylation	[3, 22]
AnkX	*Legionella pneumophila*	Rab GTPases	CDP-choline	Phosphocolination	[33, 35, 36]
Doc toxin	*Escherichia coli* Bacteriophage P1	(EF)-Tu GTPase	ATP	Phosphorylation	[32]
AvrAC	*Xanthomonas campestris*	BIK1 and RIPK	UTP	UMPylation	[37]
FicD/HYPE	Metazoans	BiP?	ATP?	AMPylation?	[41], this study

Signaling by Rho family GTPases

Rho family GTPases are essential regulators of the actin cytoskeleton [42]. They exert their activity at the inner plasma membrane through a C-terminal prenylation, but can also exist in the cytosol when bound to guanine nucleotide dissociation inhibitors (GDIs). When active, they interact with downstream effectors (not to be confused with bacterial effector proteins) such as p21-activated kinase (PAK) [43]. These interactions propagate signals that allow the polymerization and protusion of actin, providing much of cell's shape and allowing processes like motility, endocytosis, and intracellular transport. However, their influence is not limited to the actin cytoskeleton, as they can mediate signaling through numerous other pathways, such as kinase pathways and reactive oxygen species generation [44, 45].

Like other GTPases, proteins of the Rho family cycle from inactive GDP-bound states to GTP-bound active states (**Figure 5**) [46]. When GTP-bound, the proteins change conformation and are capable of interacting with downstream partners. Deactivation of these proteins is dependent on the hydrolysis of GTP, but the basal GTP hydrolyzing activity of these proteins is low. Increasing this activity is a key mechanism of regulation, which is the purpose of GTPase-activating proteins (GAPs) [46]. Binding of GAPs to GTPases speeds GTP hydrolysis and thereby inhibits their activity by decreasing the duration of their transient activated state. Conversely, the exchange of GDP for GTP is an activating mechanism, and guanine nucleotide exchange factors (GEFs) bind GTPases to expel bound

GDP [46]. As the cellular concentration of GTP is orders of magnitude higher than GDP, GTPases naturally bind free GTP and again become active, and the duration of their activity is dependent on the binding of available GAPs. Additionally, there are multiple other mechanisms of GTPase regulation, such as GDIs, that isolate GTPases in the cytosol and block binding of GEFs, relegating GTPases to a completely inactive state [46]. Each family of GTPases appear to have multiple GAPs, GEFs and GDIs that regulate their activity whose expression and localization are dependent on cell type and intracellular localization, giving Rho GTPases great diversity in function and regulation. Accordingly, these proteins are keystone signaling molecules for many different processes, and an Achilles heel that is frequently targeted by bacterial toxins to disable host cells [47].

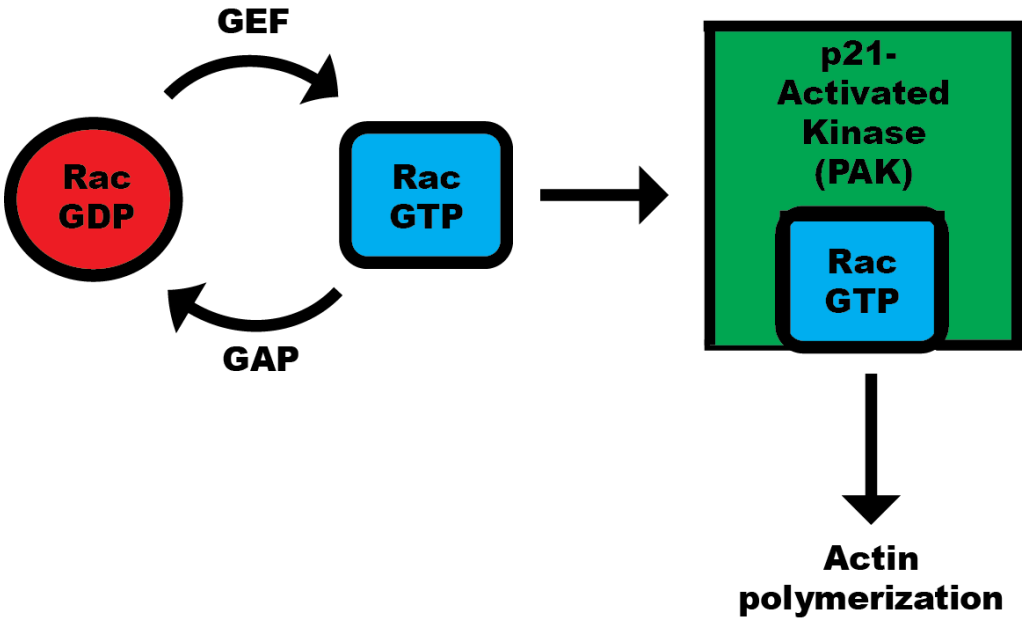

Figure 5. The GTPase cycle. Shown is a cartoon of Rac1, a Rho GTPase family protein, cycling between an inactive GDP-bound and active GTP-bound states with the assistance of GAP and GEF proteins. GTP-bound Rac1 can bind to downstream effectors like PAK. Not shown are several other mechanisms of regulation, such as guanine dissociation inhibitors, which sequester GTPases prevent the activity of GEFs.

The switch-1 loop of Rho GTPases is a frequent target for modifications such as glucosylation, deamidation and AMPylation because this is the region of the protein that mediates interactions with downstream signaling partners, such as PAK [47]. The attractiveness of this family of proteins as targets for pathogens is highlighted by recent discoveries of host pattern recognition receptors (PRRs) that monitor the activation status of Rho GTPases [48-50]. Extracellular PRRs commonly recognize molecules specific to pathogens, such as components of the gram negative bacterial membrane, secretion apparatuses, or flagella [51, 52]. NOD family proteins were shown to be intracellular PRRs that sense activated Rac1 and stimulate NFκB signaling [50, 53]. Inversely, Rho proteins that

have been inactivated through modification of the switch-1 loop can trigger the inflammasome through the novel intracellular PRR protein Pyrin via an unknown mechanism [49]. The sensitivity of the host immune system to modulation of Rho GTPases may merely be a convenient way to sense infection, or it may instead suggest that these modifications are exceptionally deleterious to the host. The majority of investigations about the effect of Rho GTPase posttranslational modifications, including AMPylation, have focused on the collapse of the actin cytoskeleton, but other signaling pathways in which these GTPases are involved may also be affected [44, 54].

Stress sensing mechanisms of eukaryotic cells are commonly subverted by bacterial effectors

Metazoan cells have multiple different signaling pathways to communicate signals perceived by PRRs. Perhaps the most essential and commonly subverted pathways are signal transduction cascades, such as the mitogen activated kinase (MAPK) and NFκB pathways (**Figure 6**) [55, 56]. Such cascades involve sequential activation and amplification of signals, allowing incredibly complex modes of propagation that are involved in governing a large range of transcriptional programs essential for normal metabolism and responses to stimuli. The termini of these pathways have cytosolic and nuclear activities, including activation of transcription factors like AP-1 for MAPK or the Rel proteins of the NFκB pathway [57]. The MAPK cascades are essential for normal eukaryotic homeostasis, but also are important for communicating various stressors, like bacterial infection. The NFκB has canonical and non-

canonical branches that can activated and propagated by different stimuli, such as the activation of toll-like receptors (TLRs) by lipopolysaccharide (LPS) or the recognition of membrane components by intracellular NOD PRRs [55]. Subverting these pathways is an attractive strategy for bacterial pathogens to colonize a host, as they are necessary for many functions of the innate immune system, such as inflammation and apoptosis.

Many bacterial toxins, secreted through T3SS, T4SS or other mechanisms, target MAPK and NFκB pathways by directly modifying one of the components in the cascade [55]. For example, the *Yersinia* effector YopJ is an acetyl transferase that modifies serine and threonine residues on MAP kinases, blocking their phosphorylation by upstream kinases to stop propagation of signals [58]. YopJ can also modify IKK, a kinase critical to signaling in NFκB to achieve the same effect. Enteropathogenic *Escherichia coli* (EPEC), a major causative agent of diarrhea, secretes an effector called NleC that cleaves a 10 amino acid peptide from the N-terminus of the NFκB transcription factor p65, preventing its dimerization with other Rel proteins and blocking its signaling [59-62]. These are merely two among dozens of bacterial effectors targeting the MAPK and NFκB pathways by directly modifying their components. For my studies, I suspected that modification of Rho GTPases, which is a common strategy of bacterial effectors such as VopS, might give some of these same effects. Rho GTPases are known to activate these pathways under some conditions, so I hypothesized that VopS and other proteins may subvert them in addition to collapsing the cytoskeleton. Such "double duty" offers extreme potential efficiency in disabling the defense of host to promote colonization, and my initial studies on this avenue are detailed in **Chapter 3.**

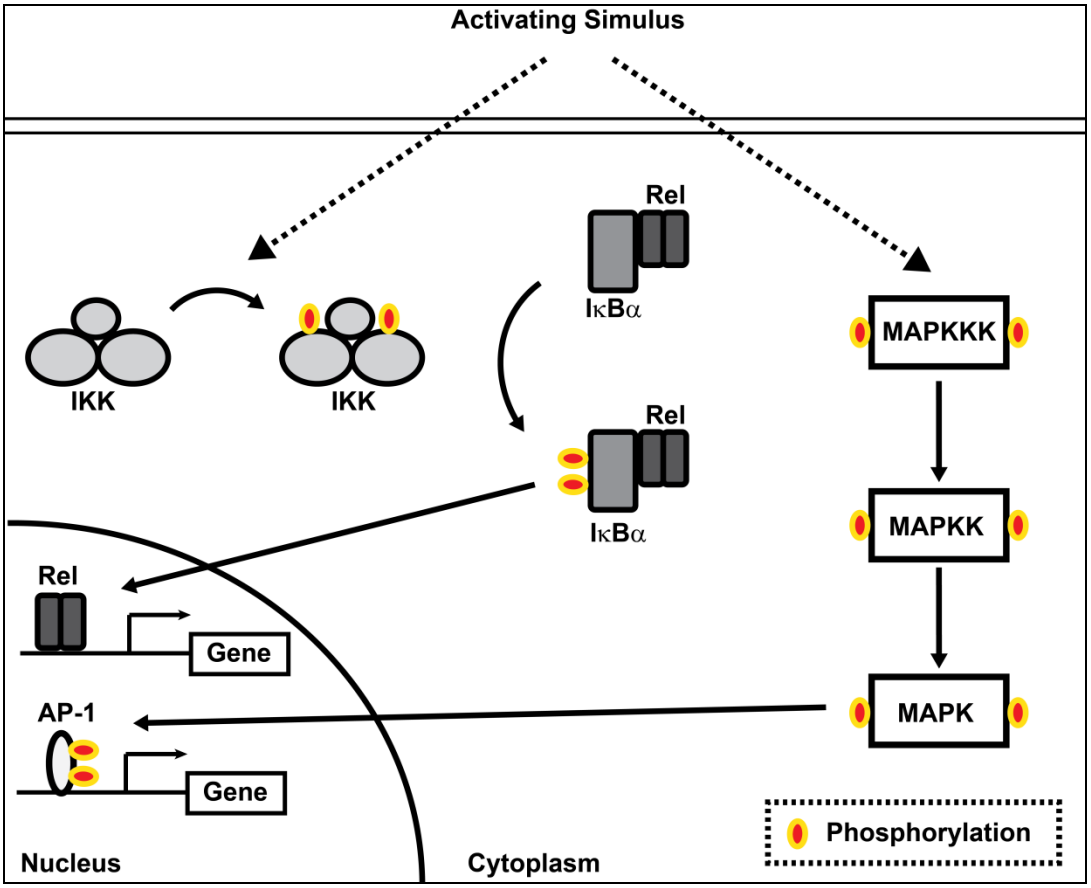

Figure 6. The MAPK and NFκB pathways are activated during infection. Extracellular and intracellular stimuli activate the NFκB and MAPK cascades, leading to changes in transcriptional profile. Upstream receptors and adaptors progagate the signal to IKK or MAPKKK, which continue the cascade. In the case of NFκB, the phosphorylation of IκBα is the penultimate, which causes its degradation and allows Rel transcription factors to enter the nucleus and bind DNA. The terminal MAPKs phosphorylates various transcription factors, including AP-1, to activate their activity.

Metazoan AMPylation: An incomplete picture

As shown in **Table 1**, most metazoans contain one Fic domain-containing protein, FicD/HYPE. Information about this protein has been the most exciting topic in the burgeoning field of AMPylation since the discovery of VopS, but information about its function and substrates has been slow to materialize. Initial studies indicated that, like VopS and IbpA, it may have AMPylation activity towards the Rho family GTPases in vitro [4]. However, FicD contains an endoplasmic reticulum signal sequence (ERSS) that may render it a lumenal protein of the secretory pathway and make AMPylation of Rho GTPases essentially impossible. It seems likely that FicD would target another lumenal protein, and while we have kept the scope of our studies on this protein broad, we favor the exploration of such lumenal proteins as potential substrates.

Unfortunately, even the enzymatic activity of FicD remains unclear. A previous study identified a shared alpha helix present in many Fic domains that prevents the binding of triphosphate nucleotides, like ATP, from binding to the Fic domain [28]. The presence of this domain renders the AMPylation activity of containing proteins essentially nil. This inhibitory alpha helix is absent in the bacterial effector proteins VopS and IbpA, which explains their robust AMPylation activity in vitro. The authors of this original study speculate that this inhibitory helix is a mechanism of regulation that can be relieved in certain conditions, allowing AMPylation of substrates and downstream signaling. Indeed, mutations that disrupt the inhibitory helix allow binding of ATP and result in considerable autoAMPylation activity of such Fic domains [28, 41]. However, other groups have speculated that these “inhibitory helices” are actually moieties that simply give the Fic domain specificity towards other

cofactors, such as more complex diphosphonucleotides. As shown above, Fic domains from other proteins have already shown promiscuity in their choice of cofactors; for example AnkX from *Legionella pneumophila* uses CDP-choline to phosphocholinate Rab proteins [34]. Frustratingly, even a recent study that solved the crystal structure of FicD has failed to settle the question once and for all [41]. While wild type FicD shows essentially no ability to bind ATP, it does have weak ability to bind ADP, perhaps indicating a diphosphonucleotide may be its preferred substrate. However, a crystal structure of FicD with a mutated "inhibitory helix" has an active site that strongly resembles AMPylators like VopS, readily binding ATP by coordinating the gamma phosphate with an arginine that is shifted into the active site by the mutation. While AMPylation activity of FicD in vitro is strong when the helix is mutated, the question of whether this activity occurs in vivo by the wild type protein or if another cofactor is favored by FicD remains an open question.

Although the catalytic activity of FicD remains ambiguous, some biological features of the gene have been gleaned using *Drosophila melanogaster* genetics. Perhaps most interestingly, deletion of the FicD gene results in flies that are blind, measured by their inability to display any measureable phototaxis [63]. This phenotype may be due to a demonstrated defect in histamine neurotransmitter recycling, although the mechanism of this defect is unclear. Complicating the matter is the fact that the final localization of FicD is uncertain. In the aforementioned study, FicD was localized in the capitate projections (ie cell membrane) of glial cells, which may be the cell type that drives the blind phenotype of FicD deficient flies [63]. However, FicD appears to be an endoplasmic reticulum resident protein in other tissues, in agreement with its localization in experiments using cultured cells. It is

also possible that FicD adopts different localizations and perhaps even functions in different cell types. However, if FicD is indeed an endoplasmic reticulum resident protein, it is likely to participate in maintaining organeller homeostasis in a manner which promotes the proper folding and processing of proteins bound for downstream sites or even other endoplasmic reticulum resident proteins.

Protein misfolding stress in the endoplasmic reticulum is dynamically regulated

The proper expression, folding, modification, and processing of proteins targeted to the secretory pathway is a significant burden for eukaryotic cells, particularly those that have high secretory activity like pancreatic or immunoglobulin-producing immune cells. Many such proteins undergo selective glycosylation and disulfide bond formation by relevant enzymes, and require extensive assistance by chaperones to fold and achieve their proper conformation. These processes are quite easily disrupted by many common insults to the cell, such as oxidative stress, glucose deprivation, increases in temperature and aging. Because many of the proteins whose processing is disrupted are critical for cell health, the cell must be able to maintain the delicate homeostasis of the secretory pathway, sense when conditions are awry, and work to correct the defect. The cell does this through a coordinated process called the "Unfolded Protein Response" (UPR).

Many factors are involved in the UPR. In the initial stages, the cell has multiple avenues to sense stress and propagate downstream signals to deal with the stress [64].

Perhaps the most central protein in this process is the ER chaperone BiP/GRP78. During normal cell homeostasis, BiP acts as an essential protein folding chaperone that comes into contact with nearly every protein translated into the ER (**Figure 7**) [65, 66]. By binding to unfolded substrates and hydrolyzing ATP, BiP provides the energy needed to prod many proteins toward their working state. This chaperone has been shown to be critical in aiding many of the processes involved in the protein folding cycle, such as glycosylation processing, disulfide bond formation, and the calnexin/calreticulin chaperone cycle [65].

In addition to its role in promoting proper protein folding, BiP is also an essential mediator of the UPR [66]. Under resting conditions with low unfolded protein load, unoccupied BiP binds to three different signaling molecules: PERK, IRE1 and ATF6. Each of these proteins spans the ER membrane, with a lumenal portion to which BiP binds to inhibit their signaling [66]. The cytosolic portions of PERK and IRE1 contain kinase and endonuclease domains, respectively, that are only active when increasing levels of improperly folded proteins compete for BiP, freeing their lumenal portions. PERK is a kinase that, when active, phosphorylates the translation initiation factor eIF2a, significantly inhibiting translation and reducing the burden of incoming proteins to the ER [67]. IRE1 is an atypical endonuclease that targets the mRNA of a transcription factor called XBP1, splicing the mRNA to a mature form that allows full and proper translation of the XBP1 [68] . This factor then goes on to promote transcription of chaperones and other proteins that will help reduce the ER stress. ATF6, the third UPR signaling molecule to which BiP binds, is itself a transcription factor whose cytosolic DNA binding remains tethered to the ER membrane when bound to BiP. When BiP is not bound, it proceeds to the Golgi apparatus,

where the DNA binding domain is cleaved and translocates to the nucleus to promote the transcription of multiple UPR genes [69, 70].

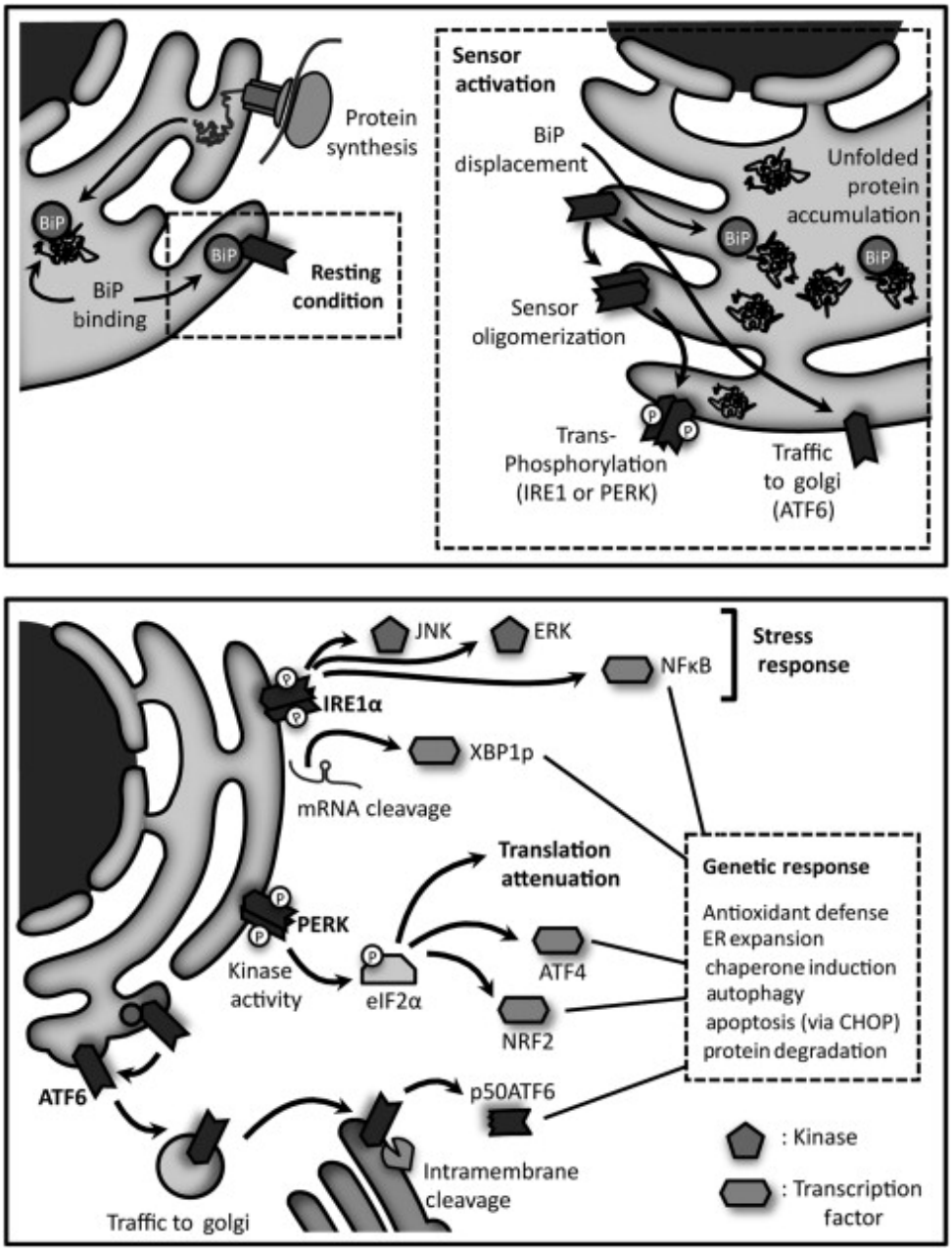

Figure 7. BiP is a key regulator of endoplasmic reticulum homeostasis. TOP: Under resting conditions, unfolded protein levels are sufficiently low for some free BiP to bind the lumenal domains of UPR signaling molecules PERK, IRE1 and ATF6, preventing their activation. When unfolded proteins accumulate, BiP is displaced, leading to activation of the molecules. **Bottom:** Upon activation, PERK, IRE1 and ATF6 use different mechanisms to help the cell return to homeostasis. Source: International Review of Cell and Molecular Biology, Volume 301, 2013, 215 – 290.

When proteins become terminally misfolded, improperly glycosylated or aberrantly modified in the ER they are translocated back to the cytosol in a process known as endoplasmic reticulum-associated protein degradation (ERAD) [71, 72]. BiP also plays an essential role in this process, as it is necessary for the degradation of many model substrates by ERAD. Suppression of BiP prevents the degradation of model ERAD substrates as BiP is a key mediator of ERAD that delivers improperly processed proteins to the ERAD retrotranslocation complex [73].

A key focus of our work on the fly and human versions of the Fic protein has been to see if FicD, as a potential ER resident protein, might affect any of these processes. Its proper function may be important to maintain ER homeostasis, or it could participate in mediating downstream conditions during the unfolded protein response. Initial evidence in this study suggests one of these may be the case, as discussed in Chapter 5.

Aims of this study

The main aim of this dissertation work was always to expand the understanding of the importance of AMPylation in eukaryotic biology, and my approach to reaching this goal was a three-pronged strategy. First, I endeavored to look more closely at the effects on host signaling caused by a toxin-mediated modification, which is the AMPylation of Rho GTPases by the T3SS effector VopS. As expected, inhibition of Rho GTPases in this manner inhibited many potential avenues of host defense, each of which is detailed in **Chapter 3**.

Second, we collaborated with the LaBaer lab at Arizona State University to develop a method to screen for AMPylation substrates using advanced protein microarray technology. Our findings in expanding the substrate catalogue of VopS and another Fic-domain containing protein is discussed in **Chapter 4**. Finally, I attempted to learn more about the human protein FicD in terms of substrates and its potential role in ER proteostasis. Studies on FicD's localization, AMPylation activity, targeting of the ER chaperone BiP, and induction during ER stress are detailed in **Chapter 5.** The findings in this work have helped to push forward the field of AMPylation and will help futures studies that lead to understanding AMPylation's role in both prokaryotic and eukaryotic biology.

CHAPTER TWO

Materials and Methods

Mammalian Cell Culture

HEK293T cells were maintained in Dulbecco's Modified Eagle Medium (DMEM, Gibco) containing 10% fetal bovine serum (FBS) and penicillin/streptomycin/glutamine at 37°C with 5% CO2. COSphox cells were maintained in low glucose DMEM (Hyclone) with 10% FBS, penicillin/streptomycin, 0.8 mg/ml G418, 200 μg/ml hygromycin and 1 μg/ml puromycin at 37°C with 5% CO2.

Bacterial strains

Escherichia coli strain Rosetta (DE3) used for protein purification was cultured with chloramphenicol in addition to antibiotics for plasmid selection. *Vibrio parahaemolyticus* strains are listed in **Table 2** and were derived from POR1 (RIMD2210633 ΔtdhAS), which was generously provided by Drs. Tetsuya Iida and Takeshi Honda. Strain genotypes and characteristics are detailed in Table 2. The CAB5 strain contains a deletion for the transcriptional regulator VtrA to prevent expression of the T3SS2 components, as well as deletions of the effectors VopQ, VopR, and VPA0450 to leave VopS as the only known T3SS effector expressed and secreted. VopS was further deleted in the CAB5ΔvopS strain, and complemented with a pBAD-VopS expression plasmid containing VopS wild type or VopS-H348A preceded by 1kb of its upstream sequence, which typically allows expression and secretion levels similar to genes encoded in the genome. CAB5ΔvopS was

complemented in the same manner, but using the pLAFR cosmid. *V. parahaemolyticus* strains were cultured in LB with 3% NaCl (marine LB, MLB). Deletions and reconstitution via plasmid mating were performed by others as previously described (22).

Mammalian Cell transfection

For transfection of 100 mm dishes, calcium phosphate transfections were used. 30 ug of expression plasmid DNA and 30 ul 2.5 M CaCl2 was added to 500 ul Hank's Buffered Salt Solution on ice and incubated for 20 minutes before addition to HEK293T cells at approximately 25% confluency with 8 ml fresh media. Media was again changed the next morning, and cells were harvested for immunoprecipitation 40 hours post transfection, at which point the cells were near full confluency.

For transfection of 6 well and smaller plates, HEK293T cells at approximately 50% confluency were transfected using Xtremegene HP transfection reagent according to manufacturer's protocol. In brief, 2 ug total DNA was combined with 2 ul transfection reagent in 200 ul serum-free OptiMEM media per reaction and incubated at room temperature for 15 minutes. Transfection reagent was then added to cells, and media was changed 4 hours later. Protein expression continued overnight, and cells were harvested for downstream applications.

Bacterial infection experiments

For immunoblot experiments, cells were seeded onto 6-well plates at a density of $4x10^5$ cells per well the day prior to infection. For immunofluorescence experiments, cells

were seeded on 6-well plates containing sterile cover slips at a density of $1x10^5$ cells per well. Bacteria were induced prior to infection by diluting overnight culture 1:10 into plain DMEM, followed by incubation at 37°C with shaking for 30 minutes. Bacteria were then diluted to multiplicity of infection (MOI) 10 relative to host cells in fresh pre-warmed DMEM. Culture media on cells was then replaced with this infection media, and were spun at 1000 rpm for 5 minutes prior to return to the incubator for indicated infection times. All infection experiments were performed three or more times with consistent results.

Western Blotting

For immunoblotting, cells were lysed in buffer containing 50 mM Tris pH 8.0, 150 mM NaCl, 1 mM EDTA, 5% glycerol, and 1% NP-40 with protease and phosphatase inhibitors (Roche) on ice prior to electrophoresis and immunoblotting. PVDF membranes were blocked with 5% milk for 30 minutes and incubated with primary antibodies at 4°C overnight with agitation. Secondary HRP linked antibodies (donkey anti-rabbit, GE; goat anti-mouse, Sigma; donkey anti-goat, Santa Cruz) were incubated at room temperature for 30 minutes at 1:10,000 dilutions in 5% milk followed by thorough washing in TBST. Chemiluminescence was generated using the Pierce ECL2 HRP substrate.

Immunofluorescence

For immunofluorescence experiments, cells were washed once with PBS, followed by fixing in 3.2% PFA for 10 minutes. Fixed cells were permeabilized with 0.5% Triton-X-100

in PBS for 4 minutes and washed prior to immunostaining with anti-p65 (Santa Cruz) at a 1:200 dilution for 1 hour. Staining was detected with anti-rabbit Alexa Fluor 568 secondary antibody (Life Technologies) incubation at 1:500 dilution for 1 hour. DNA was visualized by staining with Hoechst at 1 μg/ml for 10 minutes. Confocal images were taken using a Zeiss LSM 710 microscope and converted using ImageJ.

Recombinant protein purification

Rosetta (DE3) *E. coli* were transformed with expression plasmids on LB plates with relevant antibiotics. Proteins were expressed by inoculating large (500ml to 1.5L) cultures 1:100 with overnight cultures and growing to an OD600 between 0.5 and 0.8. 400 uM isopropyl β-D-thiogalactopyranoside (IPTG) was then added, followed by 3-5 hours of expression at room temperature. Cells were pelleted at 5,000 rpms, and pellets were resuspended in lysis buffer containing 50 mM Tris pH 8.0, 300 mM NaCl, and in the case of His-fusion proteins, 10 mM imidazole. Cells were lysed by 6-8 passages through an Emulsiflex E3 french press (Avestin), and proteins were affinity purified with either Nickel affinity resin (Pierce) or glutathione resin (Pierce) according to manufacturer's instructions. Proteins were further purified on AKTA FPLC with relevant columns as indicated. To purify VopS, GST-TEV-VopS was isolated with glutathione resin, eluted with lysis buffer containing 12.5 mM glutathione, and cleaved overnight with His-TEV protease overnight at 4 degrees Celsius. VopS was then separated from free GST by fractionation on mono Q with a linear gradient of 25 mM to 1M NaCl in 25 mM Tris, pH 8.0. AMPylated and

unAMPylated His-Rac1 V12 were purified by coexpression in Rosetta (DE3) *E. coli* with a GST-VopS fusion or empty vector. After nickel affinity step, His-Rac1 proteins were fractionated by gel filtration chromatography on Superdex 75 PG with an AKTA FPLC system in a buffer containing 20 mM HEPES pH 7.4, 150 mM NaCl with 1 mM DTT.

In vitro AMPylation assays

AMPylation assays were performed with recombinant proteins or lysates in 20-30 ul volumes with the following conditions: 50 mM Tris pH 7.5, 150 mM NaCl, 10 mM $MgCl_2$, 10 mM $CaCl_2$, and 10 mM $MnCl_2$ with 100 uM ATP. In assays with ^{32}P-α-ATP, 0.5 uCi per reaction was spiked into the master mix prior to addition. For assays with N6-ATP, the 100 uM ATP was replaced with 100 uM N6-ATP. Reactions were incubated at 30 degrees Celsius for 30 minutes. Assays with N6-ATP were then subjected to the click chemistry reaction prior to SDS-PAGE and fluorescent imaging (detailed below). In assays with ^{32}P-α-ATP, Laemmli buffer was simply added, samples were boiled and subjected to SDS-PAGE before transfer to PVDF and phosphorimaging using a phosphorscreen (KODAK).

Copper-catalyzed Click Chemistry Reactions

Lysates or recombinant proteins AMPylated with N6-adenosine or N6-ATP were precipitated by methanol:chloroform addition. Briefly, water was added to 100 ul, followed by addition of 400 ul 100% methanol and 100 ul chloroform. Samples were gently vortexed, and centrifuged at 20,000g for 5 minutes at 4 degree Celsius. The upper layer was removed, and 1 ml H2O was added before centrifugation at 20,000g for 15 minutes at 4 degree Celsius.

The supernatant was removed, and the pellet was washed with acetone and partially dried. The pellet was resuspended in 15 ul 1x PBS with 4% SDS and conjugated with azo-rhodamine by adding the following reagents at the indicated volumes and concentrations: 0.25 ul azo-rhodamine (10 mM), 1.25 ul Tris(benzyltriazolylmethyl)amine (TBTA, 2 mM), 0.5 ul tris(2-carboxyethyl)phosphine (TCEP, 50 mM), 0.5 ul $CuSO_4$ (50 mM) and 7.5 ul 1x PBS with 4% SDS. Samples were incubated for 1 hour at room temperature prior to addition of Laemmli buffer, boiling and SDS-PAGE. Gels were rinsed twice in water, fixed in 40% methanol and 10% acetic acid for 2 hours, and rinsed in water for 1 hour. Fluorescence was imaged on a STORM 860 scanner, with 532 nm excitation, 580 nm filter and 30 nm bandpass.

Pull-downs and immunoprecipitations

GST pull-downs were performed by binding purified GST proteins to glutathione beads in 50 mM Tris pH 8.0, 300 mM NaCl and 0.1% Triton X-100, followed by incubation with His-Rac1 V12 at 4°C with gentle agitation for 2 hours. Beads were washed 4 times with TBST prior to elution in Laemmli buffer and western blotting.

Immunoprecipitations were performed by incubating lysates with anti-FLAG M2 beads or anti-HA beads (Sigma) for 2 hours at 4°C, washing 4 times with TBST and eluting 3 times with 100 ug/ml FLAG peptide or once with Laemmli.

Superoxide generation assay

COSphox cells were seeded at a density of 2x105 cells per well in a 6-well plate, followed by infection as described above. Cells were then collected and superoxide generation upon stimulation with Phorbol 12-myristate 13-acetate (PMA, Sigma) was measured using the Diogenes kit (National Diagnostics) according to manufacturer's protocol. Luminescence was monitored using a FLUOstar OPTIMA (BMG LabTech) plate reader over 30 minutes. Superoxide assays were performed three times in triplicate and a representative experiment is shown.

NAPPA array fabrication

The fabrication of NAPPA arrays comprising of 10,000 highly purified DNA plasmids with full-length human ORF sequences and the procedure of protein-protein interaction screens were reported as previously described. Briefly, to accomplish the expression & display of proteins on NAPPA, the array was blocked with the Superblock solution (Pierce, Rockford, IL) for 1h at 23°C, and then incubated with the HeLa lysates based cell-free expression system (Thermo scientific, Rockford, IL) for 1.5 hrs at 30°C and 0.5 hr at 15°C. After brief washing with PBST (PBS, 0.2%Tween), the resulting protein array was blocked with PPI COLD blocking buffer (1×PBS, 1%Tween 20 and 1% BSA, pH7.4) for 1 hour at 4°C.

NAPPA AMPylation Screen

The AMPylation reaction was performed by incubation of the prepared NAPPA protein array with 40 μg/ml AMPylator proteins and 250 μM N6pATP in 160 μl AMPylation solution (20 mM HEPES pH 7.4, 100 mM NaCl, 5 mM MgCl2, 0.1 mg/ml BSA, 1 mM DTT) for 1hr at 30ºC. Following washing three times with PBST, the detection was performed with the 160 μl click reagents containing 250 μM az-rho, 1 mM TCEP, 0.1 mM TBTA and 1 mM CuSO4, as previously described (12) for 1 hr at room temperature. After washing overnight, the microarray was scanned with a Tecan's PowerScanner (Männedorf, Switzerland). The fluorescent signal was quantitated using Array-Pro Analyzer, version 6.3 (Media Cybernetics, Bethesda, MD).

Data analysis

Before statistical analysis, all the fluorescent microarray images were examined for the spot shape, dust and non-specific binding to remove false positive signals. We then normalized the raw signal intensity to decrease the variation due to different slides' background. The normalization was performed by subtracting the background signal attributable to non-specific binding of AMPylators or fluorescent molecules, which was estimated by the first quartile of the printing buffer-only control. The normalized value was calculated by dividing the result for each feature by the median background-adjusted value of all proteins on the array. Proteins with a normalized value 20% percent above the median were considered positive signals.

To choose potential substrates of VopS and IbpAFic2, we set a cut-off ratio of 1.2 fold, which was calculated by dividing the signal due to AMPylator by its buffer control. Moreover, each experiment was repeated three times on independent days and only the protein showing a positive ratio in all three experiments were selected as candidates. With this cut-off, we identified and confirmed 6 of the 7 expected targets in a preliminary test of VopS.

NAPPA interaction screen

In parallel with expression of plasmids printed on slides, 100 ng/μL DNA of Rac1-Halo proteins was added in 170 μL human HeLa lysates based cell-free expression system, and the expression was performed at 30°C for 2 hrs. To execute protein-protein interaction screening, the expressed Rac1-Halo proteins was incubated with NAPPA protein array for 16hrs at 4oC. After reaction, the array was washed three times with PPI washing buffer (PBS, 5 mM MgCl2, 0.5% Tween20, 1% BSA and 0.5% DTT, pH7.4). The binding of Rac1-Halo to its interactors on NAPPA was detected using 12.5 μM Alexa 660 conjugated Halo-ligand (Promega, Madison, WI). Finally, the microarray fluorescent images were scanned using Tecan's PowerScanner (Männedorf, Switzerland) and the signal intensity was quantitated using Array-Pro Analyzer (Media Cybernetics, Bethesda, MD).

Selection of Rac1 interactors from NAPPA screening

The selection of interaction targets was executed as previously described. Briefly, all NAPPA images were visually examined to eliminate the false positive signals caused by the spot shape, dust and non-specific bindings. Signal normalization was performed using the raw signal intensity of each spot divided by the median background-adjusted value of all features on the array. Finally, the Z-score was calculated for each protein and the selection of Rac1 interactor candidates using the following criteria (1) Z-score ≥ 2.5; (2) Z-score ratio of query protein to Halo negative control ≥ 2; (3) the targets have to meet previous criteria in two independent experiments.

wNAPPA assays

Anti-GST antibody coated 96-well plates (GE Healthcare Life Sciences, PA) with expressed GST-fused bait proteins were blocked with 5% milk at 4ºC overnight. In parallel, the Rho GTPase proteins containing a c-terminal Halo tag and their interaction proteins containing a c-terminal GST tag were expressed in 30 μL human HeLa lysates based cell-free expression system using 40 ng/μL DNA, with or without 5 ug of purified VopS added to the lysate. After expression, they were diluted with 100μL PPI blocking buffer and added into the 96-well plate. The protein-protein interaction reaction was then executed at 15ºC for 2 hrs with mild shaking. After washing three times with PBST, the detection was accomplished by incubation with 1:3000 diluted anti-Halo tag antibody (Promega, Madison, WI).

In vitro EndoH reactions

FicD-FLAG transfected HEK293T cells were harvested and lysed with 50 mM Tris pH 8.0, 150 mM NaCl, 1 mM EDTA, 5% glycerol, and 1% NP-40 with protease and phosphatase inhibitors (Roche) on ice. EndoH (New England Biolabs) cleavage assays were performed according to manufacturer's protocol, and relative mobility of FicD-FLAG with and without addition of EndoH was monitored by western blot using anti-FLAG M2 antibody.

Measurement of mRNA expression with qRT-PCR

To induced endoplasmic reticulum stress in HEK293T cells, 2 ug/ml tunicamycin or 1 uM thapsigargin were added to cells at approximately 50% confluency and incubated for indicated times. Cells were harvested by washing, scraping, snap freezing and storage at -80 until use. Total RNA was extracted using the RNeasy Plus Extraction Kit (Qiagen) according to manufacturer's protocol. cDNA was generated using 1 ug RNA with the Protoscript II First Strand cDNA Synthesis Kit (New England Biolabs) according to manufacturer's protocol, and cDNA was diluted to 200 ul in ddH_20. qPCR was performed on each sample in triplicate using Fast Sybr Green master mix (Life Technologies). 5 ul cDNA was combined with 10 ul 2x Master mix and 5 ul combined primers at 800 nM each in a 96 well plate and spun briefly to collect reactions at bottom. PCR reactions were performed and data was collected using a 7500 Fast Real-time PCR System (Life Technologies). Relative mRNA expression of indicated genes was calculated using the $\Delta\Delta$Ct method relative to GAPDH expression, calculated in Microsoft Excel.

Purification of endogenous Ala1 from Saccharomyces cerevisiae (large scale)

The large scale version of the Ala1 purification for post-translational modification analysis is listed here. The initial purification used for protein identification was approximately 1/6 of volumes used here. 50 ml overnight cultures in YPD media, 8 in total, were started by inoculation of a single BY4741 colony into each flask followed by incubation at 30ºC overnight with shaking at 225 rpm. These overnights were then used to inoculate 4 1.5 L cultures in YPD, which were grown identically for 4-6 hours until OD600 of 0.6-1.0 was reached. Yeast were washed with 300 ml ddH20 per bottle, respun and washed again in 100 ml ddH20. OD600 was recorded again to determine total amount of yeast to be spheroplasted. Cells were pelleted again and resuspended in 300 ml warmed softening buffer (0.1M Tris pH 9.3 with 10 mM DTT), and placed on shaker at 200 rpm, 30ºC, for 15 minutes. Yeast were centrifuged at 7,000 rpm for 10 minutes and room temperature, and resuspended in 300 ml warmed Digestion Buffer (1M sorbitol, 5 mM KH_2PO_4 pH 7.5). To spheroplast cells, 4 mg Zymolyase 100T was added per 1000 OD units of culture, and cells were placed on shaker at 200 rpm, 30ºC for 30 minutes. Cell wall digestion was monitored by loss of OD units. Spheroplasts were used fresh for purification steps.

For column purifications, spheroplasts were lysed by resuspension in 100 ml 25 mM Tris pH 8.0 with 25 mM NaCl, 1 mM DTT and protease inhibitors, followed by 20 strokes with a large dounce on ice. Sample was then centrifuged at 1000g for 10 minutes at 4ºC. Supernatant was then spun at 20,000g for 30 minutes, 4ºC. This supernatant (1,200 mg of protein) was then loaded onto 25 ml DEAE FF resin equilibrated with lysis buffer. Resin was

washed 4 times with lysis buffer prior to elution with lysis buffer (68 ml total) containing 155 mM NaCl. This fraction (218 mg total protein, known to contain protein of interest) was dialyzed 3x into buffer containing 20 mM HEPES pH 7.4, 25 mM NaCl. Dialyzed fraction was split into 8 equal volumes and fractionated using FPLC in 8 identical runs on 1 ml mono Q column with a 25-500 mM linear NaCl gradient and identical fractions were pooled. Fractions were assayed for presence of band of interest (strong band between 100-130 kilodaltons) by western blot with anti-Y-AMP antibody. Mono Q fractions 10-12, containing most of protein of interest, were pooled (59 mg total protein) and split into 6 identical volumes. These volumes were then loaded onto a 1 ml Blue HP column in 6 identical runs, and fractionated with a 0-2M NaCl linear gradient. Fractions were assayed as above, and strongest fractions (10-14, 9.5 mg total protein) were concentrated and exchanged into a buffer containing 20 mM HEPES pH 7.4, 1M $(NH_4)_2SO_4$ using an Amicon concentrator with 50 kDa filter. Sample was loaded in two identical runs onto a 1ml Phenyl HP column with linear gradient from 1.0-0.0 M $(NH_4)_2SO_4$. Fractions were assayed, and those containing strongest western blot signal of protein target (17-19, 0.42 mg total protein) was concentrated to 1 ml volume and loaded onto Superdex 200 column equilibrated with 10 mM sodium phosphate pH 6.8, 15 mM NaCl. Fractions 30-32 contained the most homogenous protein. These fractions were concentrated to 100 ul, subjected to SDS-PAGE, stained and sent to the UT Southwestern Mass Spectrometry for protein identification (1^{st} small scale purification) or post translational modification analysis (2^{nd} large purification). Sequential purifications were performed over a time frame of approximately 48 hours to ensure protein integrity and suitability for fractionation.

N6-Adenosine Metabolic Labeling

After 40 hours post transfection with BiP expression construct, 50-100 uM N6-Adenosine (suspended in DMSO) or DMSO alone was added to HEK293T and incubated between 6 and 8 hours. Cell were harvested and lysed in 50 mM Tris pH 8.0, 150 mM NaCl, 1 mM EDTA, 5% glycerol, and 1% NP-40 with protease and phosphatase inhibitors (Roche). Lysates were centrifuged at 20,000g for 10 minutes and the supernatant was used for pulldown with Strep-tactin Superflow Plus (Qiagen). Lysates were incubated with 30 ul resin slurry for 2 hours with end-over-end mixing at 4^{o}C for 2 hours. Resins were washed twice in TBST, followed by on-bead click chemistry reaction as described in "Copper-catalyzed Click Chemistry Reactions" with two alterations. First, SDS was omitted to allow substrates to remain on beads. Second, click master mix was added directly to beads in a final volume of 100 ul. After incubation for 1 hour, beads were washed 3 times in TBST, and proteins were eluted with 1x Laemmli buffer prior to electrophoresis and imaging as in "Copper-catalyzed Click Chemistry Reactions**".**

Table 2. Bacterial Strains

Strains	Genotype and Characteristics	Source
Vibrio parahaemolyticus		
RIMD 2210633	Parental clinical isolate of *V. parahaemolyticus* strains list below. KP positive; serotype O3:K6. Not used in this study	A gift from Takeshi Honda
CAB5	RIMD2210633 *ΔtdhAS, ΔvtrA, Δvpa1680 (vopQ), Δvpa1683 (vopR), Δvpa0450.* Allows assessment of VopS in isolation by removing TDH toxins, T3SS2 and other T3SS1 effectors	This study
CAB5Δ*vopS*	*ΔtdhAS, ΔvtrA, Δvpa1680 (vopQ), Δvpa1683 (vopR), Δvpa1686 (vopS), Δvpa0450.* Strain with deletion of TDH toxins and T3SS2, with intact T3SS1 but deletion of all characterized T3SS1 effectors including VopS	This study
CAB5Δ*vopS*/pVopS	CAB5Δ*vopS* complemented with pBAD33 (Kan^r) with full length VopS and +1kb upstream sequence containing endogenous promoter	This study
CAB5Δ*vopS*/pVopS H348A	CAB5Δ*vopS* complemented with pBAD33 (Kan^r) with full length VopS H348A (catalytically dead) and +1kb upstream sequence containing endogenous promoter	This study
Escherichia coli		
Rosetta/DE3	Allows for high expression of recombinant protein in *E. coli*	Novagen

Table 3. Primers used in this study

Cloning primers

Code	Name	Site	Sequence (5'to 3')	Purpose
AW1139	IbpA Fic2 BsaI FWD for pE-SUMO	BsaI	ATCGggtctcaAGGTAAATCATCTCCGCAAGAGGGAG	To clone the 2nd Fic domain of *H. somni* IbpA into pE-SUMO for bacterial expression
AW1140	IbpA Fic2 XbaI REV for pE-SUMO	XbaI	ATCGtctagaTTATTTTTTGCCAACTCTTTTAAAAACTC	
AW1157	FicD ND47 RF cloning FWD for pE-SUMO	N/A	gctcaccgcgaacagattggaggtGAGGAGCAGTGCTTGGCTGT	To clone FicD truncated 47 amino acids into pE-SUMO for bacterial expression
AW1158	FicD RF cloning REV for pE-SUMO	N/A	ctcgagtgcggccgcaagcttTTAGGGCTTCACAGGAAGCGTC	
AW1177	Ly-GDI FWD EcoRI pET28a	EcoRI	ATCGgaattcATGACTGAAAAAGCCCCAGAG	To clone LyGDI into pET28a for bacterial expression
AW1178	Ly-GDI REV XhoI pET28a	XhoI	ATCGctcgagTCATTCTGTCCACTCCTTCTTAATC	
AW1181	LC3 FWD EcoRI pET28a	EcoRI	ATCGgaattcCCCTCAGACCGGCCTTTC	To clone LC3 into pET28a for bacterial expression

AW1182	LC3 REV XhoI pET28a	XhoI	ATCGctcgagTCAGAAGCCGAAGGTTTCCTGG	
AW1199	RhoGDI alpha BamHI FWD	BamHI	ATCGggatccGCTGAGCAGGAGCCCACAG	To clone RhoGDI into pET28a for bacterial expression
AW1200	RhoGDI alpha XhoI stop REV	XhoI	ATCGctcgagTCAGTCCTTCCAGTCCTTCTTGATG	
AW1251	Rac2 FWD KpnI	KpnI	ATCGggtaccCAGGCCATCAAGTGTGTGG	To clone Rac2 into pET28a for bacterial expression
AW1252	Rac2 REV XhoI	XhoI	ATCGctcgagCTAGAGGAGGCTGCAGGC	
AW1253	Rac3 FWD BamHI	BamHI	ATCGggatccCAGGCCATCAAGTGCGTG	To clone Rac3 into pET28a for bacterial expression
AW1254	Rac3 REV XhoI	XhoI	ATCGctcgagCTAGAAGACGGTGCACTTCTTCC	
AW1255	CDC42 FWD Kpn	KpnI	ATCGggtaccCAGACAATTAAGTGTGTTGTTGTGG	To clone CDC42 into pET28a for bacterial expression
AW1256	CDC42 REV Not	NotI	ATCGgcggccgcTTAGAATATACAGCACTTCCTTTTGG	

Mutagenesis Primers

Code	Name	Sequence (5'to 3')	Purpose
AW1201	LyGDI T51A FWD	AGTCTAATTAAGTACA AGAAAgcaCTGCTGGGA GATGGTCCTGTG	Mutate LyGDI AMPylation site from threonine to alanine
AW1202	LyGDI T51A REV	CACAGGACCATCTCCC AGCAGtgcTTTCTTGTAC TTAATTAGACT	
AW1135	FicD E234G FWD	ATCTACCACACAGTGG CCATCggaGGCAACACC CTCACCCTCTCG	Mutate autoinhibitory helix of FicD to disrupt salt bridge that blocks ATP binding
AW1136	FicD E234G REV	CGAGAGGGTGAGGGTG TTGCCTCCGATGGCCA CTGTGTGGTAGAT	
AW1296	BiP R470A FWD	atcaaggtctatgaaggtgaagcacc cctgacaaaagacaatcat	Mutate BiP ADP-Ribosylation site from arginine to alanine
AW1297	BiP 470A REV	atgattgtcttttgtcaggggtgcttcac cttcatagaccttgat	
AW1300	BiP T366A FWD	attgttcttgttggtggctcggcacgaa ttccaaagattcagcaa	Mutate BiP AMPylation site from threonine to alanine
AW1301	BiP T366A REV	ttgctgaatctttggaattcgtgccgag ccaccaacaagaacaat	

qRT-PCR primers

Code	Name	Sequence (5'to 3')	Purpose
AW1117	GADPH FWD	CCATGAGAAGTATGACAACAGCC	Quantify GAPDH mRNA
AW1118	GAPDH REV	GGGTGCTAAGCAGTTGGTG	Quantify GAPDH mRNA
AW1115	Beta-Actin FWD	CATGTACGTTGCTATCCAGGC	Quantify Beta-Actin mRNA
AW1116	Beta-Actin REV	CTCCTTAATGTCACGCACGAT	Quantify Beta-Actin mRNA
AW1113	FicD FWD	ATTGACCATCTCACCCTACCA	Quantify FicD mRNA
AW1114	FicD REV	ATGTGCCTGATTTCCGAGAGG	Quantify FicD mRNA
AW1279	CHOP FWD	GCACCTCCCAGAGCCCTCACTCTCC	Quantify CHOP mRNA
AW1280	CHOP REV	GTCTACTCCAAGCCTTCCCCCTGCG	Quantify CHOP mRNA
AW1291	Spliced XBP1 FWD	ctgagtccgaatcaggtgcag	Quantify Spliced XBP1 mRNA
AW1292	XBP1 REV	atccatggggagatgttctgg	Quantify XBP1 mRNA
AW1293	Unspliced XBP1 FWD	cagcactcagactacgtgca	Quantify unSpliced XBP1 mRNA

Table 4. Plasmid Constructs used in this study

Plasmid	Description	Source
Mammalian Expression		
pcDNA3.1	Parental mammalian expression vector. Amp^r. Neo^r. pCMV promoter.	Life Technologies
pRL1312	Parental Gateway Mammalian Expression vector. Included N terminal FLAG tag. Amp^r. Cm^r, ccdB selection within AttR1 and AttR2 recombination sites. CMV promoter	A gift from Rueyling Lin
pSFFV-GFP		
pGEN1-DEST	Parental Gateway Mammalian Expression vector. Included N terminal TCM signal sequence, 8x His and Strep tag. Amp^r. Cm^r, ccdB selection within AttR1 and AttR2 recombination sites. CMV promoter.	DNASU
pcDNA3.1-3xHA	Parental mammalian expression vector. Amp^r. Neo^r. pCMV promoter. N-terminal 3x HA tag included.	This study
pcDNA3.1-3xHA-Rac1	*Homo sapiens* Rac1 fused with 3x HA tag	A gift from Neal Alto
pcDNA3.1-3xHA-Rac2	*Homo sapiens* Rac2 fused with 3x HA tag	This study
pcDNA3.1-3xHA-Rac3	*Homo sapiens* Rac3 fused with 3x HA tag	This study
pcDNA3.1-3xHA-LC3	*Homo sapiens* LC3 fused with 3x HA tag	This study
pRL1312-FLAG-LyGDI	*Homo sapiens* LyGDI fused with N-terminal FLAG tag	This study

pcDNA3.1-C-FLAG	Parental mammalian expression vector. Amp^r. Neo^r. pCMV promoter with C-terminal FLAG tag included.	
pcDNA3.1-FicD-FLAG	*Homo sapiens* FicD fused with C-terminal FLAG tag	This study
pSFFV-FicD-GFP	*Homo sapiens* FicD fused with C-terminal GFP tag	
pGEN1-DEST-BiP	*Homo sapiens* BiP truncated by 19 N-terminal amino acids, fused with N-terminal TCM signal sequence, 8X His and Strep tag.	DNASU

Plasmid	**Description**	**Source**
Bacterial Expression		
pET28a	Allows for high expression of recombinant protein in *E. coli.* Kan^r. T7 promoter. N terminal 6x His tag and thrombin cleavage site included. IPTG inducible	Novagen
pGEX-TEV	Allows for high expression of recombinant protein in *E. coli.* AMP^r. T7 promoter. N terminal GST tag and TEV cleavage site included. IPTG inducible.	A gift from Neal Alto
pDEST15	Allows for high expression of recombinant protein in *E. coli.* AMP^r. Cm^r, ccdB selection within AttR1 and AttR2 recombination sites.T7 promoter. N terminal GST tag. IPTG inducible.	Life Technologies
pGEX-4T	Allows for high expression of recombinant protein in *E. coli.* AMP^r. T7 promoter. N terminal GST tag and TEV cleavage site included. IPTG inducible.	GE Healthcare

pDEST17	Allows for high expression of recombinant protein in *E. coli*. AMP^r. Cm^r, ccdB selection within AttR1 and AttR2 recombination sites.T7 promoter. N terminal 6x His tag. IPTG inducible.	Life Technologies
pE-SUMO	Allows for high expression of recombinant protein in *E. coli*. Kan^r. T7 promoter. N terminal His-Smt3 (SUMO) tag. IPTG inducible.	Life Sensors
pET28a-Rac1 V12	Homo sapiens Rac1 fused to N-terminal 6x His tag. Rac1 is mutated at amino acid 12 to valine to give dominant active phenotype.	
pDEST15-p67	*Homo sapiens* p67 phox fused to an N-terminal GST tag.	This study
pGEX-4T-PAK3 PBD	*Homo sapiens* PAK3 GTPase binding domain fused to an N-terminal GST tag	A gift from Neal Alto
pGEX-TEV-VopS NΔ30	*Vibrio parahaemolyticus* VopS truncated by 30 N-terminal amino acids fused to an N-terminal GST tag	
pGEX-TEV-VopS NΔ30 H348A	*Vibrio parahaemolyticus* VopS truncated by 30 N-terminal amino acids fused to an N-terminal GST tag. Catalyically dead due to mutation of Fic domain histidine.	
pE-SUMO-IbpA Fic2	Second Fic domain (Fic2) of Histophilus somni IbpA fused to N-terminal His-SUMO tag.	This study
pE-SUMO-IbpA Fic2 H3xxxA	Second Fic domain (Fic2) of Histophilus somni IbpA fused to N-terminal His-SUMO tag. Catalyically dead due to mutation of Fic domain histidine.	This study
pET28a-RhoGDI	*Homo sapiens* RhoGDI fused to an N-terminal 6x His tag.	This study

pET28a-LyGDI	*Homo sapiens* LyGDI fused to an N-terminal 6x His tag.	This study
pET28a-LyGDI T51A	*Homo sapiens* LyGDI fused to an N-terminal 6x His tag. Mutated at threonine 51 to alanine to block AMPylation.	This study
pE-SUMO-FicD NΔ47	*Homo sapiens* FicD truncated by 47 N-terminal amino acids fused to N-terminal His-SUMO tag.	This study
pE-SUMO-FicD NΔ47 H363A	*Homo sapiens* FicD truncated by 47 N-terminal amino acids fused to N-terminal His-SUMO tag. Catalyically dead due to mutation of Fic domain histidine.	This study
pE-SUMO-FicD NΔ47 E234G	*Homo sapiens* FicD truncated by 47 N-terminal amino acids fused to N-terminal His-SUMO tag. Mutated at residue in inhibitory helix to give AMPylation activity.	This study
pDEST17-BiP NΔ19	*Homo sapiens* BiP/GRP78 truncated by 19 N-terminal amino acids fused to N-terminal His tag.	This study

CHAPTER THREE

AMPylation of Rho GTPases has multiple host cell signaling consequences

INTRODUCTION

Rho GTPases are proteins that are integral in diverse signaling pathways, including the maintenance of cell structure, coordination of cell motility, response to extracellular stimuli and activation of host defenses to pathogens. Accordingly, they represent a ripe target for virulence mechanisms of pathogenic bacteria and are frequently modified with post-translational modifications, such as glucosylation, deamidation and AMPylation . The switch-1 loop of GTPases is a frequent target of such modifications because this region of the protein mediates interactions with downstream signaling partners, such as p21-activated kinase (PAK). The attractiveness of this family of proteins as targets for pathogens is highlighted by recent discoveries of host pattern recognition receptors (PRRs) that monitor the activation status of Rho GTPases. NOD family proteins were shown to be PRRs that sense activated Rac1 and stimulate NFκB signaling. Inversely, Rho proteins that have been inactivated through modification of the switch-1 loop can trigger the inflammasome through the novel PRR protein Pyrin via an unknown mechanism. The sensitivity of the host immune system to modulation of Rho GTPases may merely be a convenient way to sense infection, or it may instead suggest that these modifications are exceptionally deleterious to the host. The majority of investigations about the effect of Rho GTPase posttranslational modifications, including AMPylation, have focused on

the collapse of the actin cytoskeleton, but other signaling pathways in which these GTPases are involved may also be affected.

One example of Rho GTPase targeting by virulence factors is the targeting of Rho, Rac and CDC42 by the type three secreted effector VopS from *Vibrio parahaemolyticus* [3]. Upon delivery into the host cell, VopS localizes to the plasma membrane via its bacterial phosphoinositide-binding domain, where it modifies Rho GTPase proteins by adding an adenosine monophosphate (AMP) to a threonine located in the switch-1 loop of the GTPase [74]. This modification has been demonstrated to cause actin cytoskeletal collapse by blocking interaction of Rac1 with p21-Activated Kinase (PAK) [3]. This phenotype has obvious implications for an infected host, but its drastic nature likely masked other important cellular consequences. In support of this, VopS has previously been shown to reduce cytokine production during infection through an unknown mechanism.

Rho family GTPases are known to have many functions in the cell beyond control of the actin cytoskeleton. For example, Rac has been shown to perform several functions in innate immunity, such as activation of the phagocytic NADPH oxidase complex, which is important for microbial killing by lymphocytes [45]. Association of activated Rac is essential for the recruitment of the p67phox subunit to the membrane, allowing generation of the killing superoxides at the phagocytic cup. Rac is also a known ubiquitination substrate for the Inhibitors of Apoptosis proteins (IAPs), though the full implications of this modification are unclear [75]. IAP's are known to ubiquitinate TRAF6 and several other proteins as a result of microbial and other stimuli to initiate downstream signaling of NFκB and MAPK pathways, leading us to speculate that Rho GTPase ubiquitination might play a role in these pathways [76]. The NFκB

and MAPK signaling cascades are critical systems that mediate cell survival outcomes for a variety of cell responses to outside stimuli, and their importance during bacterial infection is well established [55]. Manipulating these pathways are a common goal of many pathogenic bacteria, and several other diverse strategies have been elucidated, including, but not limited to, Ser/Thr acetylation, ubiquitination, phosphothreoninelyation, deamidation and ADP-ribosylation.

We sought to determine whether AMPylation of the Rho GTPase switch-1 region by VopS had effects beyond the collapse of the actin skeleton. To this end, we monitored the effects of VopS during infection on NFκB and MAPK signaling pathways, binding of IAP proteins to Rac1, and the ability of Rac1 to activate the phagocytic oxidase complex. Each of these signaling processes plays important roles in the ability of a host to clear infection, and we found that VopS had striking inhibitory effects on all of them. We also utilized a broad proteomic screen to identify a novel Rac1 binding protein C1qA. This interaction is hampered by VopS-mediated AMPylation, and thus may have implications in immunity that are yet to be explored.

RESULTS

VopS blocks activation of the NFκB and MAPK pathways

To assess the effect of VopS on host signaling, we infected cells with *V. parahaemolyticus* strains rather than transfecting cells with VopS. Transfection of cells with VopS causes cell rounding within 8 hours, precluding our ability to follow the kinetics of VopS-induced inhibition of a signaling pathway. For analysis of NFκB signaling we infected HEK293T cells with the *V. parahaemolyticus* strain CAB5 (**Table 2**), which is an attenuated

clinical isolate that is deleted for its TDH toxins, the second T3SS (T3SS2), and all known T3SS effectors except for VopS, thereby allowing T3SS1 and VopS to be studied independent of the other known *V. parahaemolyticus* virulence factors. During infection with CAB5 we found that IκBα phosphorylation and degradation of IκBα was markedly reduced relative to a CAB5 strain that is deleted for VopS (CAB5ΔvopS). Unlike CAB5, infection with CAB5ΔvopS resulted in strong IκBα phosphorylation concomitant with decreased IκBα protein levels within 1 hour of infection (**Figure 8**). IκBα phosphorylation and degradation during infection with CAB5ΔvopS complemented with wild type VopS (CAB5ΔvopS/pVopS) was similar to the parental CAB5 strain.

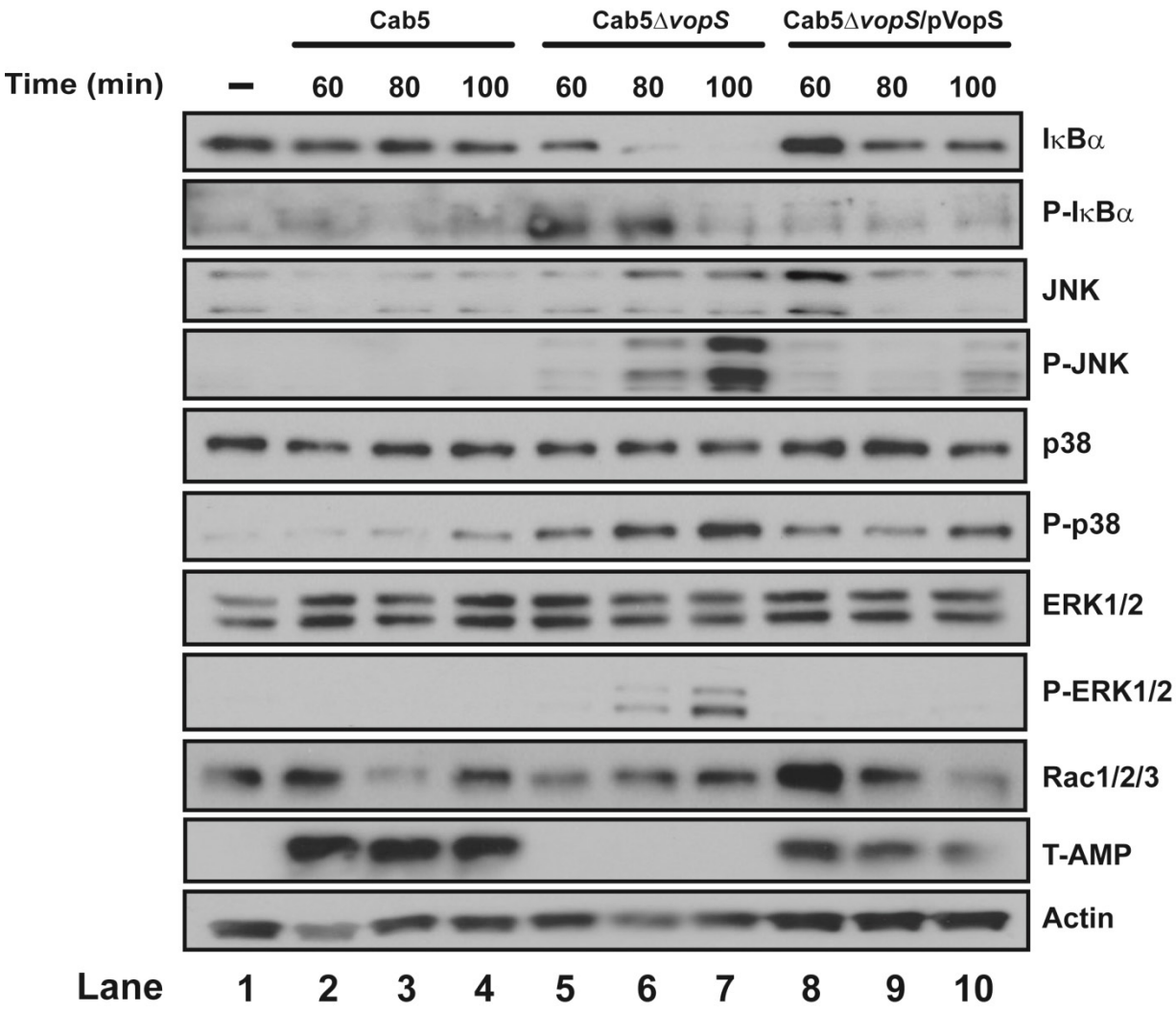

Figure 8. Phosphorylation events in NFkB, p38, JNK and Erk MAPK pathways are inhibited by VopS during infection. Phosphorylation and degradation of IκBα, Erk1/2 and JNK phosphorylation is blocked by VopS. HEK293T cells were infected at MOI=10 for the indicated times and cells were lysed and immunoblotted for phosphorylation and total protein levels. A representative experiment from three trials is presented.

To corroborate this observation, we performed anti-p65/RelA immunofluorescence of HEK293T cells infected with the CAB5 strain. After 2 hours of infection with this strain, only 18% of cells showed strong p65 nuclear localization (**Figure 9**). In contrast, greater than 95% of

cells infected with CAB5ΔvopS, which contains a further deletion for VopS, showed nuclear p65 localization. Complementation of this phenotype was observed in cells infected with the CAB5ΔvopS strain reconstituted for wild type VopS, CAB5ΔvopS/pVopS, with approximately 48% p65 translocation. Therefore, we observe p65 localization during infection in the absence of VopS and inhibition of this nuclear localization in the presence of VopS (**Figure 9**).

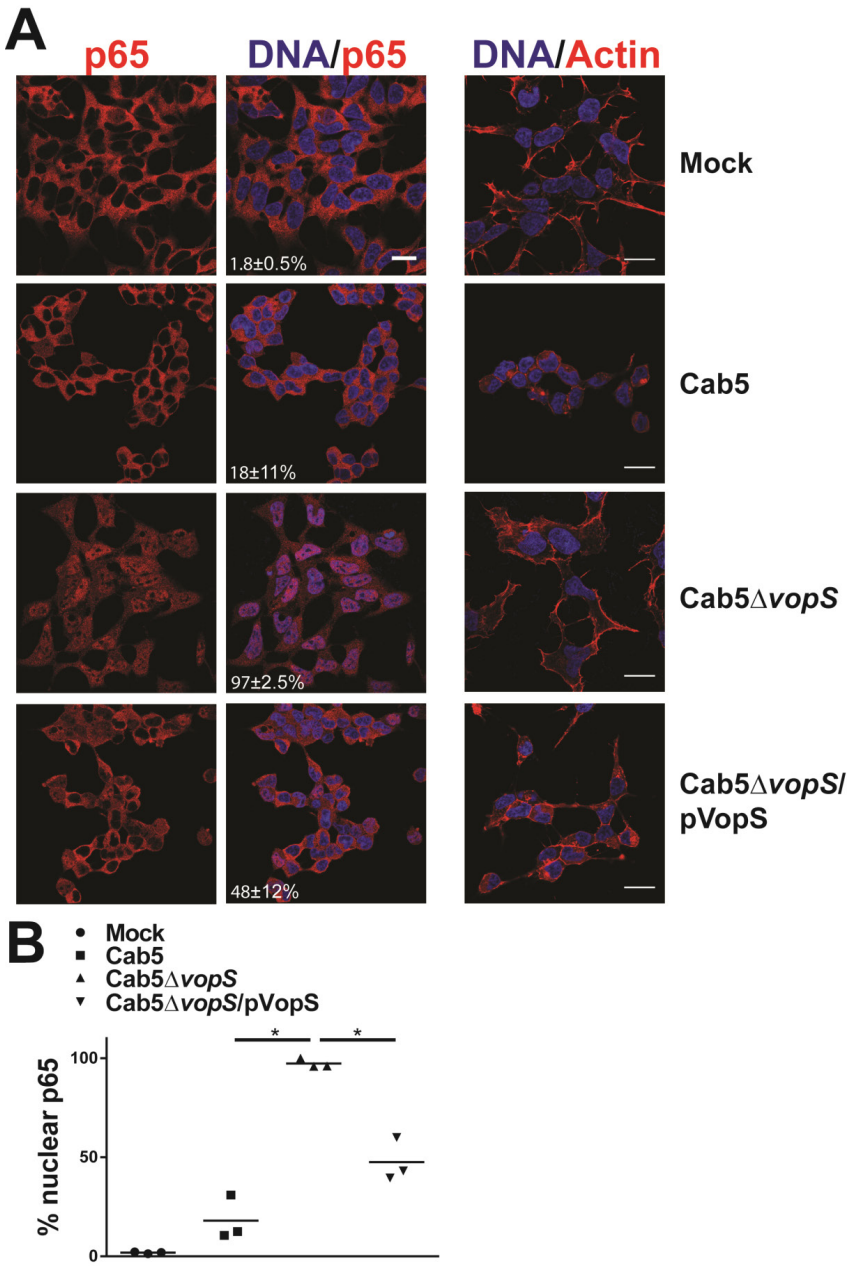

Figure 9. VopS blocks p65 nuclear translocation during infection. *A*. HEK293T cells were infected for 120 minutes with indicated strains at MOI=10 prior to fixation, permeabilization and immunofluorescence with p65 antibody (Santa Cruz) or staining with rhodamine-phalloidin. Mean percentages of cells that have nuclear p65 from 3 experiments are indicated. Error presented is standard deviation. DNA was visualized with Hoechst stain. Scale bar= 20 μm. *B*. The percentages of cells that have nuclear P65 are indicated. Cell counts are between 75-150 cells from multiple fields for each condition and experiment, in three separate experiments. Asterisk represents P value < 0.01 with two-tailed test.

The MAP kinases Erk, p38 and c-jun activated kinase (JNK) are commonly activated during infection, and along with NFκB share many upstream activators that can be activated by Rho GTPases [44]. Activation of these proteins is characterized by phosphorylation of their activation loops on their signature –TXY- motifs. With profiles similar to IκBα activation, we found that during infection with *V. parahaemolyticus* CAB5 and CAB5ΔvopS/pVopS, JNK and Erk activation was inhibited (**Figure 8**). p38 activation did not appear to be strongly affected by VopS, and the CAB5ΔvopS strain induced activation of all MAP kinases tested. This observation indicates that NFκB, Erk, p38 and JNK are activated during *V. parahaemolyticus* infection and that VopS disrupts an upstream activator of shared strongly by NFκB, Erk and JNK, but perhaps only moderately p38.

To test interactions of AMPylated and unAMPylated Rac1 in vitro, we generated His-Rac1-V12, a dominant active mutant, with and without the modification by coexpression with VopS or empty vector in *E. coli*. Rac-V12 co-expressed with VopS is insensitive to further AMPylation in a secondary AMPylation assay, indicating that nearly all of the protein is modified (**Figure 10A**). AMPylated Rac1 also showed no interaction with PAK, as demonstrated previously (**Figure 10B**) and is the likely cause of most signaling effects observed as this kinase is known to contribute to those pathways under certain conditions.

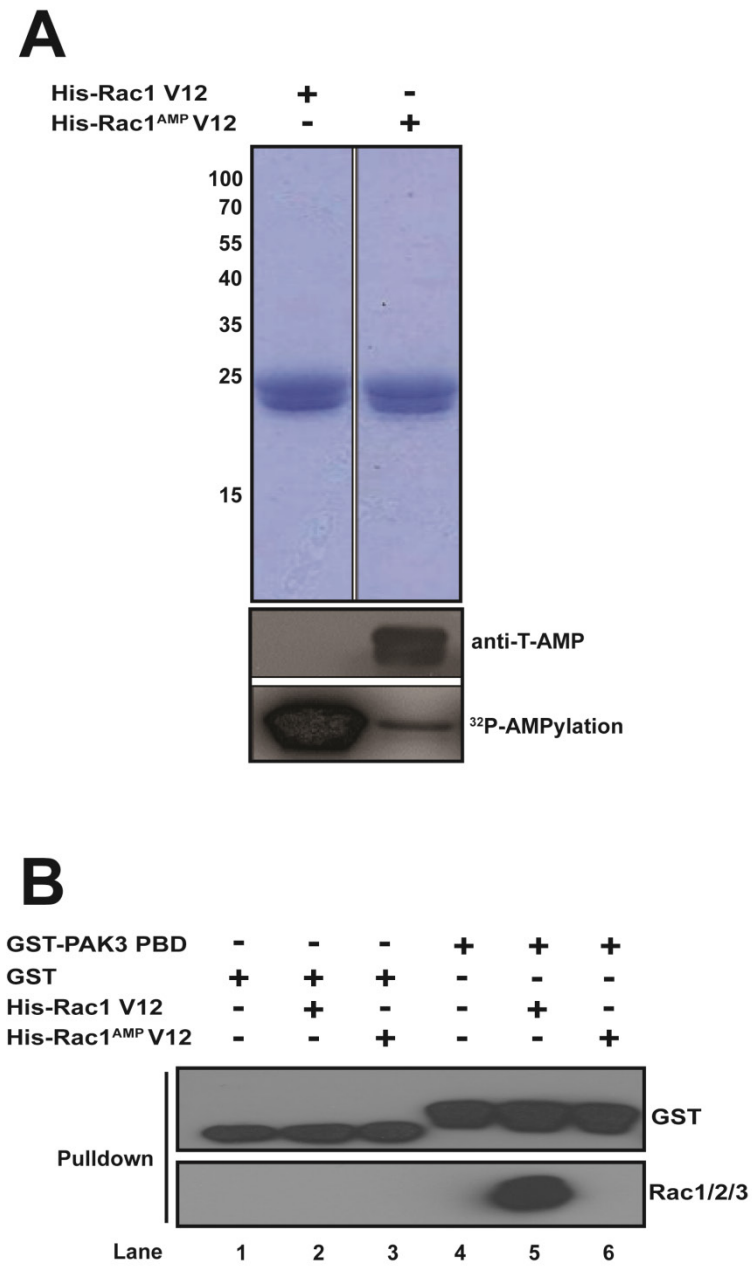

Figure 10. Purified, AMPylated Rac1 does not bind p21-activated kinase. Purification of AMPylated Rac1. His-Rac1 V12 proteins were expressed in Rosetta *E. coli* cells with empty vector (His-Rac1 V12) or GST-VopS (His-Rac1^{AMP} V12) and purified. His-Rac1^{AMP} V12 is richly AMPylated as seen with T-AMPylation antibody. A secondary VopS AMPylation assay of the proteins with ^{32}P-α-ATP shows that His-Rac1^{AMP} V12 cannot be AMPylated further, indicating >95% AMPylation from coexpression. *B*. AMPylated Rac1 does not bind PAK3. PD=pulldown, IB=immunoblot

Production of superoxide by Nox2 is inhibited by VopS

Microbial killing by lymphocytes is largely a function of phagocytosis followed by generation of reactive oxygen species (ROS) to kill the engulfed microbes [77]. The phagocytic NADPH oxidase (NOX2) complex, which is composed of at least 5 proteins, generates these superoxides at the site of engulfment, which activates proteolytic enzymes that mediate killing and immune signaling. The complex is composed of gp91, p22, p47, p67 and Rac1 or Rac2 [45]. Rac1/2 is essential for the function of the complex, as its activation, localization to the membrane and binding to p67 activates the complex. Accordingly, we hypothesized that AMPylation may inhibit superoxide generation by this complex, as the interaction between p67 and Rac1 could be disrupted. To test this we utilized the COSphox cell line, which is stably transfected with all required components of the NOX2 system mentioned above [78]. Superoxide generation was monitored by luminescence for 30 minutes using the Diogenes kit, and this cell based assay was validated by ensuring that generation of oxygen radicals upon stimulation with the NOX2 activator PMA could be inhibited with superoxide dismutase (**Figure 11**).

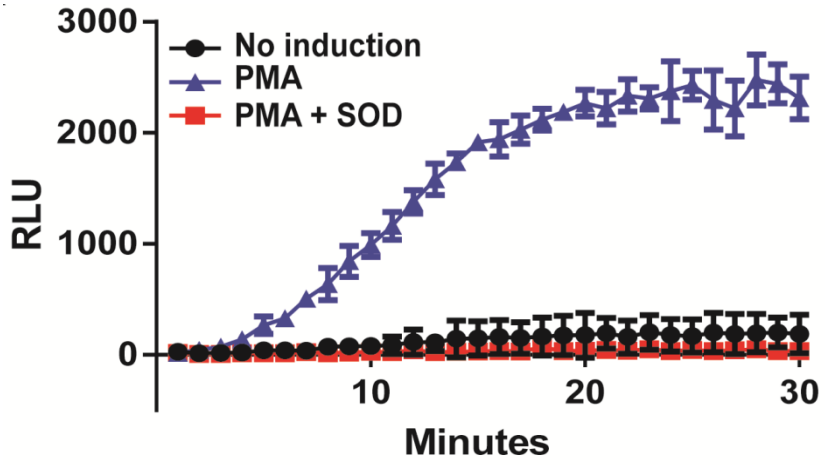

Figure 11. Validation of the NOX2 superoxide assay. COSphox cells stably transfected with gp91, p22, p47 and p67 were stimulated in triplicate by the addition of 2 μM PMA (blue). Cells were collected, induced with PMA for 5 minutes in 96 well plates, and production of superoxide was measured over 30 minutes using a plate reader. Addition of 50 U of SOD (red) completely inhibited the assay, demonstrating that the chemiluminescence is superoxide-dependent. Data points are the mean and error bars are standard deviation.

COSphox cells were then infected with *V. parahaemolyticus* strains for 2 hours, collected, and stimulated with PMA for 5 minutes before measurement. We found that cells infected with CAB5 reduced superoxide generation to levels similar to cells that were uninfected and uninduced (**Figure 12**). By contrast, cells infected with CAB5ΔvopS strain generated robust superoxide signal upon PMA stimulation. Similarly, infection with CAB5Δvops/pVopS-H348A strain containing a plasmid encoding the catalytically inactive VopS mutant H348A did not inhibit superoxide generation, while CAB5ΔvopS/pVopS strain reduced superoxide generation to levels similar to cells that were unstimulated (**Figure 12**). These results indicate that targeting of Rho GTPases by pathogens may allow them to avoid killing by lymphocytes. Interestingly, AMPylation of Rac1 appears to modestly but consistently reduce binding to the NOX2 subunit

p67 in a GST pulldown assay (**Figure 13**). This may indicate that AMPylation prevents the association of Rac proteins with the NOX2 complex.

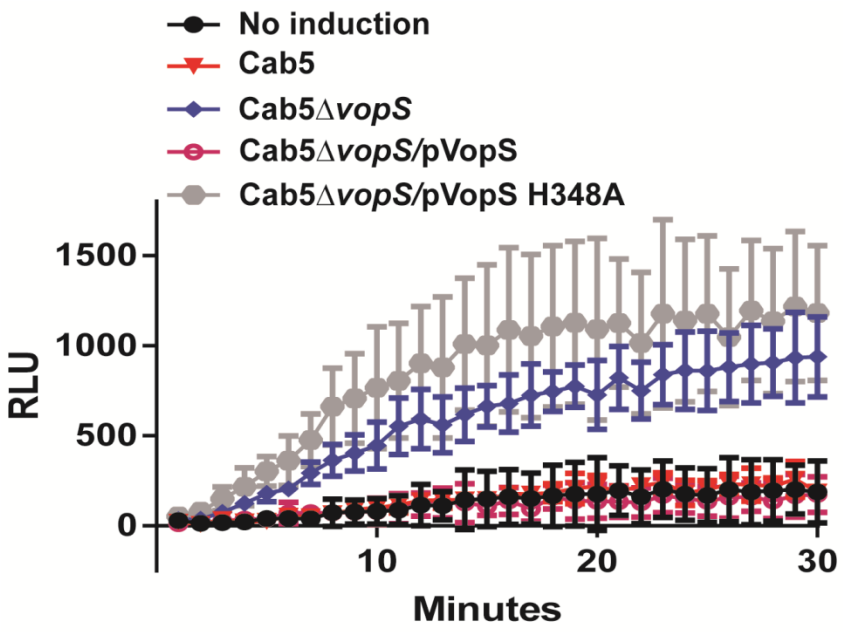

Figure 12. VopS blocks generation of superoxides during infection. VopS inhibits ROS produced by NOX2. Prior to stimulation with PMA, COSphox cells were infected in triplicate with the indicated strains at MOI 10 for 2 hours.

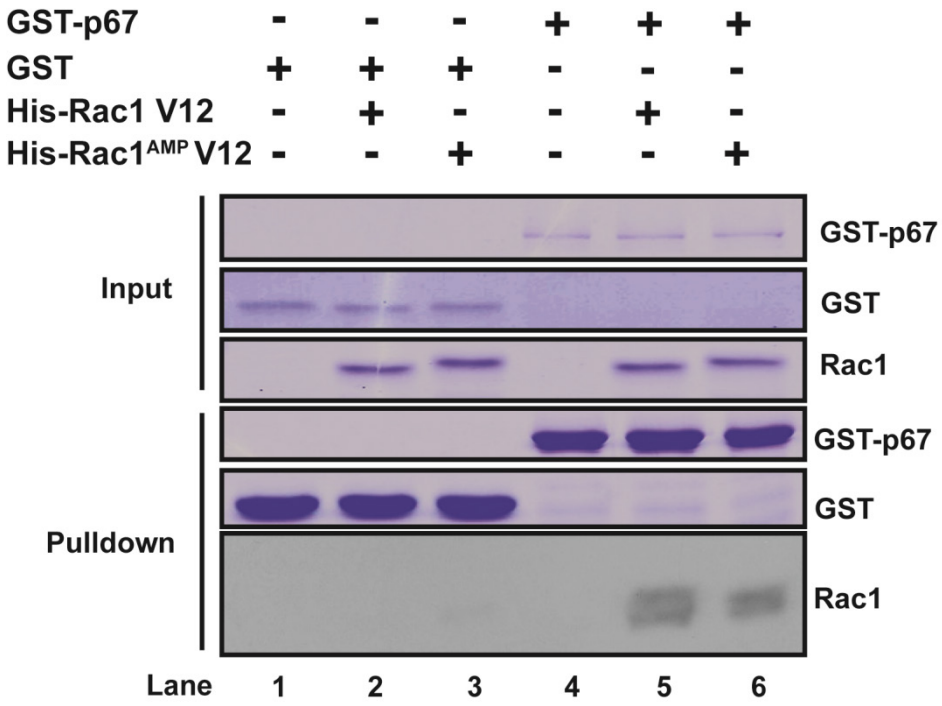

Figure 13. In vitro binding of Rac1 to p67phox is reduced by AMPylation. 25 ug His-Rac1 V12 proteins were incubated with glutathione beads loaded with 50 ug GST-p67 or GST for 2 hours at 4C. Beads were washed and co-eluting Rac1 proteins were observed by immunoblot with Rac antibody. GST-p67 showed a modest but consistent reduction in binding His-Rac1^{AMP}-V12 in comparison to His-Rac1-V12.

Binding of IAP proteins to Rho GTPases is blocked by AMPylation

IAP proteins are well studied factors in their inhibition of apoptosis and activation of NFκB, but the breadth of their involvement in these processes is not well understood. Their E3 ligase activity is important for this function, as ubiquitination of target substrate proteins is required to create necessary docking sites for interactions between proteins in the NFκB pathway, such as TRAF proteins [76]. Interestingly, IAPs were recently found to also be E3 ligases for Rac1 [75]. It is not known if the IAP-mediated ubiquitination of Rac proteins might play a role in infection and NFκB activation, or if it merely targets them for proteosomal degradation. GST fused cIAP

and XIAP were incubated with recombinantly purified His-Rac1-V12. Unmodified Rac1 bound readily to both cIAP and XIAP, but AMPylated His-Rac1-V12 did not bind either protein (**Figure 14**), demonstrating that AMPylation may disrupt this direct interaction.

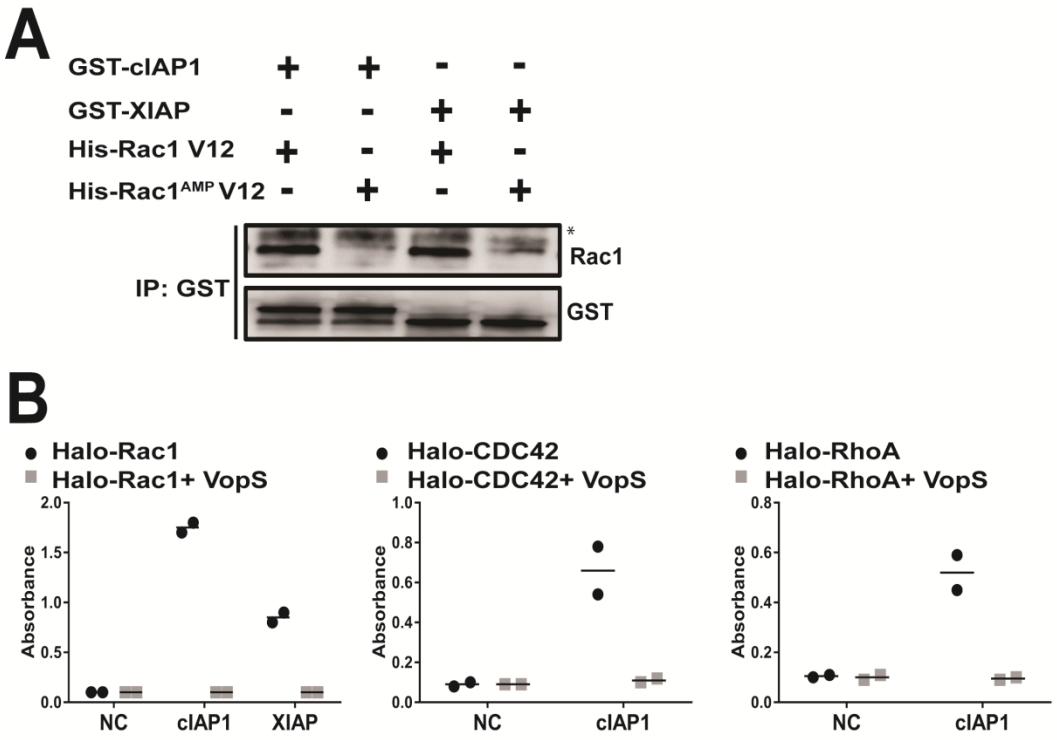

Figure 14. Rac1, CDC42 and RhoA bind to cIAP in vitro, but binding is blocked by AMPylation. AMPylation inhibits Rac1 binding to IAP proteins. IAP proteins expressed in human cell free lysates were incubated with recombinantly purified His-Rac1-V12 or His-Rac1^{AMP}-V12. IAP proteins were then immunoprecipitated with GST antibody and immunoblotted for interacting Rac1 protein with His antibody. *B*. UnAMPylated but not AMPylated CDC42, RhoA and Rac1 are binding partners of IAPs. IAP-GST proteins presented in wNAPPA format were incubated with Halo-Rac1, CDC42 or RhoA with and without the presence of 5ug of VopS. Binding was measured by fluorescein signal after incubation with fluorescein-conjugated Halo ligand. All GTPases were able bind cIAP, but addition of VopS abrogated binding. IP-immunoprecipitation. Asterisk-non-specific band.

This loss of interaction may explain another phenomenon observed during infections with *V. parahaemolyticus,* which is that Rho GTPase levels decrease at later times of infection. When HEK293T cells are infected with CAB5, which contains VopS, Rho and Rac levels remain relatively constant throughout the infection (**Figure 15**). However, during infection with CAB5ΔVopS, Rho and Rac levels decrease to considerably lower levels at 3 to 4 hours post infection. When this strain is complemented with VopS, GTPase levels again remain constant throughout the infection. The exact mechanism of this GTPase degradation that is disrupted by VopS is not a certainty, but the phenomenon coincides with the induction of the expression cIAP, which could be targeting it for degradation through ubiquitination.

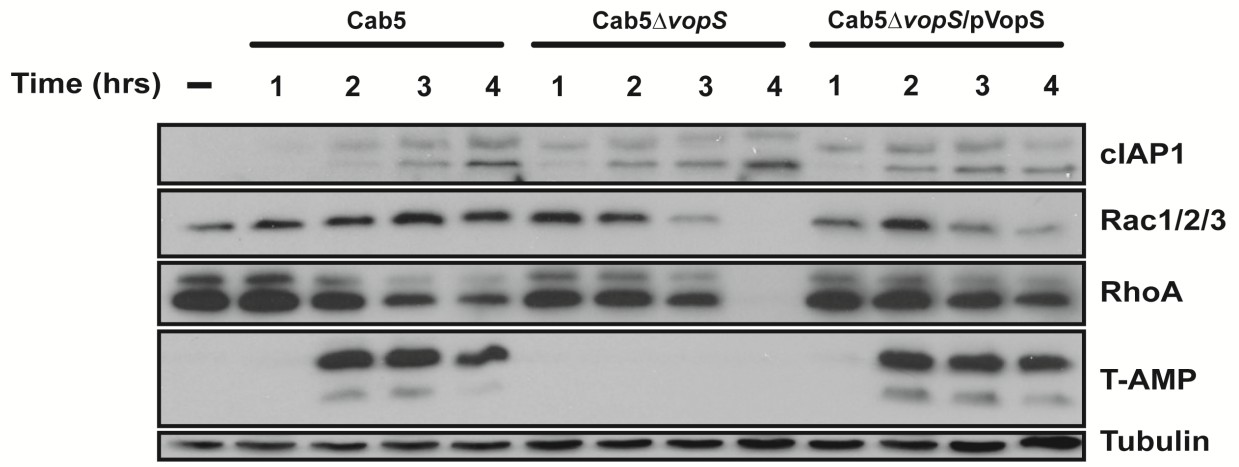

Figure 15. Rac and RhoA degradation is blocked during infection by VopS. VopS inhibits degradation of Rac1 and RhoA during infection. HEK293T cells were infected with indicated strains at MOI of 10 for the indicated times and cells were lysed and immunoblotted. Rac and RhoA protein levels were considerably higher at late time points in infection in the presence of VopS.

DISCUSSION

Bacterial pathogens and their multicellular hosts are involved in a molecular arms race that has stretched through the millennia. Host strategies to recognize and clear infections have appeared in many evolutionary conserved systems, including PRRs, adaptive immunity, and inflammatory responses. Pathogens are forced to evolve counterstrategies that can weaken or thwart these host responses, and they have found many critical nodes in signaling pathways to subvert for their own survival.

One of these nodes is the Rho family of GTPases. While the susceptibility of Rho GTPases in relation to their control of the actin cytoskeletal has been well documented, it is possible that the other functions of these proteins in host defense have been overlooked. Here, we sought to explore other potential effects of Rho GTPase targeting by a bacterial pathogen. Our findings suggest that targeting the Rho GTPases may provide some of the same NFκB and MAPK inhibition advantages as effectors that target the pathways directly.

We found that AMPylation by VopS inhibits activation of the NFκB pathway, measured by the phosphorylation state of the NFκB inhibitor IκBα and the nuclear translocation of p65. Activation of the MAP kinases JNK and Erk were also inhibited, but little change was observed in p38 phosphorylation. Loss of NFκB, Erk and JNK activation by VopS may be explained by the previous observation that AMPylation of Rho GTPases inhibits interaction with PAK (**Figure 10B**) which along with Rhotekin is known to signal through these pathways. However, the crosstalk in these immune sensing pathways is complex and not completely understood. For example, Rac1 is known to be involved in pathogen sensing by NOD1, and is also a substrate of

the NFκB mediator cIAP1. It is possible that AMPylation of Rho GTPases inhibits these pathways at multiple levels.

Other factors in the NFκB pathway that may be inhibited during *V. parahaemolyticus* infection are the IAP proteins. Ubiquitination by IAP proteins is known to be important for NF*κ*B activation, and Rac1 is a known substrate of these proteins. Cellular Rac and RhoA levels were observed to decrease during late stages of *V. parahaemolyticus* infection with a strain lacking VopS, whereas, the presence of VopS appeared to inhibit their degradation. In agreement, recombinant Rac1 AMPylated with VopS was unable to bind to this E3 ligase, which could explain the persistence of Rac1 levels in the presence of VopS. However, the importance of Rho GTPase ubiquitination by IAP proteins for NFκB activation has not been determined. The combination of NFκB inhibition and loss of IAP binding as a result of Rho GTPase AMPylation observed in this work indicates that IAP ubiquitination of Rho GTPases could be important for immune signaling and merits further study. Such ubiquitination could be a form of immune signaling, or it is also possible that the ability of the cell to turnover Rho GTPases is important. The accumulation of AMPylated and sterically blocked Rho GTPases in the cell is potentially deleterious. Interestingly, the region of Rho GTPases involved in binding IAP proteins is not known, but these results suggest that the switch-1 loop plays some role in the interaction, or AMPylation causes a conformational change that does not allow binding of the E3 ligases.

Perhaps the most direct and obviously beneficial effect of AMPylation by VopS is the inability of the phagocytic NADPH oxidase to be activated. This complex is essential for fighting bacterial pathogens, as patients deficient in any of the complex subunits suffer from

chronic granulomatous disease with recurrent and often deadly infections . Disabling this host weaponry by targeting the Rac GTPases offers bacteria a distinct survival advantage. As other bacterial effectors modify the switch-1 region of RhoGTPase, this may be an overlooked common mechanism used to disrupt the host cell activation of ROS.

The sum of the findings presented here indicates that the targeting of Rho family GTPases provides complex and multifaceted advantages for microbial pathogens, highlighting the status of Rho GTPases as an "Achilles' Heel" in host immunity (**Figure 16**) [79]. At least six different signaling functions mediated by Rho GTPases are sabotaged: collapse of the actin cytoskeleton, inactivation of NFκB, Erk and JNK pathways, lack of degradation of Rho GTPases, and lack of superoxides produced by the NOX2 complex. The critical nature of this modification is further supported by recent findings that cytosolic PRRs are dedicated to sensing both deactivated and over-activated versions of Rho GTPases. As other bacteria use virulence factors to inactivate Rho GTPases by modifying the switch-1 loop with a variety of post-translational modifications, the conserved mechanisms disrupted by VopS will likely be applicable for many other bacterial infection models. We have also identified other potential molecules affected by Rho GTPase AMPylation through two protein microarray screens, discussed in **Chapter Four**.

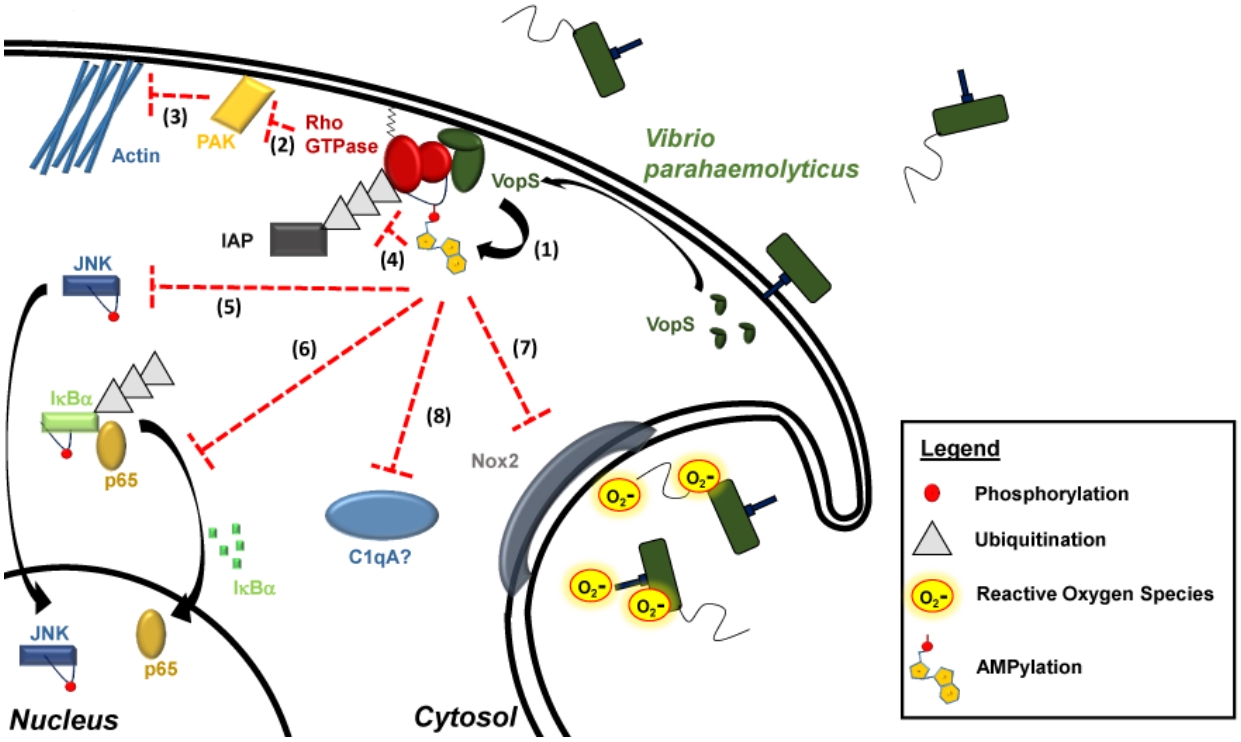

Figure 16. Expanding the understanding of cell signaling pathways inhibited by AMPylation. Upon translocation into the host cell, VopS localizes to the host membrane via its BPD and AMPylates Rho GTPases on their switch-1 loop **(1)**. AMPylation inhibits GTPase binding to PAK **(2)**, which compromises cell control of the actin cytoskeleton **(3)**. Binding of the E3 ligase to Rac1 is also inhibited, reducing ubiquitin mediated degradation **(4)**. Phosphorylation of JNK, Erk and IκBα are reduced by VopS **(5,6)**, as is degradation of IκBα and nuclear translocation of p65. Production of reactive oxygen species by the Nox2 complex is abrogated, likely promoting bacterial survival from lymphocytes **(7)**. Although the implications of the C1qA-Rac1 interaction are unknown, AMPylation blocked this interaction and could inhibit downstream signaling **(8)**.

CHAPTER FOUR

Newly developed Nucleic Acid programmable protein array screens reveal novel proteins affected by AMPylation

INTRODUCTION

Our understanding of the breadth of AMPylation substrates remains limited in scope. While we expanded our knowledge about the phenotype of infections involved AMPylation of Rho GTPases, including stress signaling inhibition and actin cytoskeleton collapse, which members of the Rho GTPase family can be targeted is not known. It is also possible that VopS and other Fic proteins target additional unknown proteins in the host cell milieu. Additionally, candidate substrates for the human Fic protein, FicD/HYPE, remain a subject of intense interest.

In an attempt to address these questions, we chose to collaborate with the lab of Joshua LaBaer at the University of Arizona State, who is a specialist in Nucleic Acid Programmable Protein Arrays (NAPPA). NAPPA is perhaps the most advanced of the current cell-free protein array technologies that have been developed over the past decade [80]. Cell-free arrays do not require protein purification and provide rapid a approach for fabricating protein arrays in terms of cost, shelf life, and storage [81]. In these arrays, a nucleotide template is printed on the slide and used to produce proteins with a cell-free expression systems derived from *E.coli*, wheat germ and rabbit reticulocyte lysate. These proteins can be engineered to contain fusion tags that enable their capture to the array surface with an appropriate agent allowing the NAPPA to produce both high-density and high

content slides (~2,300 – 8000 proteins) [82]. In NAPPA, plasmid-based cDNAs configured including an epitope tag are printed on a microscope slide along with the corresponding tag-specific binding reagent, such as an anti-tag antibody. At the time of experimentation, the cDNA is transcribed and translated into recombinant protein and captured/displayed in situ by the binding reagent. Using a rabbit reticulocyte lysate-based cell-free expression system, NAPPA has been applied towards the identification of novel protein-protein interactions and disease-related antibody biomarkers [83]. However, cell-free protein arrays have yet to be employed in the study of post-translational modification, the primary subject of this chapter.

In this work, we established a novel, non-radioactive unbiased AMPylation screening platform by developing a novel click chemistry-based detection assay for use on high-density cell-free protein microarrays displaying human proteins [84]. Using this technology, we were able to confirm that VopS and another Fic protein, IbpA Fic2, are capable of modifying the entire Rho GTPase family and also modified multiple additional potential substrates, though these are low confidence. We also used NAPPA to perform a Rac1 interaction screen, in which we identified two novel Rac interactions that could be disrupted by AMPylation [79].

We screened 10,000 human proteins with two bacterial pathogen AMPylators, VopS and IbpAFic2, identifying more than twenty new substrates each. Two novel Rho GTPases (Rac2 and Rac3) were validated in vivo as substrates of the virulence factor VopS in HEK293T cells during *V. parahaemolyticus* infection. Using mass spectrometry, we verified that a non-GTPase protein, ARHGDIB/LyGDI, was AMPylated by VopS on its threonine 51, which is located in a highly regulated part of this protein. This modification inhibited phosphorylation of LyGDI by Src kinase in vitro. Finally, the identification of these new

targets allowed us to build the first bacteria-host interaction AMPylation network revealing signaling interactions that could potentially be important for bacterial pathogenesis in the future functional studies.

RESULTS

AMPylation of Rho GTPases on NAPPA array

Purified and active VopS and IbpA were used with the NAPPA array for an AMPylation screen by Xiaobo Yu in the LaBaer lab (**Figure 17**). This venture was successful due to the availability of an alkyne-modified ATP molecule allowing it to be modified with fluorophores or affinity tags [18]. Labeling AMP-modified substrates covalently with a fluorophore and the use of human ribosomal machinery and chaperones to produce proteins resulted in a much higher sensitivity and signal to noise (R/N) ratio compared with previous studies. Xiaobo screened 10,000 human proteins with both VopS and IbpAFic2, identifying the entire RhoGTPase family as substrates and more than twenty new, low-confidence substrates (**Figure 18, Table 5**).

Normalized signals showing a 1.2 fold increase over the buffer-only control were considered positive. Only the substrates showing a positive ratio in all three experiments on different days were selected as final candidates. With these criteria, a total of 20 and 21 substrates for VopS and IbpAFic2 were discovered from the screening, respectively (Table x). The annotations showed that many of the VopS and IbpAFic2 substrates were RhoGTPases, 8 and 7, respectively. In addition, we found dozens of novel potential non-GTPase substrate proteins.

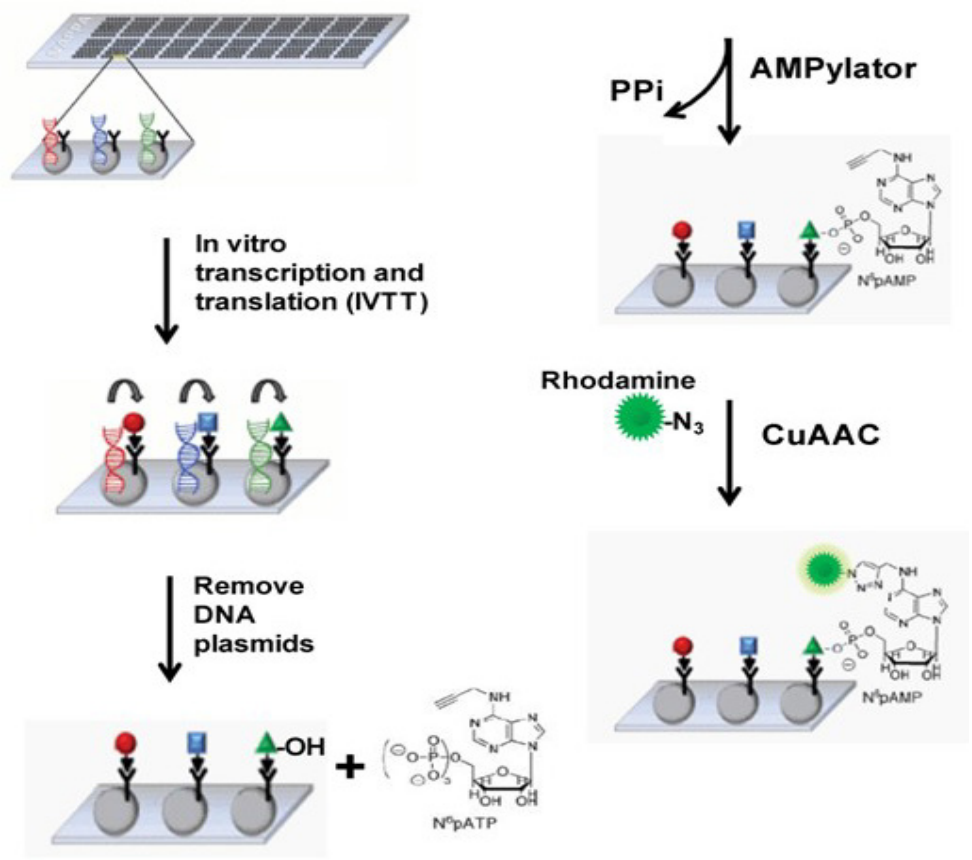

Figure 17. Development of the NAPPA AMPylation assay. The principle of AMPylation assay on NAPPA arrays. Expression plasmids are printed on slides, followed by expression of proteins with IVTT lysate. After removal of DNA, click AMPylation assay is performed and slides are scanned for AMPylated proteins.

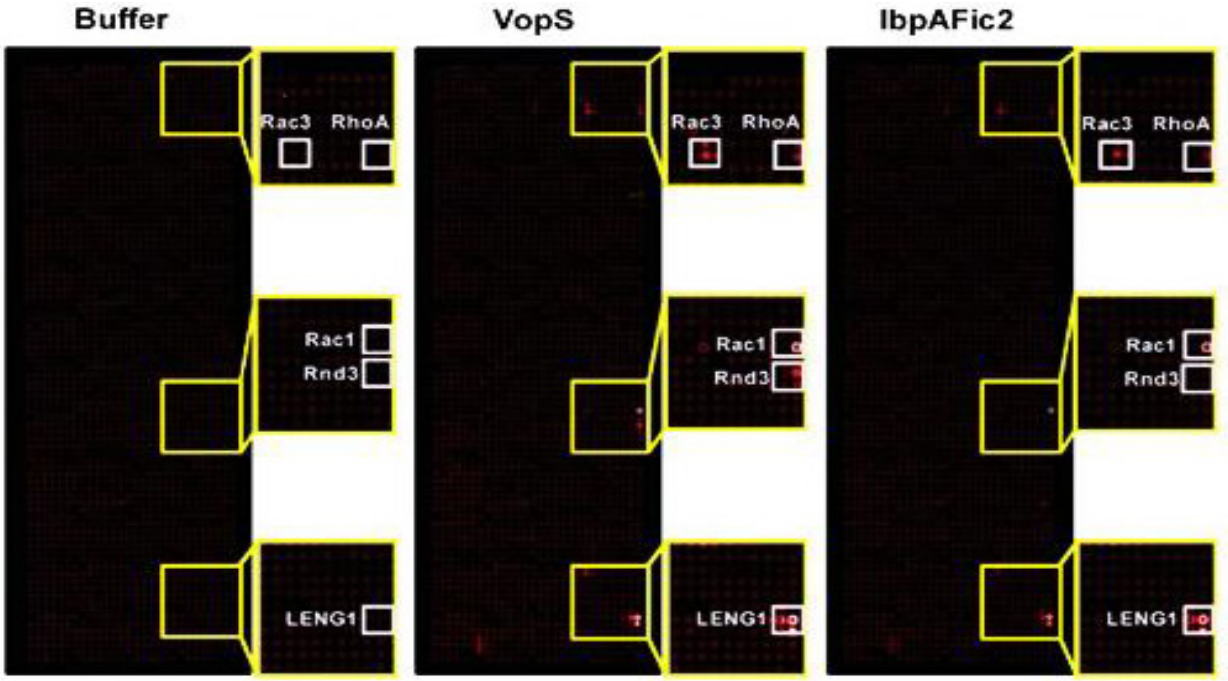

Figure 18. VopS and IbpA activity on the NAPPA array. Representative NAPPA fluorescent images show human targets with strong fluorescent signals from VopS and IbpA AMPylation.

Sequence alignment of all eight GTPases identified as targets for IbpAFic2 and VopS in the NAPPA screening revealed a highly conserved motif of YxPTVF (**Table 6**). A motif scan using ScanProsite (http://prosite.expasy.org/scanprosite/) identified seven more proteins with this motif, including six GTPases and a non-GTPase, ERGIC2. Xiaobo Yu confirmed that every member of the Rho GTPase family could be AMPylated in vitro by both VopS and IbpAFic2.

To determine if this substrate flexibility of VopS might be possible during an infection, we transiently expressed Rac1, Rac2 and Rac3 in HEK293T cells, followed by infection with *V. pararahaemolyticus* and immunoprecipitation of the target substrate (**Figure 19**). Using a strain that expresses and secretes VopS as the only known T3SS

effector (CAB5), we found that VopS AMPylated the known substrate Rac1 and two new GTPases, Rac2, and Rac3 (**Figure 19**). This indicates that VopS can AMPylate most Rho GTPase family members during infection and can serve as a general inhibitor of all Rho GTPase activity. We also tested AMPylation of three in vitro confirmed non-GTPase substrates (LyGDI, LC3 and LENG1) in vivo, but did not observe the modification when transfected cells were infected under these conditions. The inability to detect AMPylation of these substrates may be because the modification is transient or is prevented by another PTMs (such as phosphorylation). Alternatively, we may have failed to evaluate the cells at the relevant time or condition to detect this modification. As a result, we sought to confirm a non-GTPase substrate and elucidate the effect of AMPylation on its potential function in vitro.

No.	Name	Motif IbpA *  VopS *						VopS	IbpAFic2
1	Cdc42	Y	v	P	T	V	F	NAPPA	NAPPA
2	Rac1	Y	i	P	T	V	F	NAPPA	NAPPA
3	RhoA	Y	v	P	T	V	F	NAPPA	NAPPA
4	Rac2	Y	i	P	T	V	F	NAPPA	NAPPA
5	Rac3	Y	i	P	T	V	F	NAPPA	NAPPA
6	RhoB	Y	v	P	T	V	F	NAPPA	NAPPA
7	RhoC	Y	v	P	T	V	F	NAPPA	NAPPA
8	Rnd3	Y	v	P	T	V	F	NAPPA	Prediction*
9	RhoD	Y	t	P	T	V	F	Prediction*	Prediction*
10	RhoG	Y	i	P	T	V	F	Prediction*	Prediction*
11	RhoJ	Y	v	P	T	V	F	Prediction*	Prediction*
12	RhoQ	Y	v	P	T	V	F	Prediction	Prediction
13	Rnd1	Y	v	P	T	V	F	Prediction	Prediction
14	Rnd2	Y	v	P	T	V	F	Prediction	Prediction
15	ERGIC2	Y	e	P	T	V	F	Prediction	Prediction

Table 5. VopS and IpbA AMPylate the entire Rho GTPase family, revealing a recognition motif. The NAPPA array and subsequent validation experiments reveal that VopS and IbpA can AMPylate the entire Rho GTPase family by recognizing the peptide sequence YxPTVF.

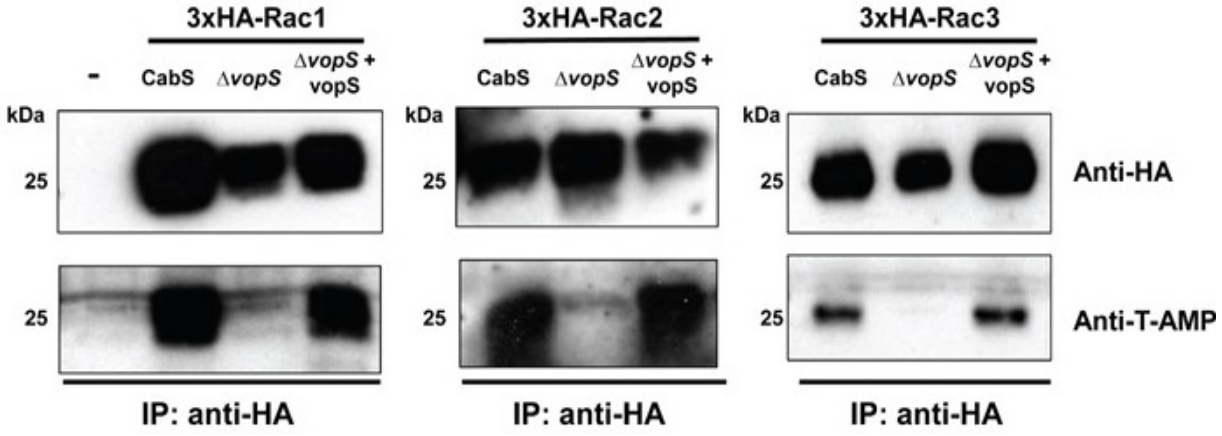

Figure 19. VopS AMPylates Rac1, Rac2 and Rac3 during infection. Transfected 3xHA tagged Rac1, Rac2 and Rac3 were immunoprecipitated from HEK293T cells infected with Cab5, Cab5Δ*vopS* or Cab5Δ*vopS*/pVopS cells and immunoblotted for AMPylation.

Characterization of LyGDI AMPylation

ARHGDIB/LyGDI (LyGDI) was chosen for further study because it represents a new class of substrate that nevertheless plays important roles in GTPase regulation for innate immunity, including T-cell activation, phagocytosis of bacteria by macrophages, and reactive oxygen species production for microbial killing [85]. LyGDI is primarily expressed in hematopoietic cells and some cancers, and belongs to the RhoGDI family of which there are three members: ARHGDIA/RhoGDI, LyGDI and ARHGDIG/RhoGDI3. Unlike the GTPase substrates, LyGDI does not have a YxPTVF motif, suggesting that if LyGDI were AMPylated, modification must occur at a novel recognition sequence.

To test these non-GTPase substrates for VopS modification, I co-expressed either LyGDI or RhoGDI with VopS. These purified proteins were sent the UTSW proteomics core for total mass analysis to test for AMPylation. Comparison of the apparent mass of His-

LyGDI co-expressed with GST-VopS revealed the appearance of a protein population with an increase in molecular weight of 328-329 Daltons over the LyGDI coexpressed with empty vector, which is indicative of a protein modified with AMP (**Figure 20**).

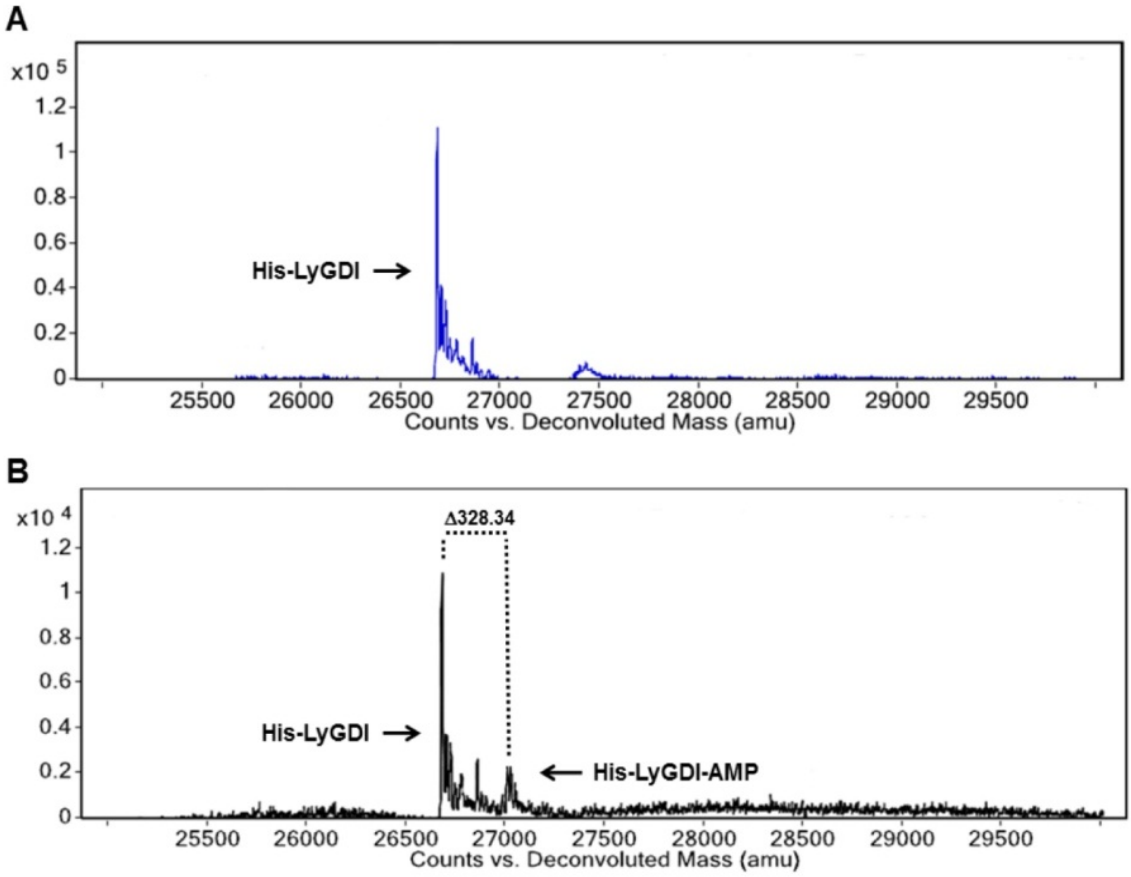

Figure 20. Total mass of LyGDI expressed alone or with VopS shows partial AMPylation. *(A)* and *(B)* are the co-expression of His-LyGDI protein with empty vector and GST-VopS ND30, respectively, which was run on an Agilent 6540 UHD Accurate-Mass QTOF machine and a partial mass shift of 328.34 daltons was observed.

To identify the AMPylated residue(s) on LyGDI, I again collaborated with the UTSW proteomics core to use LC-MS/MS, as previously described. Only one residue, threonine 51,

was identified in the peptide T51LLGDGPVVTDPK63 to be modified with AMP (**Figure 21**). Analysis of the reporter ions eliminated threonine 60 as the possible site for AMPylation.

T(+329.05)LLGDGPVVTDPK
1 x Phosphoadenosine (T)
Charge: 2, Exp. m/z: 820.887, Calc. m/z: 820.887

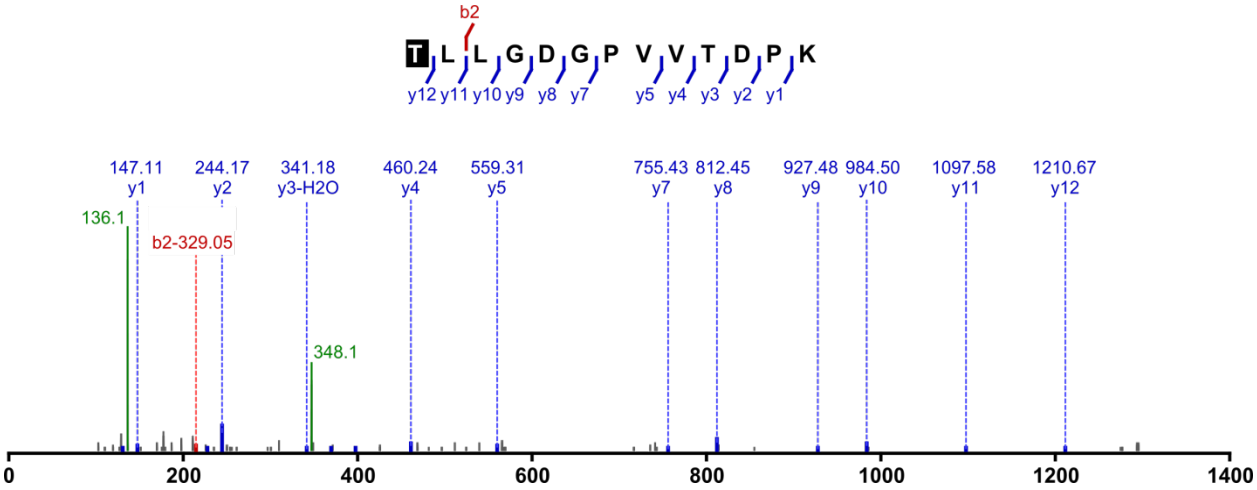

Key:	m/z out of range of spectrum	matched c-term ion	unmatched c-term ion	matched n-term ion	unmatched n-term ion

		a	b	b-18.01	b-329.05	y	y-17.03	y-18.01	y (2+)	y-17.03 (2+)	y-18.01 (2+)		
T	1											13	T
L	2	516.20	544.19	526.18	215.14	1210.67	1193.64	1192.66	605.84	597.32	596.83	12	L
L	3		657.28	639.27	328.22	1097.58	1080.56	1079.57	549.30	540.78	540.29	11	L
G	4		714.30	696.29	385.24	984.50	967.47	966.49	492.75	484.24	483.75	10	G
D	5		829.32	811.31	500.27	927.48	910.45	909.47	464.24	455.73	455.24	9	D
G	6		886.35	868.34	557.29	812.45	795.42	794.44	406.73	398.22	397.72	8	G
P	7		983.40	965.39	654.35	755.43	738.40	737.42	378.22	369.71	369.21	7	P
V	8		1082.47	1064.46	753.41	658.38	641.35	640.37	329.69	321.18	320.69	6	V
V	9		1181.54	1163.53	852.48	559.31	542.28	541.30	280.16	271.64	271.15	5	V
T	10		1282.58	1264.57	953.53	460.24	443.21	442.23	230.62	222.11	221.62	4	T
D	11		1397.61	1379.60	1068.56	359.19	342.17	341.18	180.10	171.59	171.09	3	D
P	12		1494.66	1476.65	1165.61	244.17	227.14		122.59	114.07		2	P
K	13					147.11	130.09		74.06	65.55		1	K

Figure 21. LC-MS/MS reveals LyGDI is AMPylated on threonine 51. LS-MS/MS analysis of recombinantly purified, AMPylated LyGDI protein was performed on a Q Exactive mass spectrometer after tryptic digestion and spectra were examined manually for phosphoadenosine. Ions characteristic of phosphoadenosine (136.1 and 348.1, green) were observed, and y and b-series fragment ions identify threonine 51 as the site of AMPylation. Greater than 97% sequence coverage of LyGDI was achieved, with 30 Threonine 51-AMPylated peptides identified.

To confirm these mass spectrometry findings, I analyzed RhoGDI and LyGDI with antibodies that recognize AMPylated threonine (T-AMP) or tyrosine (Y-AMP). I observed that purified His-LyGDI co-expressed with VopS, but not empty vector, was strongly recognized by the T-AMP antibody (**Figure 22**). Interestingly, despite strong homology between the RhoGDI family members, RhoGDI was not AMPylated by VopS. Mutation of threonine 51 to alanine in LyGDI abrogated its AMPylation, demonstrating that threonine 51 is a specific AMPylation site (**Figure 22**). The targeting of this specific residue in LyGDI is reminiscent of the way in which VopS precisely targets the threonine in the Switch I region of Rho GTPases to inhibit their interaction with downstream effectors.

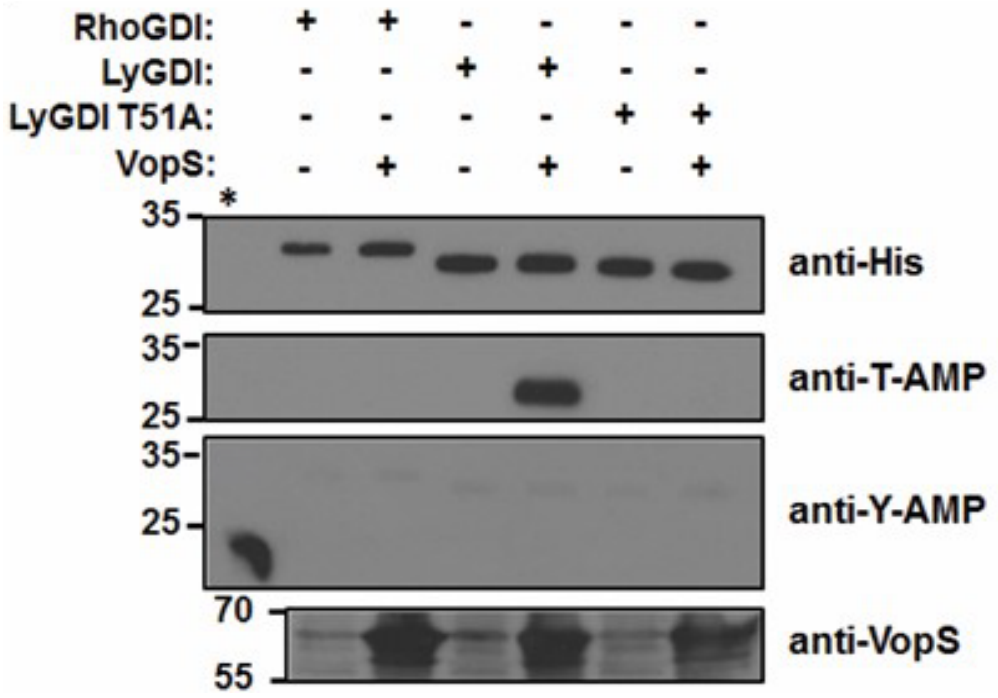

Figure 22. Threonine 51 is the single site of AMPylation on threonine 51. His-RhoGDI and His-LyGDI proteins were expressed in *E. coli* with GST-NΔ30VopS or empty vector and blotted for total protein (anti-His), threonine AMPylation (anti-T-AMP), tyrosine AMPylation (anti-Y-AMP), and VopS expression (anti-VopS, total lysate). Lane 1 (*) is tyrosine AMPylated Cdc42.

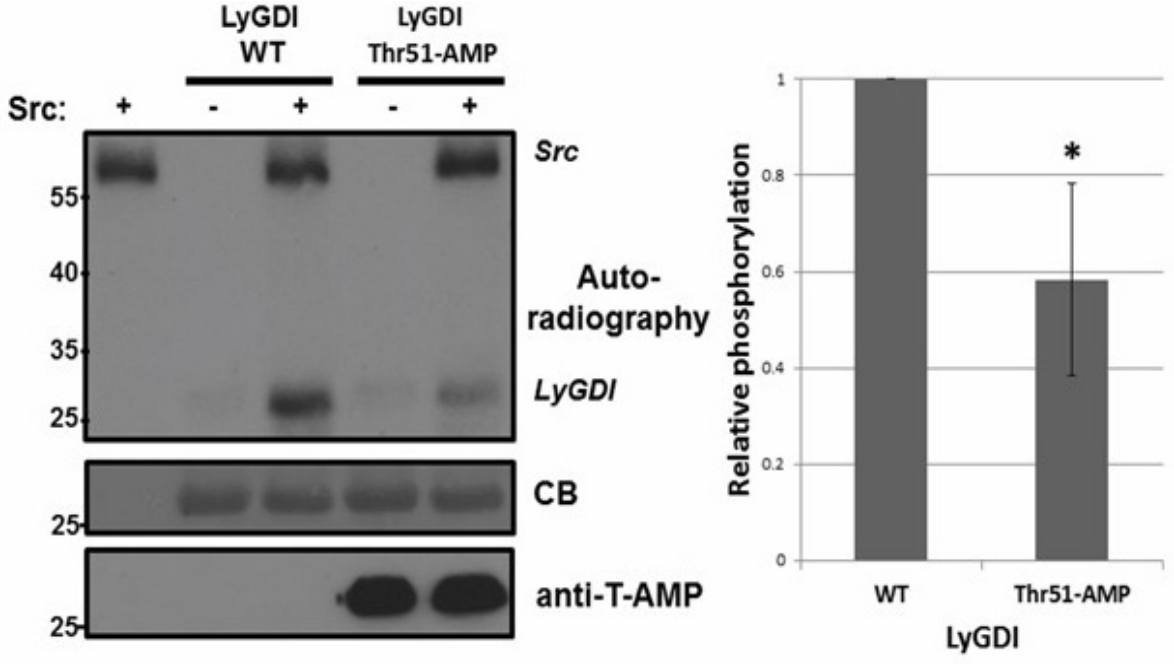

Figure 23. AMPylation of LyGDI inhibits phosphorylation by Src. AMPylated or unAMPylated LyGDI incubated with Src kinase, 100 μM ATP and 5 μCi [γ-32P] ATP for 45 minutes. CB, coomassie staining. (C) Relative phosphorylation of AMPylated vs. unAMPylated LyGDI over three experiments. P= 0.034.

Sequence analysis of RhoGDIs reveals that the site of AMPylation is present only in LyGDI, not RhoGDI or RhoGDI3, explaining its specificity (**Figure 22**). Interestingly, the site of AMPylation of LyGDI by VopS is located in an N-terminal alpha helix that neighbors the location of several PTMs, including phosphorylation by Src kinase [86, 87]. The diversity of regulation on and around the N-terminal helical region of LyGDI presents multiple avenues by which AMPylation by VopS could disrupt its function.

Inhibition of Src phosphorylation of LyGDI by VopS AMPylation

To test if AMPylation by VopS might have potential as a competitive PTM, we assessed the ability of AMPylated LyGDI to be phosphorylated by Src. We observed that unmodified LyGDI is readily phosphorylated by Src, but LyGDI previously AMPylated by VopS is phosphorylated at a significantly lower (58%) level than unmodified LyGDI (**Figure 23**), indicating that AMPylation of LyGDI may be competitive with Src phosphorylation and potentially other sites of modification in the N-terminus of LyGDI. A complete loss of phosphorylation was not expected, as the previous total mass analysis of of AMPylated-LyGDI showed a mixed population of modified and unmodified LyGDI, although the relative amounts cannot be deduced from unquantitative mass spectrometry (**Figure 20**). It is possible but not certain the portion resistant to Src phosphorylation also represents the portion of AMPylated LyGDI.

AMPylation of LyGDI during an infection was not observed in preliminary experiments, but further studies will be required to rule it out as a naturally occurring modification. Nevertheless, the ability of this in vitro AMPylation to compete with naturally occurring PTMs presents a tool to understand the regulation of this protein in processes like immunity and cancer.

Rac interaction screen reveals novel interactors

We further hypothesized that there may be additional unknown roles of Rho GTPases that might be disrupted by switch-1 modification. To screen for potentially novel interactions that could be blocked by AMPylation, we utilized a second type of NAPPA, a protein interaction screen [88]. To probe for novel Rac1 interactions, we expressed a Halo-Rac1 fusion using a human cell-free expression system. Lysates containing GTP-loaded Halo-Rac1 or Halo alone were incubated overnight with NAPPA slides presenting more than 10,000 unique proteins, followed by washing and labeling with Halo-ligand fused to alexa660 (**Figure 24A,B**).

As expected, known interactors such as PAK6, cIAP1/BIRC2 and XIAP/BIRC4 gave positive signals (**Figure 24C**). Additionally, a few potentially novel interactors were observed, including another Rho GTPase, RhoB and the complement subunit C1qA (**Figure 24C**). C1qA is the first component of the serum complement system, a secreted ligand binding factor that bridges the innate and adaptive immune systems .

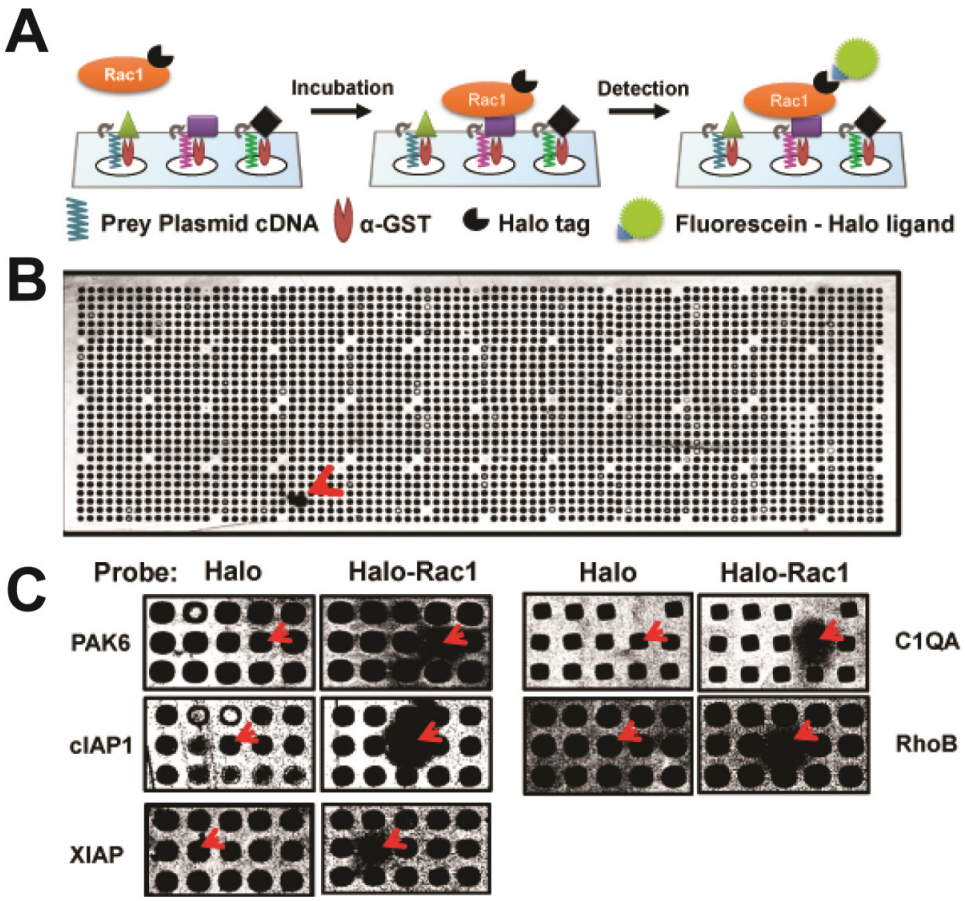

Figure 24. Rac interaction screen reveals C1qA and RhoB as novel interactors. NAPPA slides were incubated with Halo alone or Halo-Rac1 fusion protein. After washing, bound Halo-Rac1 was conjugated to Fluorescein using Halo ligand and slides were scanned. *B*. A representative NAPPA slide. Red arrowhead=bound Halo-Rac1. *C*. Rac1 binds multiple proteins in NAPPA screen. Enhanced view of spots with bound Halo-Rac1. Arrowheads indicate spot representing labeled prey gene.

AMPylation of Rac inhibits interaction with C1qA and RhoB

We next sought to test if AMPylation of the switch-1 loop might disrupt any of these novel interactions and used an in vitro binding assay to test for disrupted interactions. Interestingly, the novel interactors RhoB and C1qA were able to bind Rac1 in the absence but not the presence of VopS (**Figure 25A**). This observation was further confirmed in an immunoprecipitation experiment in which recombinantly AMPylated Rac1 was unable to bind either GST fused RhoB or C1qA (**Figure 25B**). These results support the conjecture that Rac1 mediates additional unknown function(s) in innate immunity by binding to C1qA and Rho proteins and these interactions are inhibited by modification of the switch-1 loop on Rho GTPases.

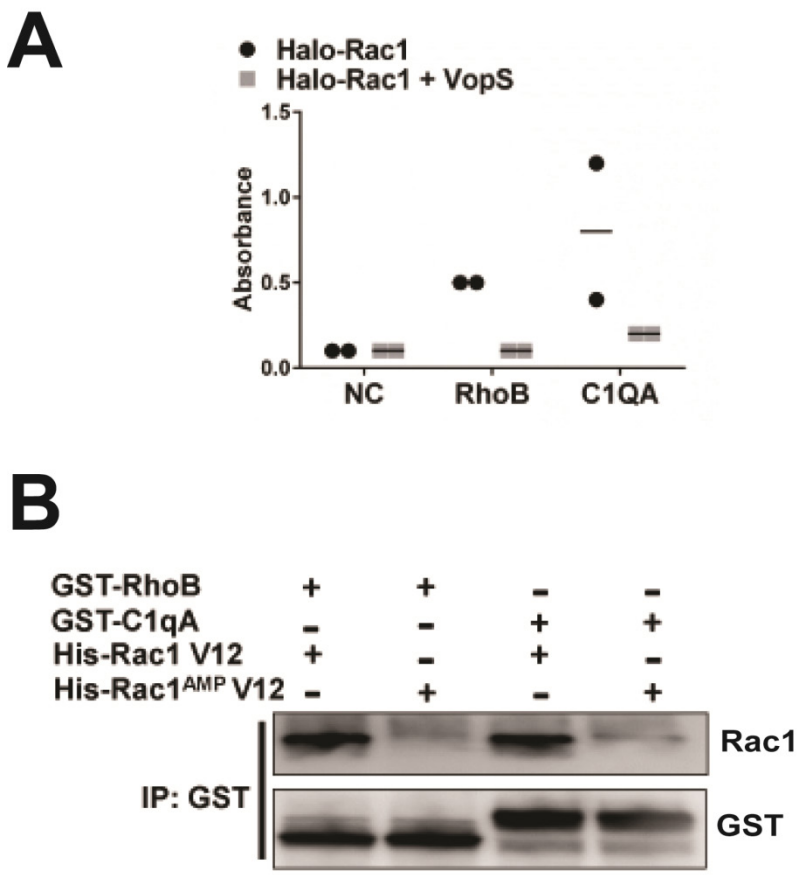

Figure 25. AMPylation of Rac1 blocks binding to C1qA and RhoB. A. VopS inhibits binding of C1qA and RhoB to Rac1. Indicated prey plasmids were printed in a 96 well ELISA plate coated with anti-GST antibody prior to cell free expression. Plates were then incubated with Halo-Rac1 with or without the addition of 5 ug VopS, washed, and conjugated with Fluorescein-Halo ligand before analysis. Addition of VopS inhibited interaction of each of the prey with Halo-Rac1. B. AMPylated Rac1 does not bind C1qA or RhoB. C1qA and RhoB proteins expressed in human cell free lysates were incubated with recombinantly purified His-Rac1 V12 or His-Rac1AMP V12. GST-fused proteins were then immunoprecipitated with GST antibody and immunoblotted for interacting Rac1 protein with His antibody. IP=immunoprecipitation, IB=immunoblot

DISCUSSION

Our collaboration with Joshua LaBaer and Xiaobo Yu was very fruitful in establishing new technologies for the study of AMPylation and other post-translational modifications. The development of this high throughput screening method could lead to discoveries with any type of modification that has a suitable reporter for use with the NAPPA array. The NAPPA AMPylation screen and further validation confirmed that the entire Rho GTPase family are likely targets of bacterial AMPylators. We also found that LyGDI can be AMPylated in vitro, determined the site of modification and showed that AMPylation can be a competitive modification with phosphorylation by Src kinase. Further work will be required to establish if LyGDI can be AMPylated in vivo.

Our NAPPA interaction screen has also revealed another potential role of Rac1 in innate immunity, which is the binding of C1qA. As part of the large, secreted complement complex, C1qA makes little sense as a signaling partner of Rac1, but recent research has revealed that C1qA also plays a key cytosolic role in innate immunity [89]. C1qA was shown to enhance the retinoic acid-inducible gene-I-like receptor (RLR) pathway through the binding of several cytosolic factors, leading to reduced viral replication [89]. However, little else is known about the cytosolic role of C1qA, particularly in regards to bacterial infection. It is possible that binding to Rac1 is important for an undiscovered function of C1qA in the innate immune system. Considering that at least two PRRs for altered Rho GTPases exist in the cell, it is possible that binding of C1qA to Rac1 is important for one of these processes. We observed that AMPylation disrupts this interaction, which may serve to inhibit or promote the activation of downstream signaling. Dimerization of Rho GTPase proteins have

been previously observed, but the full implication of these and potential Rac1 and Rho heterodimers identified in this screen are not fully understood [90]. This NAPPA interaction system can also be used in the future to screen for Rac1 and other Rho GTPase interactions against a larger pool of proteins to identify novel binding partners and possible activities.

CHAPTER FIVE

The human Fic protein is induced during endoplasmic reticulum stress and can AMPylate the chaperone protein BiP/GRP78

INTRODUCTION

While significant success has been achieved in deciphering the activities, targets and functional consequences of AMPylation by bacterial Fic proteins, the human Fic protein FicD/HYPE remains enigmatic. Studies with toxins have the benefit of uncontrolled, robust activity resulting in dramatic phenotypes in cells, such as the collapse of the actin cytoskeletal by VopS. These features are a great boon when attempting to identify potential targets and pathways in which the protein may be involved, and stem from the fact that toxins and effectors are essentially unregulated signaling agents working inside the host cell to cause a change during an infection. The complexity of metazoan biology, on the other hand, often requires multiple modes of regulation for any given signaling pathway. The activity of such proteins can be regulated in cis, within the protein itself, or in trans by other proteins and factors inside the cell.

Such complications are the likely reason that little is still known about the function of the metazoan Fic-domain containing protein FicD. Potential examples of in cis and in trans regulation can be found when studying the topology of FicD (**Figure 26**) [41]. In addition to an N-terminal ER signal sequence and transmembrane helices, FicD contains two tetracopeptide repeats (TPR) that are likely to mediate interactions with other proteins. These interactions may be necessary for binding to AMPylation

substrates, or could be responsible for mediating interactions with regulating proteins or anchoring to a larger protein complex. This protein also has an obvious example of in cis regulation, as it contains an inhibitory helix that blocks the ATP binding site of the C terminal Fic domain [28]. A glutamate residue (234 in human FicD) forms a salt bridge with a critical arginine in the active site of the Fic domain, sterically preventing it from interacting with the gamma phosphate of ATP molecules. Mutation of the glutamate residue in the inhibitory helix allows proper positioning of the arginine to coordinate ATP, allowing AMPylation activity.

These potential mechanisms of regulation have slowed the progress of determining FicD function, as endogenous AMPylation in cells is much more difficult to identify than that catalyzed by the unregulated bacterial effectors. In this study, I attempted to gain further insights into the functions of FicD in terms of localization, activity, targets and potential roles in the cell. In synergy with work done on the fly version of this protein by my fellow graduate student Hyeilin Ham, we now know that the Drosophila Fic-containing protein (dFic) is localized in the lumen of the endoplasmic reticum (ER), has robust AMPylation activity when the inhibitory helix is disrupted, can AMPylate the ER chaperone BiP in vitro and is upregulated during unfolded protein response conditions [91].

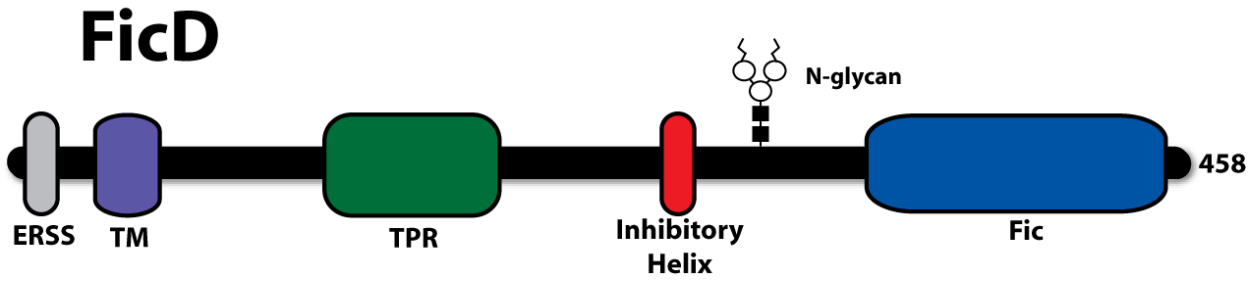

Figure 26. Features of the FicD protein. The human fic protein contains an ER signal sequence, a single pass transmembrane helix, two TPR motifs, an inhibitory helix, an N-linked glycosylation site and the eponymous Fic domain.

RESULTS

Overexpressed FicD is localized in the endoplasmic reticulum

Encoded in the FicD gene is a predicted ER signal sequence that could target it to the secretory pathway and a predicted N-linked glycosylation site, suggesting that FicD may localize to the endoplasmic reticulum or further along the secretory pathway (**Figure 26**). To test if FicD does indeed localize to the ER, I transfected HEK293T cells with FicD fused to a C-terminal FLAG tag. Transfected lysates were then treated with EndoH, an enzyme that cleaves N-linked sugars from glycosylated proteins. Treatment with EndoH increased the mobility of FicD on a western blot, indicating it is N-linked glycosylated (**Figure 27A**). Additionally, this indicates that FicD is likely an ER resident protein, as EndoH recognizes only glycosylation that has not been further process at later stages of the secretory pathway (i.e. Golgi Apparatus). I also transfected HEK293T cells

with FicD fused to a C-terminal GFP tag to visualize its morphology inside cells and found that it adopts a lace-like localization, reminiscent of ER localized proteins (**Figure 27B**).

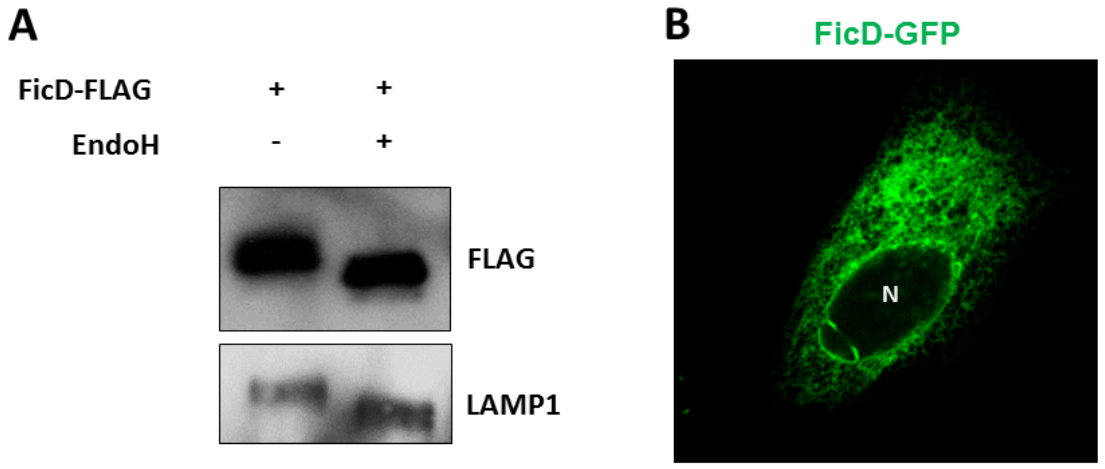

Figure 27. FicD is N-glycosylated, EndoH sensitive and shows ER-like localization. A. Treatment with EndoH causes a mobility shift of transfected FicD, showing that the protein is N-glycosylated and lumenal. Sensitivity to EndoH suggests it does not travel beyond the endoplasmic reticulum. B. Transfected FicD-GFP shows a lace-like morphology, supportive of ER localization. N=nucleus.

These findings support the hypothesis that FicD is localized in the ER, and that its AMPylation activity may target another ER resident protein. This knowledge is key in defining potential substrates for this protein. As FicD does not contain a C-terminal KDEL sequence or known mechanism to retain it in the ER, it is possible that FicD is secreted to the extracellular media. To test this, I again expressed FicD-FLAG in HEK293Tcells, and attempted to immunoprecipitate FicD using anti-FLAG beads from either the cells or the extracellular media. I did this by first collecting the conditioned

media, followed by collection and lysis of the cells with NP-40 detergent prior to immunoprecipitation. As expected, FicD was readily precipitated from the cells, but no FicD was detected in the media (**Figure 28**).

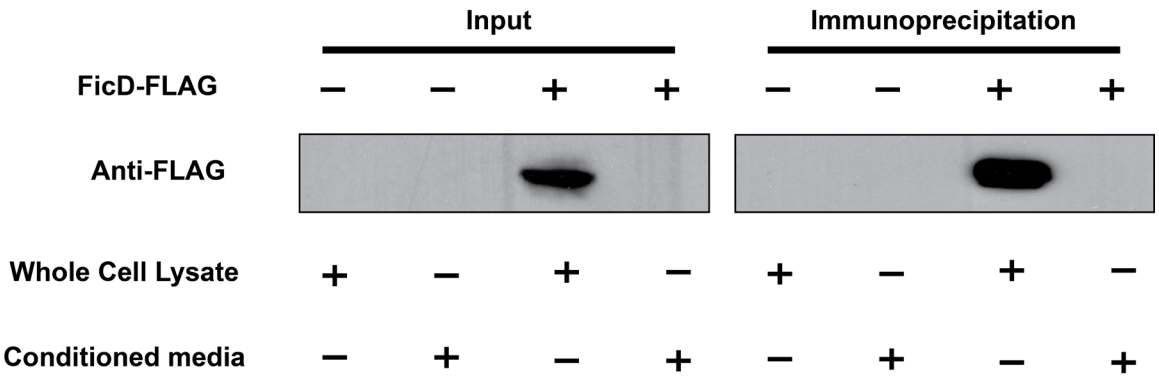

Figure 28. FicD-FLAG is not secreted to extracellular media. HEK293T cells were transfected with either FicD-FLAG or empty vector, and lysates or conditioned media were immunoprecipitated with anti-FLAG M2 beads. FicD was detected only in lysates.

Mutation of inhibitory salt bridge in FicD results in robust AMPylation activity

Identifying potential substrates of FicD is greatly complicated by the poor activity of the wild type form of the protein. Fortunately, an exhaustive bioinformatics study of Fic proteins recently revealed the presence of an inhibitory helix, which is absent in many of the bacterial Fic proteins [28]. This helix is present in FicD, and is likely the cause of the poor activity. To produce highly active FicD protein for use in vitro assays, FicD proteins were N-terminally truncated by 47 amino acids to remove the signal sequence and hydrophobic transmembrane helices and fused to an N-terminal His-SUMO tag for affinity purification and solubility. I mutated human FicD at glutamate-234, which is the

acidic residue responsible for occluding ATP from the FicD active site, and created an additional inactive control protein mutated at the critical histidine-363 in the FicD active site. Expression of these His-SUMO fused proteins was induced in Rosetta (DE3) E. coli and purified by nickel affinity chromatography. Proteins were further purified by AKTA FPLC using mono Q anion exchange and Superdex 75 gel filtration, yielding relatively pure FicD proteins (**Figure 29**).

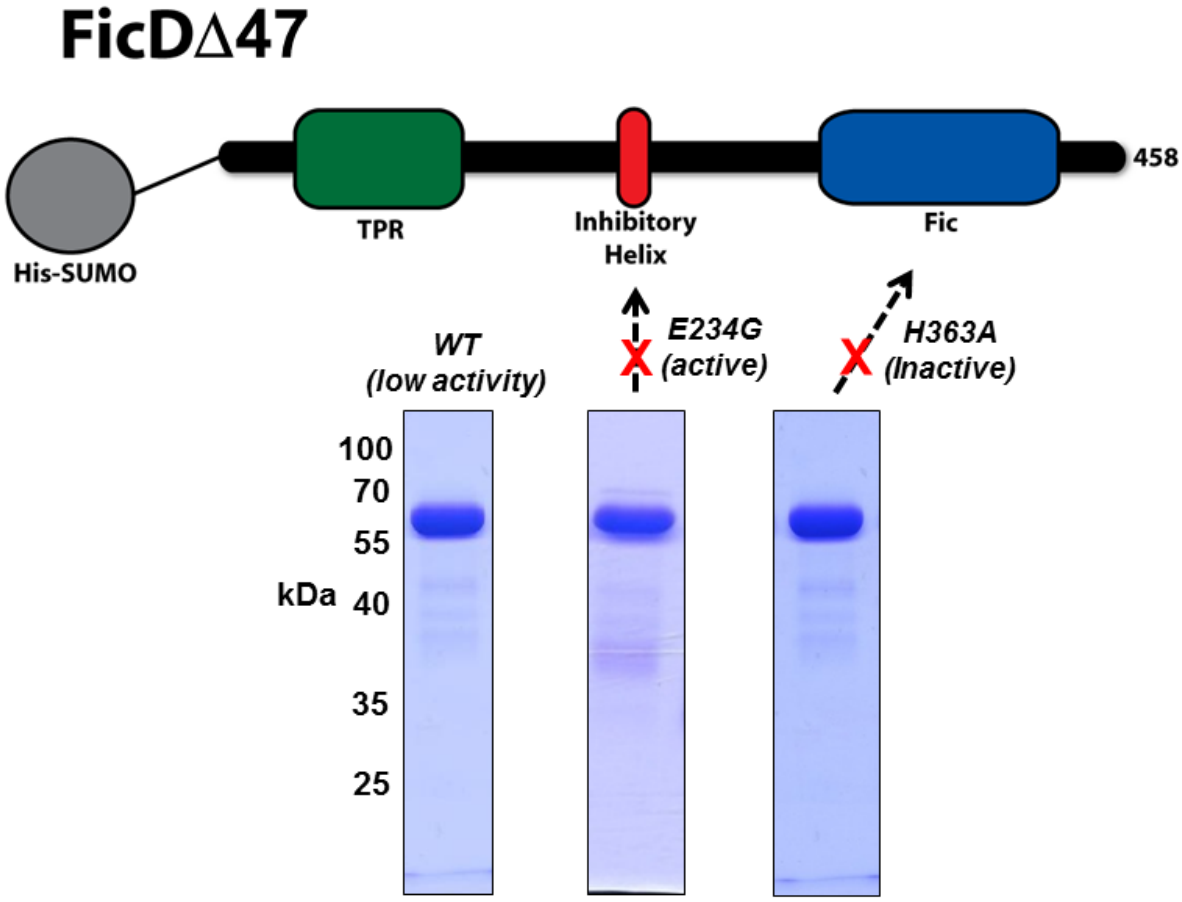

Figure 29. Purification of recombinant FicD. Wild type, E234G and H363A FicD cDNAs truncated to remove the first 47 amino acids were fused to an N-terminal His-SUMO tag, and purified by nickel affinity. The proteins were further purified by AKTA FPLC on monoQ and Superdex 75. Shown is the purity of the final product of each.

To test if the FicD protein mutated in the inhibitory helix may have higher AMPylation activity, I performed an AMPylation assay with radioactive ^{32}P-α-ATP and equal amounts of wild type or FicD E234G protein to see if autoAMPylation could be observed. The wild type protein showed little activity, as was previously observed. By contrast, the mutated FicD E/G showed robust autoAMPylation activity as observed by autoradiography and a complete band shift of the total protein seen on the coomassie blue stain (**Figure 30**). Unfortunately, the sites of autoAMPylation were not able to be discerned by LC-MS/MS. Multiple sites of AMPylation were observed but the mapping to specific amino acids was inconclusive with low confidence in the results (data not shown).

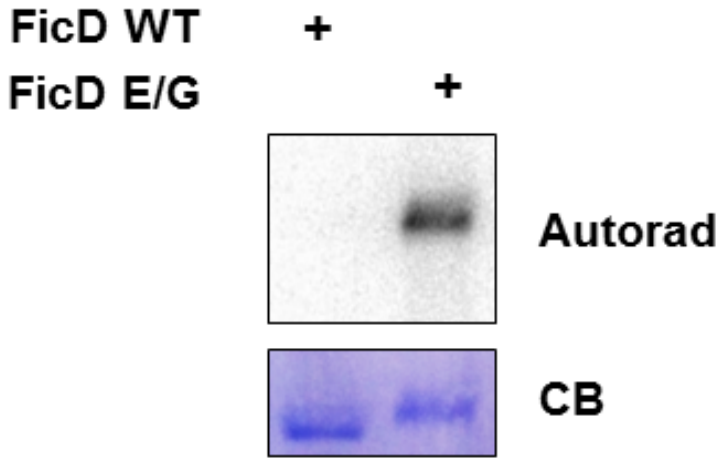

Figure 30. FicD protein mutated in the inhibitory helix has strong autoAMPylation activity. Mutating the salt bridge-forming glutamate 234 to glycine gives robust autoAMPylation activity to FicD, observed by autoradiography after treatment with ^{32}P-α-ATP and complete mobility shift of total protein by coomassie stain.

FicD AMPylates BiP/GRP78 in vitro

A previous report demonstrated that FicD, like VopS or IbpA, was capable of AMPylating Rho GTPases in vitro. However, it seems unlikely that Rho GTPases are true substrate of FicD , considering that Rho GTPases are localized in the cytosol or attached to the inner plasma membrane via palmitoylation and FicD is localized to the secretory pathway. To attempt to identify potential substrates of FicD, I used the purified FicD proteins in in vitro AMPylation assays against HEK293T lysates. No significant activity was observed by either FicD H363A or wild type. FicD E/G showed robust autoAMPylation, but no activity in the molecular weight range of Rho GTPases in comparison to IbpA (**Figure 31**). However, FicD E/G did appear to AMPylate a protein between 70 and 100 kilodaltons, which was consistent through multiple experiments with different lysates, including detergent extract from mouse pancreas.

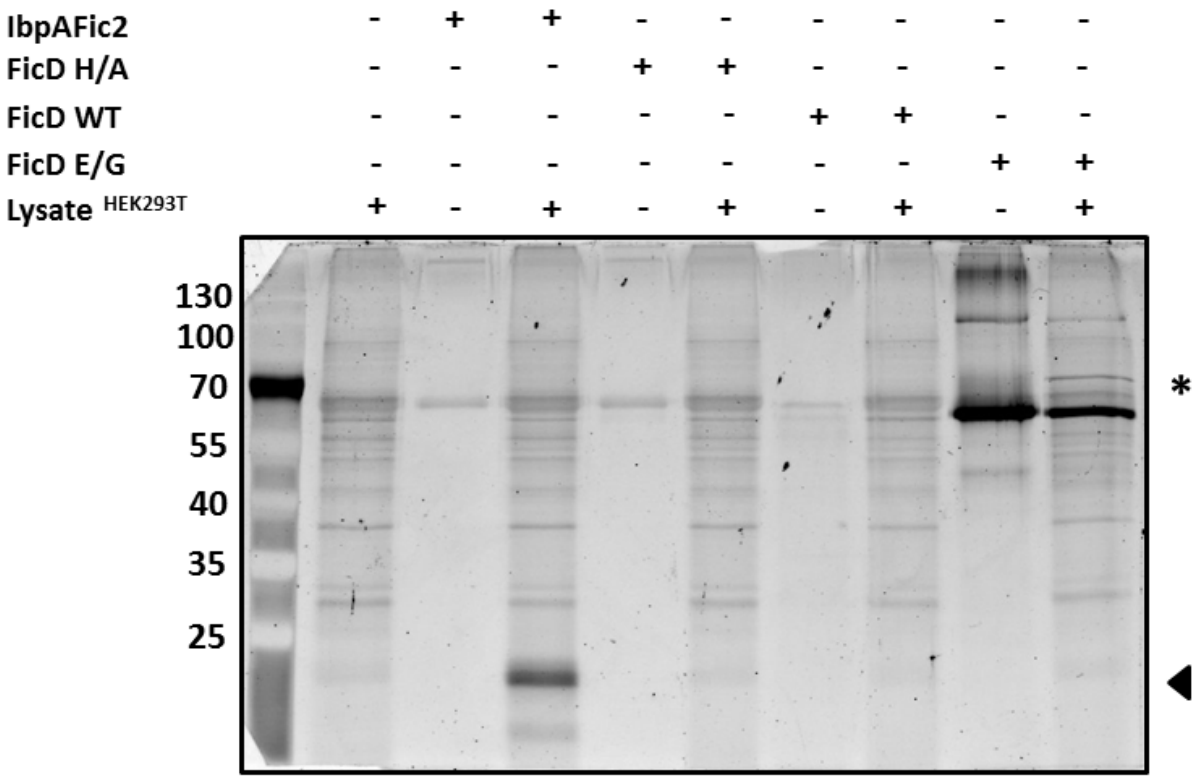

Figure 31. A 70+ kDa protein is AMPylated by FicD in mammalian lysates. Unlike VopS and IbpA Fic2, FicD does not AMPylate RhoGTPases (arrowhead) in HEK293T lysate. FicD E/G mutant appears to AMPylate a protein between 70-100 kDa in the lysate (asterisk).

Concurrent work by Hyeilin Ham in our lab on the *Drosophila melanogaster* homologue of FicD (dFic) had recently identified the ER chaperone BiP/GRP78 as a potential AMPylation substrate. BiP is a strong candidate substrate, as it shares the most likely subcellular localization of FicD, which is in the lumen of the endoplasmic reticulum. BiP, with a molecular weight of approximately 75 kilodaltons, also has a molecular weight matching the range of the substrate in mammalian lysates AMPylated by FicD E/G.

To produce recombinant BiP for use in in vitro assays, I cloned human BiP into a bacterial expression vector containing an N-terminal 6x His tag, and also truncated the first 19 N-terminal amino acids, representing the signal sequence that is cleaved during normal processing in the ER. His-BiP was expressed in Rosetta (DE3) *E. coli* and purified by nickel affinity chromatography, followed by fractionation on a Superdex 75 gel filtration column (**Figure 32**). His-BiP separated into two species on the gel filtration column. The higher molecular weight species (fractions <52) likely represents BiP bound to poorly folded proteins from the E. coli lysate or aggregates of BiP. The lower molecular weight species (fractions 52-58) presumably represents unbound, monomeric BiP. The latter elution pattern resembles that of a protein with similar molecular weight used in column calibration, conalbumin (MW 75 kilodaltons). The fractions of the predicted unbound, monomeric BiP were used in the experiments described below.

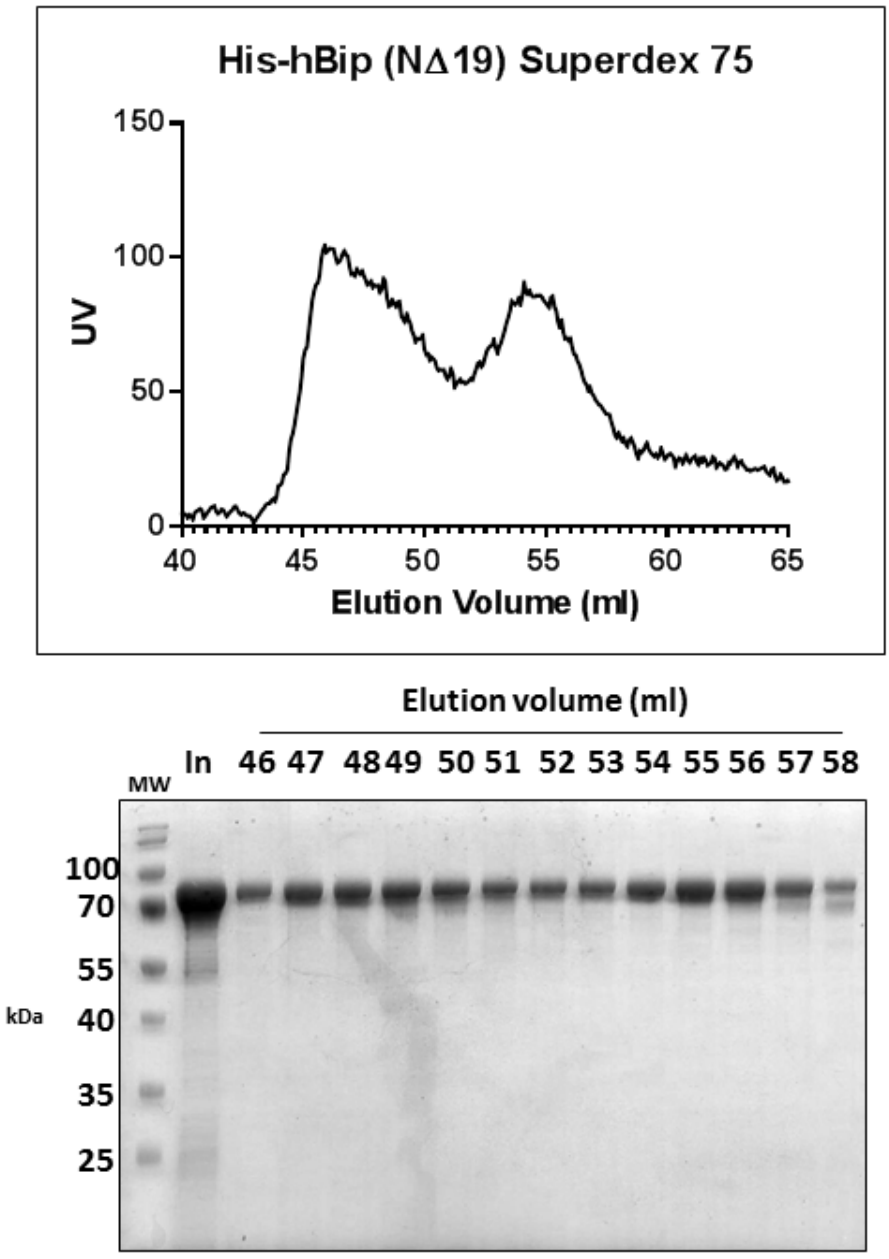

Figure 32. Purification of recombinant human BiP. His-tagged BiP expressed in Rosetta E. coli was captured on nickel affinity resin, eluted, concentrated and fractionated by gel filtration on a superdex 75 column. Recombinant BiP separated into two populations. Fractions 53-57, representing the correct molecular weight and therefore substrate-free population were pooled for use in assays. In=input

To test if BiP might be a potential substrate of FicD, I performed an in vitro AMPylation assay by incubating each of the FicD protein with or without recombinant BiP and ^{32}P-α-ATP. As before, FicD H363A and wild type proteins showed no autoAMPylation, and also had no activity towards against BiP (**Figure 33**). However, FicD E/G shows robust AMPylation activity against recombinant BiP, indicating it is a strong in vitro substrate.

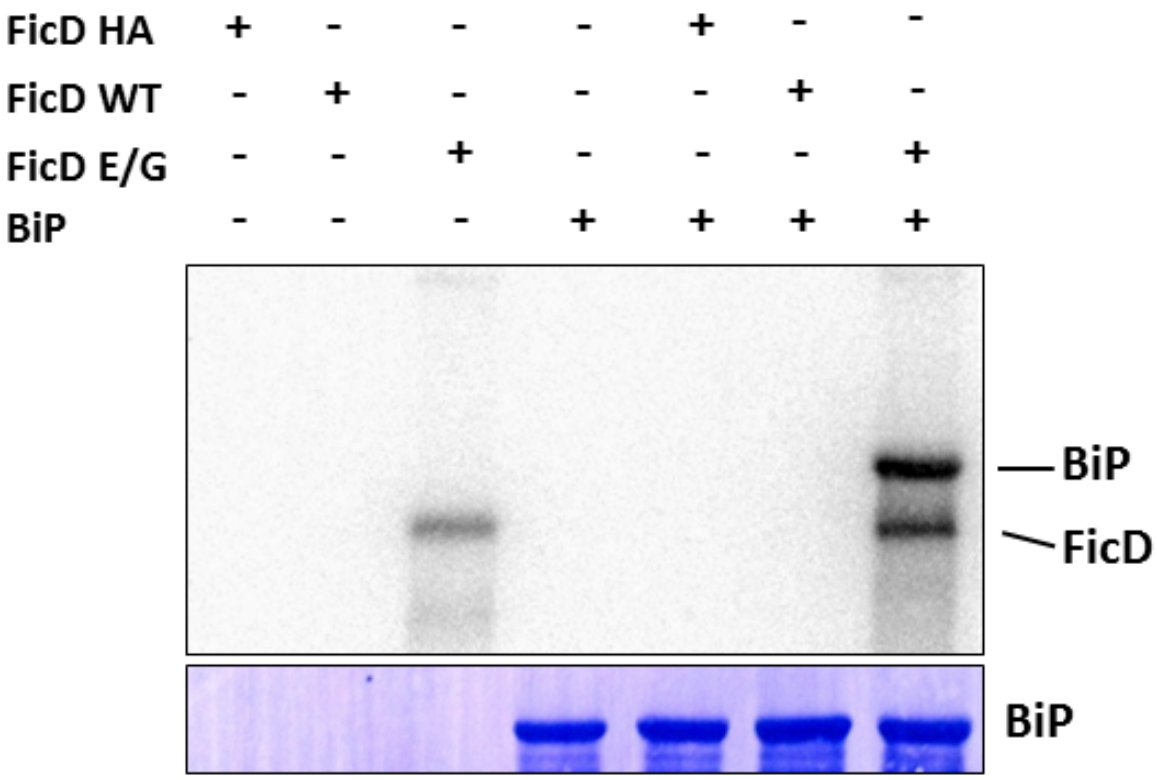

Figure 33. FicD E/G robustly AMPylates human BiP in vitro. FicD mutated to disrupt its inhibitory helix, but not wild type FicD, shows strong AMPylation activity to BiP. Top image is autoradiography after treatment with 32P-a-ATP, while bottom image is coomassie stain of filter with total BiP.

FicD activity may be related to the endoplasmic reticulum unfolded protein response

The discovery of BiP as a potential substrate of FicD led to an obvious question: is FicD involved in the unfolded protein response? BiP is an integral part of the cell's response at multiple levels to increasing loads of unfolded protein in the endoplasmic reticulum, and modification of BiP by FicD could be a novel mechanism of modulating BiP activity. One potential piece of data that supports this hypothesis is observed in the *Δdfic* knockout flies, which were previously found to be blind [63]. I found that total levels of BiP protein in the knockout flies were significantly increased (**Figure 34**). Increased levels of BiP are a hallmark of increased ER stress and the unfolded protein response, as cells increase BiP levels to help manage increases in misfolded or poorly folded proteins. This result may indicate that absence of dFic leads to a defect that perturbs the endoplasmic reticulum and may trigger the unfolded protein response. The blind phenotype of *Δdfic* knockout flies could potentially be explained by increased ER stress leading to aberrant processing and transport to the cell surface of receptors critical for visual neurotransmission.

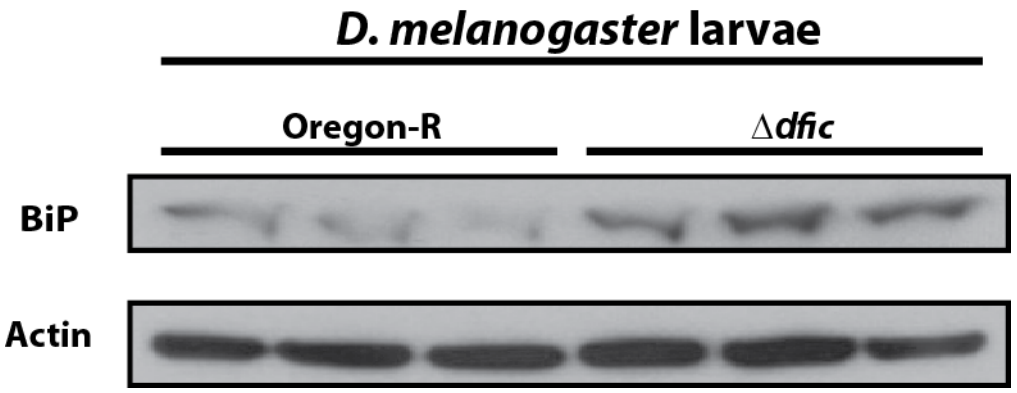

Figure 34. *dFic* mutant flies show elevated levels of endogenous BiP. *Drosophila melanogaster* dFic mutants show increased endogenous levels of BiP over wild type Oregon-R flies, indicating ER stress. Each lane represent a single larva.

Genes that help maintain endoplasmic reticulum homeostasis or help return the cell to homeostasis are commonly upregulated at the mRNA level under conditions that induce the unfolded protein response (UPR). Multiple examples exist, such as BiP, the endoplasmic reticulum chaperone, and CHOP, a key mediator of apoptosis when the stress cannot be brought under control [92]. This is in contrast to unrelated genes, whose mRNA levels remain the same or decrease due to transcription factors and atypical mRNA decay mediated by IRE1, a multipurpose endonuclease critical for the UPR [93]. To test if FicD might be upregulated during conditions that induce the unfolded protein response, I stressed HEK293T cells with two commonly used inducers, tunicamycin and thapsigargin, for 6 hours. Tunicamycin inhibits N-linked glycosylation, while thapsigargin drastically reduces the levels of calcium in the endoplasmic reticulum, which is a critical cofactor for many chaperones. Using quantitative RT-PCR, I found that FicD mRNA levels increased significantly under both conditions relative to the cells

treated with DMSO only (**Figure 35**). This induction happened in the same time scale relative to CHOP, an endoplasmic reticulum stress regulated gene. These findings support the hypothesis that FicD is an endoplasmic reticulum stress regulated gene.

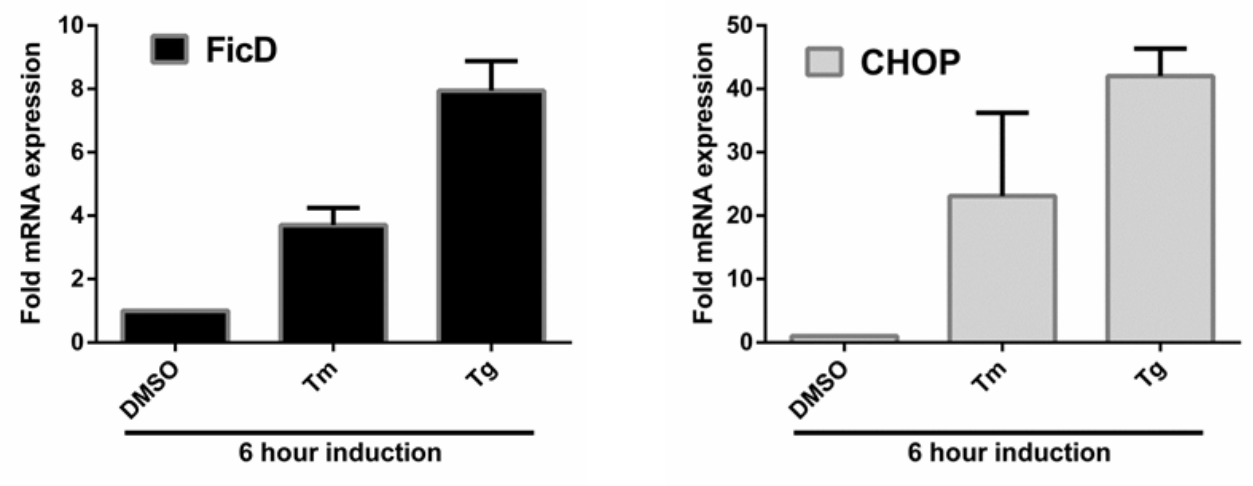

Figure 35. FicD mRNA levels are increased in cells undergoing ER stress. Treatment of HEK293T cells with ER stress inducers tunicamycin (Tm, 2ug/ml) or thapsigargin (Tg, 1 uM) results in increased levels of FicD mRNA relative to GAPDH mRNA. CHOP is a gene known to be induced under ER stress conditions.

To further understand the regulation of FicD during the unfolded response, I performed a time course to observe the induction of mRNA from 0 to 33 hours in the presence of tunicamycin. I found that FicD mRNA levels increased between 2 and 4 hours post-addition of tunicamycin relative to the uninduced mRNA control **(Figure 36)**. These data show a slight (1-2 hours) delay in comparison to other UPR induced mRNAs such as CHOP (**Figure 36**). XBP1 mRNA splicing leads to the translation of an active XBP1 transcription factor that upregulates multiple genes involved in the UPR,

potentially indicating that the FicD promoter may be targeted by XBP1 or other UPR transcription factors. Interestingly, each of these factors shows only an acute increase in mRNA, with levels decreasing after about 12 hours post-addition of the stress stimulator.

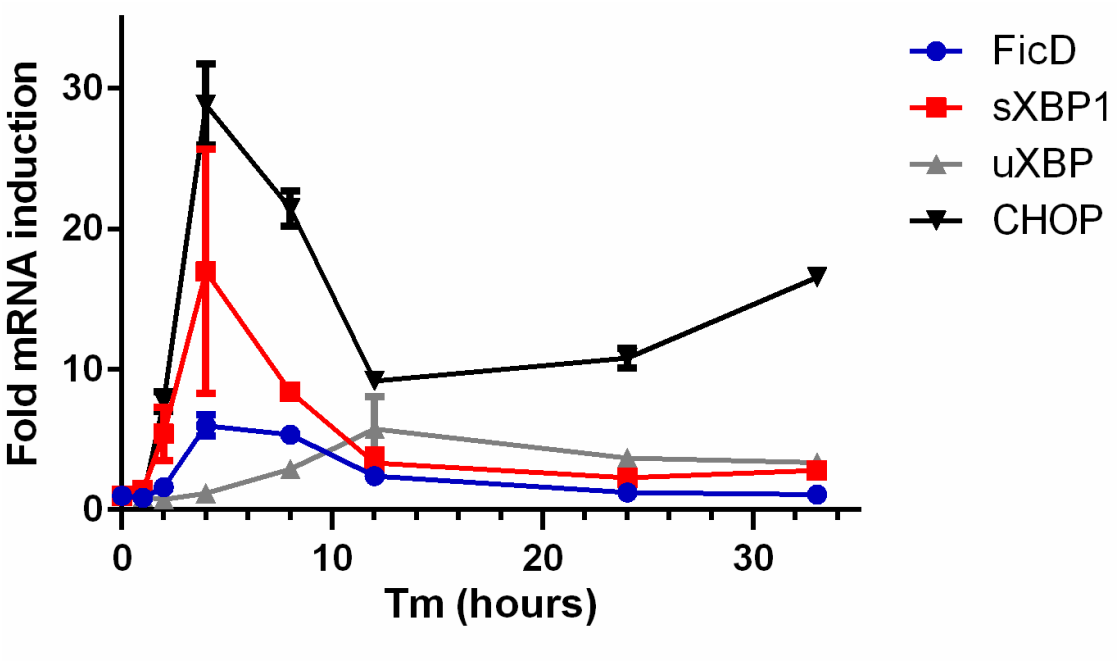

Figure 36. Induction of FicD expression under ER stress. HEK293T cells were treated with tunicamycin (Tm, 2 ug/ml) for indicated times. FicD mRNA levels increase between 4-10 hours post treatment before returning to near normal levels, coinciding with the splicing of XBP1. uXBP1: unspliced XBP1 mRBA. sXBP1: spliced XBP1 mRNA.

DISCUSSION

Since the discovery that the VopS Fic domain transfers AMP to protein substrates, understanding the role of the human homologue FicD has been a subject of intense interest. While much work remains to decipher the function of this gene, my work and the work of others has given a few insights into the processes in which FicD might be involved. Studies using *Drosophila* genetics in collaboration with Helmut Kramer's lab provided the critical finding that flies lacking dFic are blind [63]. This initial finding was accompanied with evidence that dFic was expressed on the capitate projections (i.e. the plasma membrane extension thought to be derived from the ER) of glial cells and that neurotransmitter recycling was reduced in these knockout flies. This led to the hypothesis that dFic plays a direct role in neurotransmitter release or uptake, perhaps by modulating the function of a key receptor. However, our work suggests that dFic may be an ER resident protein, but the overall primary localization in most cell types in a complex multicellular organism remains unclear.

My work and that of others has demonstrated that ATP is a poor cofactor in vitro for the wild type FicD protein, which requires disruption of the inhibitory helix to use it effectively [28, 41]. Two hypotheses can be immediately drawn from this: (1) the inhibitory helix is a mechanism of regulating AMPylation catalyzed by this protein, and during conditions in which AMPylation is desired this inhibition is relieved by an unknown mechanism, or, (2) FicD uses a nucleotide cofactor other than ATP. While the recently published structure of FicD shows that the active site is functionally identical to other AMPylators when the inhibitory helix is disrupted, other groups have speculated

that it may not be an "inhibitory helix" at all [34]. Rather, factors that occlude the gamma phosphate of ATP from the active site of Fic proteins may actually give them specificity for diphosphate nucleotides. The precedent for this is AnkX, a Fic protein which uses CDP-choline as a cofactor. Interestingly, it was found that while wild type FicD showed no binding to ATP, it did bind ADP, although weakly [41]. However, limited trials by myself and others with potential diphosphate cofactors, such as CDP-choline and NAD, have met with no success, making the inhibitory helix hypothesis presumably the more likely option. Nevertheless, consideration of both possibilities is prudent in future studies about the biochemical mechanisms of FicD.

My primary contributions to deciphering this enigmatic protein are support for ER localization, confirmation of BiP as an in vitro substrate and evidence showing FicD is a UPR-regulated gene, suggesting it may be important for ER homeostasis. Further work will be required to determine if BiP AMPylation occurs naturally in mammalian cells, as it appears to in *Drosophila* S2 cells. If BiP is a true substrate of FicD AMPylation, a potential hypothesis is that AMPylation will modulate one of its functions. BiP is a multifunctional protein that interacts with many signaling components of the UPR, but its primary function is a chaperone to help proteins fold. As AMPylation has thus far been an inhibitory modification, it is likely that FicD would have a negative regulatory effect, in the vein of glutamine synthetase adenylyl transferase in *E. coli [2]*.

One potential mechanism is that AMPylation of BiP occurs in the ATPase domain, which could inhibit the ATP binding or hydrolysis that is necessary for its chaperone activity (**Figure 37A**). Indeed, AMPylation of the *D. melanogaster* BiP occurs

at threonine-366, which is situated near the ATP binding pocket of the ATPase domain of BiP [91]. It is also possible that AMPylation of BiP could occur at the substrate binding domain and inhibit its interaction with misfolded substrates (**Figure 37B**). A third possibility is that the binding of BiP to the UPR signaling proteins PERK, IRE1 or ATF6 could be disrupted by AMPylation, which may affect their downstream signaling (**Figure 37C**). Considering it is unlikely to ever be beneficial for the cell to inhibit a large fraction of its ER chaperone at any given time, a potential hypothesis is that AMPylation of the human BiP might maintain a smaller, inactive pool of BiP that can be readily deAMPylated and brought into service. This could offer a more rapid response to stress than traditional activation through increased transcription and translation. However, more work is required to confirm in vivo AMPylation and test these hypotheses.

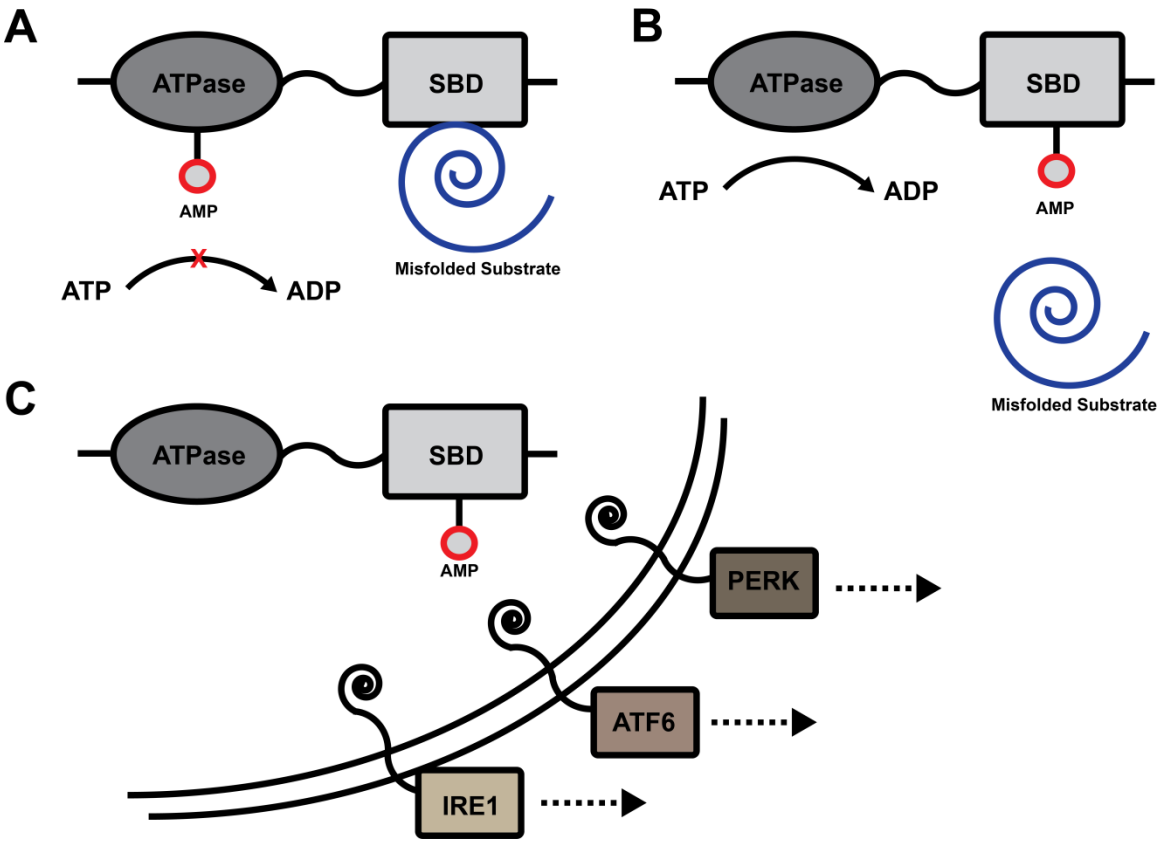

Figure 37. Potential roles for BiP AMPylation by FicD in endoplasmic reticulum homeostasis. A. AMPylation of the BiP ATPase domain could inhibit the binding or hydrolysis of ATP, which supplies the energy BiP uses to help proteins fold. B. AMPylation of the substrate binding domain of BiP could block the binding of misfolded proteins. C. AMPylation of BiP could block binding to the UPR regulators PERK, ATF6 and/or IRE1, which would promote UPR signaling.

CHAPTER SIX

Discussion and Future Directions

DISCUSSION

Implications for AMPylation and other modifications on the Rho GTPase switch-1 loop

The switch-1 loop of Rho GTPases is a critical polypeptide for cell signaling and mediating the interaction with numerous downstream effectors involved in processes such as cell shape, motility, phagocytosis, signaling cascades and reactive oxygen species production. As such, the switch-1 is an Achilles' heel that is often targeted to cripple host cells during infection, using posttranslation modifications such as ADP-ribosylation, AMPylation and glycosylation. In this study, I have, with the help of several collaborators, provided novel insight into the cell signaling events that can be affected by modification of this interaction loop. While studies on these disruptive modifications have focused primarily on the changes in the actin cytoskeleton, other cellular functions can also be affected. Disrupting the host defense signaling cascades such a NFκB and MAPK are very advantageous for bacteria attempting to keep a low profile. It seems likely that any bulky modification of the switch-1 loop will cause these signaling defects, and determining if ADP-ribosylation and glycosylation do so is an interesting avenue for further research.

It is also possible that the full significance of the actin cytoskeleton inhibition is not fully appreciated, considering that a bacteria attempting to establish a niche in the

host might want to shut down multiple roles of the cytoskeleton, including but not limited to, adhesion of epithelium, motility and phagocytic competence of immune cells that might chase them. Unfortunately, the drastic nature of this phenotype would make it difficult to parse out which functions of the actin cytoskeleton are most affected during an infection, as all are likely to be completely shut down. Modification of the switch-1 loop of different GTPases is not feasible, as this is known to interrupt interactions even in the absence of other modifications.

This work I think truly highlights the power of studying bacterial toxins to identify potentially important interactions in the host cell, as a few open questions about Rho GTPase interactions have arisen. Is ubiquitinylation of Rho GTPases during infection an important signaling mechanism in immunity? AMPylation of Rho GTPases blocks its interaction with Inhibitors of Apoptosis proteins, IAPs, which are known E3 ligases that promote immune signaling complex formation. It is possible that ubiquitination of Rho GTPases by IAPs does not merely target them for degradation, but under some conditions, might inhibit the formation or function of an unknown or known immune protein complex or interaction. Future studies could focus on determining if abrogation of GTPase ubiquitination leads to any signaling defects during infection by transfection with Rho GTPases mutated at their ubiquitination site and analyze downstream signaling events.

Development of protein microarray tools for the study of AMPylation

Our Rac1 interaction screen revealed another interesting protein: the complement head subunit C1qA. Recent studies revealed that the cytosolic function of C1qA is as a pattern recognition receptor to promote sensing of viral DNA [89]. Many of the details of how this protein performs its cytosolic function are unknown, including many of its key binding partners. It is possible that interacting with Rac1 is an important mechanism to activate immune signaling for various pathogenic signals, such as bacterial peptidoglycan components and aberrant host signaling. It is also possible that C1qA might serve as a direct sensor of modified Rho GTPases, which has recently been observed with the PRR Pyrin [94]. Future studies could test if coexpression of C1qA in the cytosol with Rac1 proteins under various conditions might induce stress signaling pathways. Using wild type, dominant negative, or dominant active Rac1 with or without C1qA will show if different active states of Rac play a role in the ability of C1qA to sense stimuli and signal downstream. Alternatively, pairing C1qA expression with transient knockdown of Rac1 will determine if Rac1 is necessary for C1qA signaling.

In this work we also designed and validated a powerful tool for screening post-translational modifications using the NAPPA array. This protein microarray technique is a powerful technology in its own right, capable of rapidly and conveniently displaying thousands of proteins for different uses, but its potential has not been fully tapped. Using NAPPA to screen for post-translational modification substrates is a natural extension of the technology, and AMPylation served as a useful modification to validate the strategy. In our screen, we examined the entire Rho GTPase family as AMPylation substrates of

bacterial Fic proteins. The use of a click-fluorescent AMPylation probe demonstrates that any sufficiently adaptable fluorescent or luminescently-conjugated probe could serve tool for this screening method. For example, alkyne conjugated glycans could be used to screen for glycosylation substrates, or GFP-fused ubiquitin could be used to screen for substrates of E3 ligases. The potential power of this screening method would be very powerful for elucidating the function or target of enigmatic enzymes.

Since the discovery of Fic as a versatile transferase domain, the human homologue FicD has been one of the aforementioned enigmatic enzymes. Accordingly, we attempted to use in the NAPPA array screen as well, unfortunately, with little success. The wild type version of this protein showed very little activity, with all hits having low scores and many with incorrect subcellular localization. No hits from the screen could be validated by other methods. Conversely, the activity of the deinhibited version of the FicD protein was very high, generating too much background in the NAPPA for any kind of reliable reading. The robust autoAMPylation activity of the FicD protein likely results in the trace amounts of this protein bound to the slide obscuring the visualization of any potential hits. Unfortunately the functions and substrates of FicD must be elucidated using another method.

Potential yeast AMPylation could reveal novel AMPylators

Only two domains are currently known to catalyze protein AMPylation: the Fic and nucleotidyll transferase domains. While both domains are widely conserved among bacteria, metazoans contain only one copy of the Fic domain and no obvious homologues of the adenylyl transferase domain, although some nucleotide transferases (i.e. polymerases) could be potential AMPylators. Interestingly, no potential AMPylators can be bioinformatically predicted with any confidence in yeast, as it has no Fic domain proteins or obvious adenylyl transferase homologues. However, despite the lack of obvious AMPylator candidates in yeast, we were able to detect what appears to be AMPylation through both radioactive assays and western blot. Incubation of BY4741 yeast whole cell lysates with ^{32}P-α-ATP results in labeling of numerous proteins, as seen in a radioactive exposure of lysates run on SDS-PAGE (**Figure 38A**). Further evidence for yeast AMPylation can be observed using immune serum inoculated with a tyrosine-AMPylated peptide (Y-AMP antibody), as at least two proteins appear to be recognized by this serum but not by serum from uninoculated rabbits (**Figure 38B**). Interestingly no signal above background was observed in yeast extracts with rabbit serum raised against a threonine-AMPylated peptide (T-AMP antibody, data not shown).

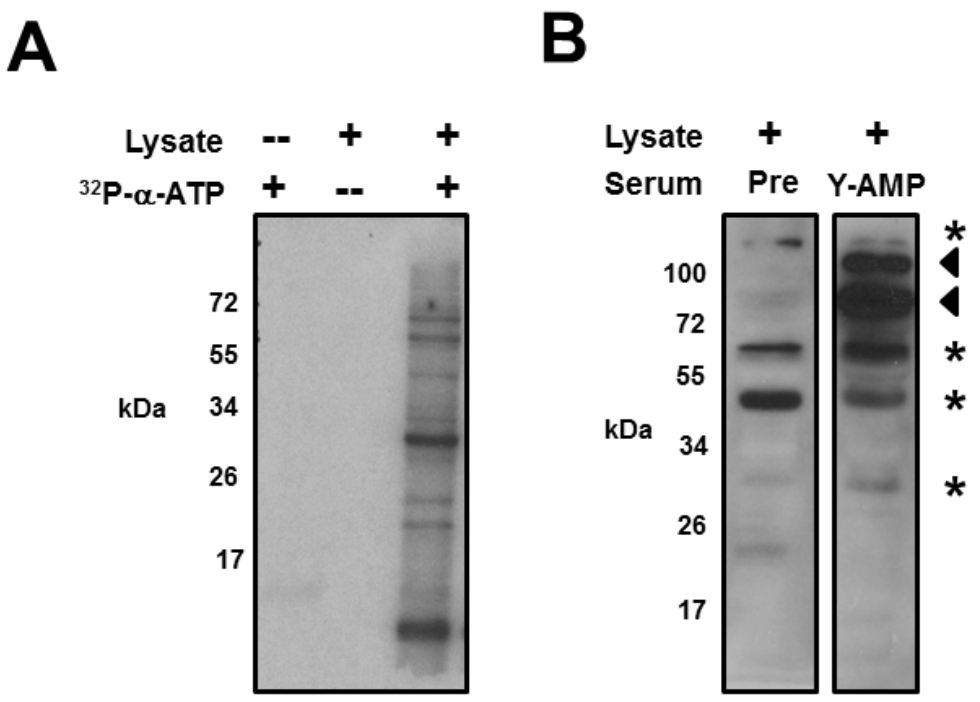

Figure 38. Potential AMPylation in BY4741 yeast extracts. A. Whole cell yeast lysates were incubated with ^{32}P-α-ATP for 30 minutes, and radioactivity of SDS-PAGE transfers were exposed to film overnight. Multiple apparently AMPylated bands are observed. B. Immunoblotting of BY4741 yeast extracts with either pre-immune rabbit serum (left) or serum of rabbits inoculated with a tyrosine AMPylated peptide (right), show potential AMPylated substrates. Pre: preimmune serum from rabbits. Arrowheads: Potential AMPylation substrates. Asterisk: background bands (appear in both preimmune and immune sera).

To attempt to identify AMPylated proteins in yeast, I endeavored to purify endogenously AMPylated proteins from the lysates using sequential column chromatography. After extensive optimization, I decided that purification of the 100+ kilodalton band (top arrowhead, **Figure 38B**) using western blot with the Y-AMP antibody as an assay was the most tractable method. By testing the binding of this protein to multiple columns, including ion exchange, hydrophobic, size exclusion and mixed

mode/affinity matrices, I was able to conceive a purification plan that allowed me to isolate this protein to near homogeneity (**Figure 39A, B**). Using reverse phase LC-MS/MS, Yan Li with the UT Southwestern Proteomics core identified this protein as alanine-tRNA synthetase (Ala1), which is a key protein in activation of alanine amino acid during translation. Ala1 promotes the attachment of alanine to its cognate tRNA in a two-step process: first it activates alanine by conjugating it to AMP from ATP in a high energy bond, and the energy of this reaction is used to then transfer alanine to the acceptor region of the tRNA, where it can then be used in translation. AMP transfer by Ala1 is not considered AMPylation, as it is a transient modification that is not on a hydroxyl side chain, but instead on the carboxyl moiety.

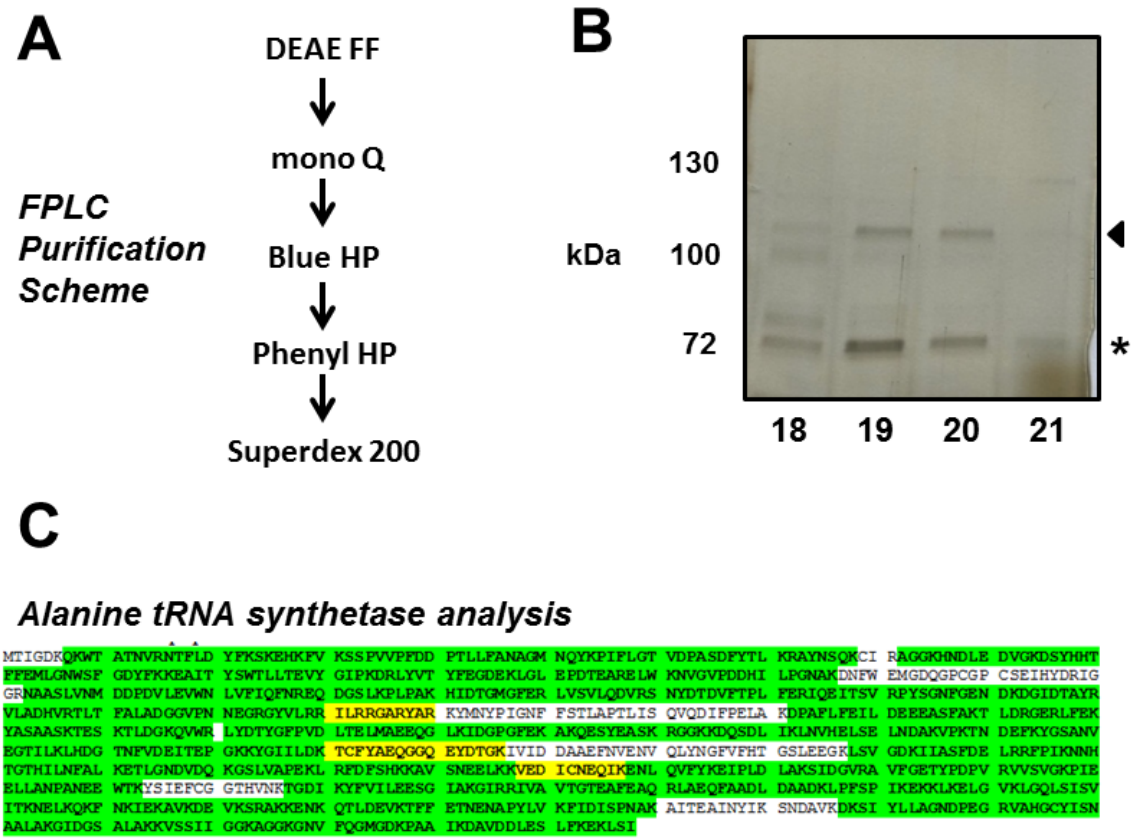

Figure 39. The potential AMPylation substrate Ala1 was purified from Saccharomyces cerevisiae lysates. A. Purification scheme of the 100+ substrate B. Silver stain of fractions from final show a band corresponding to correct molecular weight (arrowhead). This band was identified as alanine rRNA synthetase (Ala1). Asterisk: unrelated coeluting band. C. Coverage of mass spectrometry analysis of endogenous Ala1 for AMPylation. No AMPylated peptides were observed with 87% coverage of protein.

I next attempted to identify any potential sites of AMPylation by mass spectrometry analysis. I scaled up the aforementioned purification scheme and produced sufficient quantities of endogenous Ala1 (approximately 10 micrograms) for peptide analysis and a search for AMPylated peptide. Unfortunately, despite achieving 87% coverage of the protein in our analysis, no AMPylated peptides could be detected. It is

possible that AMPylated peptides of Ala1 simply are not amenable to mass spectrometry analysis or occur at levels too low for detection. It is also possible that the recognition of Ala1 by the Y-AMP antibody is due to the alanine-AMP transferase activity of Ala1, which could cause automodification of Ala1 as accidental byproducts that resemble autoAMPylation. Future studies may be conducted to determine if AMPylation of Ala1 is a naturally occurring phenomenon, or if other potential AMPylation substrates in yeast exist.

Potential roles for FicD in endoplasmic reticulum stress?

Some clues as to the potential role of FicD in metazoan biology have been found. The cell pursues multiple avenues to relieve the stress of misfolded proteins. The observation that Δd*fic* knockout flies may have an overall higher level of ER stress, observed by increased BiP protein, indicates that dFic may play a role in alleviating such stress. Additionally, FicD mRNA expression is induced during the UPR. Genes involved in assisting protein folding, expanding the size of the endoplasmic reticulum, limiting translation of new proteins and promoting the degradation of terminally misfolded proteins are all commonly upregulated during the UPR. Therefore, it is possible that FicD is involved in one of these or other unfolded protein response processes, and its absence prevents the complete resolution of endoplasmic reticulum stress.

The discovery of BiP as an in vitro substrate of FicD presents an interesting possibility to explain this observed potential role in ER stress and has opened up

interesting avenues of study. We have found that FicD mutated at the inhibitory helix robustly AMPylates recombinant BiP. In *Drosophila* S2 cells, AMPylation of BiP appears to happen during endoplasmic reticulum homeostasis, and disappears during instances of stress, like reducing conditions or inhibition of N-glycosylation. It is possible that AMPylation of BiP during unstressed conditions is a mechanism used by the cell to maintain a stable population of inactive BiP that can be readily activated by removal of the modification. Perhaps AMPylation of BiP is a method of resolving low levels of stress without the need for more dramatic cell responses, which include altering the global transcriptional and translational programs in the cell.

Assessment of BiP as a bona fide FicD substrate

Future studies on BiP AMPylation will need to confirm that AMPylation occurs in mammalian cells, as it appears to in *Drosophila* S2 cells. Unfortunately, preliminary studies with AMPylation antibodies have not detected any AMPylation at the molecular weight range corresponding to BiP in HEK293T lysate or on BiP immunoprecipitated from cells. We also have not been able to identify high confidence AMPylated peptides using mass spectrometry. The caveat with these experiments is that HEK293T cells are transformed cells and abnormally high, possibly unregulated, BiP is frequently associated with cancer cells and may not reflect the cell type in which FicD regulation of BiP could occur.

An alternative method of detecting AMPylation from mammalian cells is to utilize metabolic labeling of live cells. Previously, studies have monitored what is

believed to be ADP-ribosylation of BiP in cells by incubating with H3-labeled adenosine [95]. Indeed, the ADP-ribosylation observed in such studies may serve a similar role to our model of BiP AMPylation, which is transient inhibition of BiP in normal homeostatic conditions. As adenosine is a precursor for both ATP (AMPylation) and NAD (ADP-ribosylation), labeled adenosine can serve to monitor either modification. For convenience, we can also use a non-radioactive approach to this labeling by instead using alkyne labeled adenosine (N6-adenosine), which can be conjugated with fluorescent rhodamine for detection of the modifications. As a preliminary experiment, cells were transfected with BiP fused to an N-terminal Strep tag and incubated with N6-adenosine for 6 hours. Cells were then lysed, BiP was isolated with Streptactin beads and modified BiP was conjugated with Rhodamine via copper chemistry. Eluted BiP protein was then visualized with by fluorescence in an SDS-PAGE polyacrylamide gel (**Figure 40**). Using this method, BiP can be assayed for modification, but the assay cannot differentiate between AMPylation and ADP-ribosylation. Using point mutants of BiP altered at known and suspected sites of modification, such as threonine-366 and arginine-470, we can meticulously identify sites that are modified with either ADP-ribosylation or AMPylation.

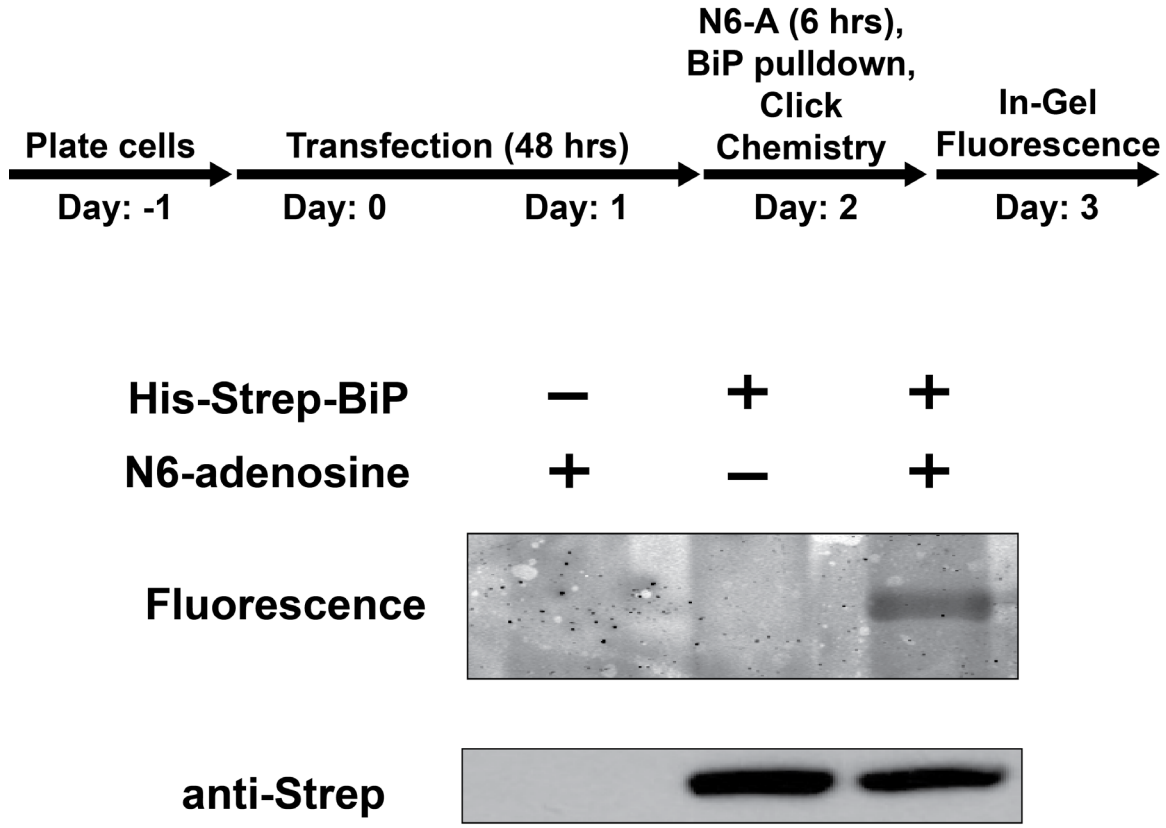

Figure 40. BiP is AMPylated and/or ADP-ribosylated in HEK293T cells. HEK293T cells were transfected with His-Strep-BiP for 48 hours, followed by metabolic labeling for 6 hours with 100 uM N6-adenosine, which is a precursor for both N6-ATP and N6-NAD. Transfected BiP was pulled down from lysates with Streptactin Beads, and modified BiP was conjugated to azo-Rhodamine with click chemistry, followed by imaging of in gel fluorescence.

An alternative and less technically challenging method of analyzing BiP AMPylation would be to create a new and more effective AMPylation antibody. The current AMPylation antibody used in the lab was raised against an AMPylated Rac1 peptide, and it is possible that this antibody simply does not recognize AMPylated human BiP with high efficiency. To this end, I have designed an antibody to recognize BiP AMPylated at threonine-366, the site known to be AMPylated. In collaboration with

Haydn Ball, we synthetically generated the AMPylated peptide Val-Gly-Gly-Ser-Thr(AMP)Arg-Ile corresponding to residues 362-368 of BiP, with the threonine-366 AMPylated (**Figure 41**). This peptide was used to immunize rabbits, and as the serum becomes available it will be tested for recognition of *Drosophila* and human BiP, AMPylated and AMPylated. Increasing the efficiency of recognition of BiP AMPylation will make such studies considerably more tractable.

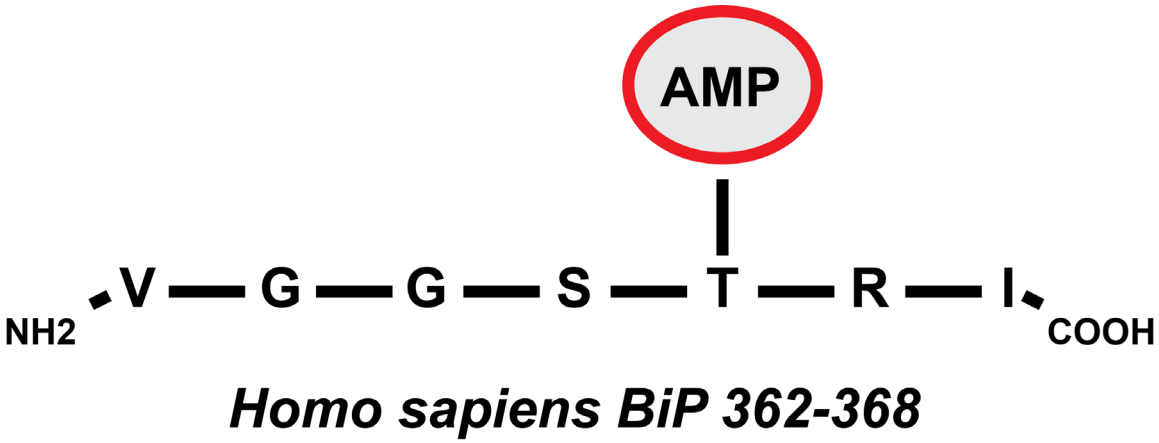

Figure 41. Synthetic AMPylated BiP peptide used for new AMPylation antibody. Production of a new antibody for recognizing BiP AMPylation is underway and could help the study of this modification.

Regulation of FicD AMPylation activity

Another open question about FicD activity is the mechanism of regulation of its AMPylation activity. If the "inhibitory helix" is truly a mechanism of regulating AMPylation activity and not a moiety that gives it specificity towards a diphosphonucleotide cofactor, then there must be a separate method of relieving the inhibition. One possible mechanism could be a transient modification of FicD in the ER, such as phosphorylation, that could displace the salt bridge and allow FicD to become active. Removing this modification would then likely return FicD to an inactive state.

Another possibility is that binding to another protein in the endoplasmic reticulum protein promotes AMPylation by FicD. A possible method to identify a potential binding partners of FicD would be to affinity purify FicD-FLAG from HEK293T cells, and identify coeluting proteins by mass spectrometry. Potential interacting proteins could be identified using coimmunoprecipitation or yeast-2-hybrid analysis. Their ability to promote FicD AMPylation activity could be assessed by adding recombinant versions of identified proteins to in vitro FicD AMPylation assay and/or assessing relative AMPylation rates on whole cell lysates.

CRISPR knockout technology opens new avenues for FicD studies

A potentially powerful tool recently developed in the lab is a Δ*ficD* HEK293T genetic knockout cell line generated by Anju Sreelatha using CRISPR technology. Future studies will be able to use this tool to analyze global changes in cell signaling due to the loss of FicD in a mammalian cell line. As FicD has been implicated in the UPR, a future avenue of study will be to determine if the Δ*ficD* cell line is deficient in any specific aspect of UPR signaling, such as the IRE1 or PERK signaling pathways. For IRE1 signaling, we can compare the rate of splicing of its primary mRNA substrate, XBP1 during endoplasmic reticulum stress. Additionally, total phosphorylation of the PERK substrate eIF2α will be measured, as well as global translation rates during stress to determine if this pathway is altered by loss of FicD. We can also assess other general factors in the cell, such as total ER size during stress, and the ability of the cell to perform endoplasmic reticulum-associated degradation (ERAD). It is also possible that some information about its overall role in cell signaling during ER stress could be gleaned by performing RNAseq on Δ*ficD* cells and the parental HEK293T cells under different stress conditions at different times, such as loss of disulfide bonds from reducing agents like DTT or loss of N-glycosylation from tunicamycin. Parsing differences in the timing of activated genes in the presence and absence of FicD could reveal in which aspects of cell biology FicD is involved.

The FicD knockout cell line will also be invaluable if BiP is found to be a bona fide substrate of FicD, by allowing studies on differences in BiP activity in the absence of FicD AMPylation. Folding and secretion of a model substrate such as bovine pancreatic

trypsin inhibitor (BPTI) in presence and absence of FicD can also be assayed to determine if the processing of ER proteins is affected by FicD, either through AMPylation of BiP or other substrates. Mutants of BiP deficient for AMPylation can be used in the parental HEK293T strain to determine which effects observed for FicD are BiP-dependent.

Concluding remarks

The field of AMPylation is still in its infancy, with many open questions remaining. Numerous bacterial Fic effectors with unclear substrates and functions still exist that may have interesting effects on host cell signaling. Additionally, many bacterial species have multiple Fic domain proteins present in their genomes that likely have no pathogenic function, but serve some unknown purpose in bacterial cell signaling. Also unknown are the functions of the human Fic protein, which may have multiple substrates in the endoplasmic reticulum. This study and others like it will continue to expand the knowledge of this burgeoning field and will reveal the full importance of AMPylation and other Fic-mediated modifications in biology.

BIBLIOGRAPHY

1. Woolery, A.R., et al., *AMPylation: Something Old is New Again.* Front Microbiol, 2010. **1**: p. 113.
2. Stadtman, E.R., et al., *Multiple molecular forms of glutamine synthetase produced by enzyme catalyzed adenylation and deadenylylation reactions.* Advances in enzyme regulation, 1970. **8**: p. 99-118.
3. Yarbrough, M.L., et al., *AMPylation of Rho GTPases by Vibrio VopS disrupts effector binding and downstream signaling.* Science, 2009. **323**(5911): p. 269-72.
4. Worby, C.A., et al., *The fic domain: regulation of cell signaling by adenylylation.* Mol Cell, 2009. **34**(1): p. 93-103.
5. Muller, M.P., et al., *The Legionella effector protein DrrA AMPylates the membrane traffic regulator Rab1b.* Science, 2010. **329**(5994): p. 946-9.
6. Yarbrough, M.L. and K. Orth, *AMPylation is a new post-translational modiFICation.* Nat Chem Biol, 2009. **5**(6): p. 378-9.
7. Mangum, J.H., G. Magni, and E.R. Stadtman, *Regulation of glutamine synthetase adenylylation and deadenylylation by the enzymatic uridylylation and deuridylylation of the PII regulatory protein.* Arch Biochem Biophys, 1973. **158**(2): p. 514-25.
8. Brown, M.S., A. Segal, and E.R. Stadtman, *Modulation of glutamine synthetase adenylylation and deadenylylation is mediated by metabolic transformation of the P II -regulatory protein.* Proc Natl Acad Sci U S A, 1971. **68**(12): p. 2949-53.

9. Jiang, P., A.E. Mayo, and A.J. Ninfa, *Escherichia coli glutamine synthetase adenylyltransferase (ATase, EC 2.7.7.49): kinetic characterization of regulation by PII, PII-UMP, glutamine, and alpha-ketoglutarate.* Biochemistry, 2007. **46**(13): p. 4133-46.

10. Jaggi, R., et al., *The two opposing activities of adenylyl transferase reside in distinct homologous domains, with intramolecular signal transduction.* EMBO J, 1997. **16**(18): p. 5562-71.

11. Kinch, L.N., et al., *Fido, a novel AMPylation domain common to fic, doc, and AvrB.* PLoS One, 2009. **4**(6): p. e5818.

12. Kawamukai, M., et al., *Cloning of the fic-1 gene involved in cell filamentation induced by cyclic AMP and construction of a delta fic Escherichia coli strain.* J Bacteriol, 1988. **170**(9): p. 3864-9.

13. Daniels, N.A., et al., *Vibrio parahaemolyticus infections in the United States, 1973-1998.* J Infect Dis, 2000. **181**(5): p. 1661-6.

14. Daniels, N.A., et al., *Emergence of a new Vibrio parahaemolyticus serotype in raw oysters: A prevention quandary.* JAMA, 2000. **284**(12): p. 1541-5.

15. Makino, K., et al., *Genome sequence of Vibrio parahaemolyticus: a pathogenic mechanism distinct from that of V cholerae.* Lancet, 2003. **361**(9359): p. 743-9.

16. Broberg, C.A., T.J. Calder, and K. Orth, *Vibrio parahaemolyticus cell biology and pathogenicity determinants.* Microbes Infect, 2011. **13**(12-13): p. 992-1001.

17. Zhang, L., et al., *Type III effector VopC mediates invasion for Vibrio species.* Cell Rep, 2012. **1**(5): p. 453-60.

18. Grammel, M., et al., *A chemical reporter for protein AMPylation.* J Am Chem Soc, 2011. **133**(43): p. 17103-5.

19. Neunuebel, M.R., et al., *De-AMPylation of the small GTPase Rab1 by the pathogen Legionella pneumophila.* Science, 2011. **333**(6041): p. 453-6.

20. Li, Y., et al., *Characterization of AMPylation on threonine, serine, and tyrosine using mass spectrometry.* J Am Soc Mass Spectrom, 2011. **22**(4): p. 752-61.

21. Hao, Y.H., et al., *Characterization of a rabbit polyclonal antibody against threonine-AMPylation.* J Biotechnol, 2011. **151**(3): p. 251-4.

22. Luong, P., et al., *Kinetic and structural insights into the mechanism of AMPylation by VopS Fic domain.* J Biol Chem, 2010. **285**(26): p. 20155-63.

23. Pieles, K., et al., *An experimental strategy for the identification of AMPylation targets from complex protein samples.* Proteomics, 2014. **14**(9): p. 1048-52.

24. Hardiman, C.A. and C.R. Roy, *AMPylation is critical for Rab1 localization to vacuoles containing Legionella pneumophila.* MBio, 2014. **5**(1): p. e01035-13.

25. Lewallen, D.M., et al., *Inhibiting AMPylation: a novel screen to identify the first small molecule inhibitors of protein AMPylation.* ACS Chem Biol, 2014. **9**(2): p. 433-42.

26. Chen, Y., et al., *Structural basis for Rab1 de-AMPylation by the Legionella pneumophila effector SidD.* PLoS Pathog, 2013. **9**(5): p. e1003382.

27. Xiao, J., et al., *Structural basis of Fic-mediated adenylylation.* Nat Struct Mol Biol, 2010. **17**(8): p. 1004-10.

28. Engel, P., et al., *Adenylylation control by intra- or intermolecular active-site obstruction in Fic proteins.* Nature, 2012. **482**(7383): p. 107-10.

29. Itzen, A., W. Blankenfeldt, and R.S. Goody, *Adenylylation: renaissance of a forgotten post-translational modification.* Trends Biochem Sci, 2011. **36**(4): p. 221-8.

30. Goody, R.S., et al., *The versatile Legionella effector protein DrrA.* Commun Integr Biol, 2011. **4**(1): p. 72-4.

31. Tan, Y. and Z.Q. Luo, *Legionella pneumophila SidD is a deAMPylase that modifies Rab1.* Nature, 2011. **475**(7357): p. 506-9.

32. Cruz, J.W., et al., *Doc toxin is a kinase that inactivates elongation factor Tu.* J Biol Chem, 2014. **289**(11): p. 7788-98.

33. Mukherjee, S., et al., *Modulation of Rab GTPase function by a protein phosphocholine transferase.* Nature, 2011. **477**(7362): p. 103-6.

34. Campanacci, V., et al., *Structure of the Legionella effector AnkX reveals the mechanism of phosphocholine transfer by the FIC domain.* EMBO J, 2013. **32**(10): p. 1469-77.

35. Tan, Y., R.J. Arnold, and Z.Q. Luo, *Legionella pneumophila regulates the small GTPase Rab1 activity by reversible phosphorylcholination.* Proc Natl Acad Sci U S A, 2011. **108**(52): p. 21212-7.

36. Goody, P.R., et al., *Reversible phosphocholination of Rab proteins by Legionella pneumophila effector proteins.* EMBO J, 2012. **31**(7): p. 1774-84.

37. Feng, F., et al., *A Xanthomonas uridine 5'-monophosphate transferase inhibits plant immune kinases.* Nature, 2012. **485**(7396): p. 114-8.

38. Xu, R.Q., et al., *AvrAC(Xcc8004), a type III effector with a leucine-rich repeat domain from Xanthomonas campestris pathovar campestris confers avirulence in vascular tissues of Arabidopsis thaliana ecotype Col-0.* J Bacteriol, 2008. **190**(1): p. 343-55.

39. Castro-Roa, D., et al., *The Fic protein Doc uses an inverted substrate to phosphorylate and inactivate EF-Tu.* Nat Chem Biol, 2013. **9**(12): p. 811-7.

40. Liu, M., et al., *Bacterial addiction module toxin Doc inhibits translation elongation through its association with the 30S ribosomal subunit.* Proc Natl Acad Sci U S A, 2008. **105**(15): p. 5885-90.

41. Bunney, T.D., et al., *Crystal Structure of the Human, FIC-Domain Containing Protein HYPE and Implications for Its Functions.* Structure, 2014.

42. Bustelo, X.R., V. Sauzeau, and I.M. Berenjeno, *GTP-binding proteins of the Rho/Rac family: regulation, effectors and functions in vivo.* Bioessays, 2007. **29**(4): p. 356-70.

43. Wang, J., et al., *Reciprocal signaling between heterotrimeric G proteins and the p21-stimulated protein kinase.* J Biol Chem, 1999. **274**(44): p. 31641-7.

44. Frost, J.A., et al., *Actions of Rho family small G proteins and p21-activated protein kinases on mitogen-activated protein kinase family members.* Mol Cell Biol, 1996. **16**(7): p. 3707-13.

45. Hordijk, P.L., *Regulation of NADPH oxidases: the role of Rac proteins.* Circ Res, 2006. **98**(4): p. 453-62.

46. Cherfils, J. and M. Zeghouf, *Regulation of small GTPases by GEFs, GAPs, and GDIs.* Physiol Rev, 2013. **93**(1): p. 269-309.

47. Aktories, K., *Bacterial protein toxins that modify host regulatory GTPases.* Nat Rev Microbiol, 2011. **9**(7): p. 487-98.

48. de Zoete, M.R. and R.A. Flavell, *Detecting "different": Pyrin senses modified GTPases.* Cell Res, 2014. **24**(11): p. 1286-7.

49. Xu, H., et al., *Innate immune sensing of bacterial modifications of Rho GTPases by the Pyrin inflammasome.* Nature, 2014. **513**(7517): p. 237-41.

50. Keestra, A.M. and A.J. Baumler, *Detection of enteric pathogens by the nodosome.* Trends Immunol, 2014. **35**(3): p. 123-30.

51. Broz, P. and D.M. Monack, *Newly described pattern recognition receptors team up against intracellular pathogens.* Nat Rev Immunol, 2013. **13**(8): p. 551-65.

52. Takeuchi, O. and S. Akira, *Pattern recognition receptors and inflammation.* Cell, 2010. **140**(6): p. 805-20.

53. Keestra, A.M., et al., *Manipulation of small Rho GTPases is a pathogen-induced process detected by NOD1.* Nature, 2013. **496**(7444): p. 233-7.

54. Frost, J.A., et al., *Cross-cascade activation of ERKs and ternary complex factors by Rho family proteins.* EMBO J, 1997. **16**(21): p. 6426-38.

55. Reddick, L.E. and N.M. Alto, *Bacteria fighting back: how pathogens target and subvert the host innate immune system.* Mol Cell, 2014. **54**(2): p. 321-8.

56. Krachler, A.M., A.R. Woolery, and K. Orth, *Manipulation of kinase signaling by bacterial pathogens.* J Cell Biol, 2011. **195**(7): p. 1083-92.

57. Arthur, J.S. and S.C. Ley, *Mitogen-activated protein kinases in innate immunity.* Nat Rev Immunol, 2013. **13**(9): p. 679-92.

58. Mukherjee, S., et al., *Yersinia YopJ acetylates and inhibits kinase activation by blocking phosphorylation.* Science, 2006. **312**(5777): p. 1211-4.

59. Pearson, J.S., et al., *A type III effector protease NleC from enteropathogenic Escherichia coli targets NF-kappaB for degradation.* Mol Microbiol, 2011. **80**(1): p. 219-30.

60. Yen, H., et al., *NleC, a type III secretion protease, compromises NF-kappaB activation by targeting p65/RelA.* PLoS Pathog, 2010. **6**(12): p. e1001231.

61. Muhlen, S., M.H. Ruchaud-Sparagano, and B. Kenny, *Proteasome-independent degradation of canonical NFkappaB complex components by the NleC protein of pathogenic Escherichia coli.* J Biol Chem, 2011. **286**(7): p. 5100-7.

62. Baruch, K., et al., *Metalloprotease type III effectors that specifically cleave JNK and NF-kappaB.* EMBO J, 2011. **30**(1): p. 221-31.

63. Rahman, M., et al., *Visual neurotransmission in Drosophila requires expression of Fic in glial capitate projections.* Nat Neurosci, 2012. **15**(6): p. 871-5.

64. Hetz, C., *The unfolded protein response: controlling cell fate decisions under ER stress and beyond.* Nat Rev Mol Cell Biol, 2012. **13**(2): p. 89-102.

65. Otero, J.H., B. Lizak, and L.M. Hendershot, *Life and death of a BiP substrate.* Semin Cell Dev Biol, 2010. **21**(5): p. 472-8.

66. Bravo, R., et al., *Endoplasmic reticulum and the unfolded protein response: dynamics and metabolic integration.* Int Rev Cell Mol Biol, 2013. **301**: p. 215-90.

67. Owen, C.R., et al., *PERK is responsible for the increased phosphorylation of eIF2alpha and the severe inhibition of protein synthesis after transient global brain ischemia.* J Neurochem, 2005. **94**(5): p. 1235-42.

68. Yoshida, H., et al., *XBP1 mRNA is induced by ATF6 and spliced by IRE1 in response to ER stress to produce a highly active transcription factor.* Cell, 2001. **107**(7): p. 881-91.

69. Yamamoto, K., et al., *Differential contributions of ATF6 and XBP1 to the activation of endoplasmic reticulum stress-responsive cis-acting elements ERSE, UPRE and ERSE-II.* J Biochem, 2004. **136**(3): p. 343-50.

70. Ye, J., et al., *ER stress induces cleavage of membrane-bound ATF6 by the same proteases that process SREBPs.* Mol Cell, 2000. **6**(6): p. 1355-64.

71. Olzmann, J.A., R.R. Kopito, and J.C. Christianson, *The mammalian endoplasmic reticulum-associated degradation system.* Cold Spring Harb Perspect Biol, 2013. **5**(9).

72. Kopito, R.R., *ER quality control: the cytoplasmic connection.* Cell, 1997. **88**(4): p. 427-30.

73. Stolz, A. and D.H. Wolf, *Endoplasmic reticulum associated protein degradation: a chaperone assisted journey to hell.* Biochim Biophys Acta, 2010. **1803**(6): p. 694-705.

74. Salomon, D., et al., *Effectors of animal and plant pathogens use a common domain to bind host phosphoinositides.* Nat Commun, 2013. **4**: p. 2973.

75. Oberoi, T.K., et al., *IAPs regulate the plasticity of cell migration by directly targeting Rac1 for degradation.* EMBO J, 2012. **31**(1): p. 14-28.

76. Estornes, Y. and M.J. Bertrand, *IAPs, regulators of innate immunity and inflammation.* Semin Cell Dev Biol, 2014.

77. Rada, B. and T.L. Leto, *Oxidative innate immune defenses by Nox/Duox family NADPH oxidases.* Contrib Microbiol, 2008. **15**: p. 164-87.

78. Price, M.O., et al., *Rac activation induces NADPH oxidase activity in transgenic COSphox cells, and the level of superoxide production is exchange factor-dependent.* J Biol Chem, 2002. **277**(21): p. 19220-8.

79. Woolery, A.R., et al., *AMPylation of Rho GTPases subverts multiple host signaling processes.* J Biol Chem, 2014. **289**(47): p. 32977-88.

80. Ramachandran, N., et al., *Next-generation high-density self-assembling functional protein arrays.* Nat Methods, 2008. **5**(6): p. 535-8.

81. Ramachandran, N., et al., *Self-assembling protein microarrays.* Science, 2004. **305**(5680): p. 86-90.

82. Saul, J., et al., *Development of a full-length human protein production pipeline.* Protein Sci, 2014.

83. Wright, C., et al., *Detection of multiple autoantibodies in patients with ankylosing spondylitis using nucleic acid programmable protein arrays.* Mol Cell Proteomics, 2010.

84. Yu, X., et al., *Copper-catalyzed azide-alkyne cycloaddition (click chemistry)-based detection of global pathogen-host AMPylation on self-assembled human protein microarrays.* Mol Cell Proteomics, 2014. **13**(11): p. 3164-76.

85. Griner, E.M. and D. Theodorescu, *The faces and friends of RhoGDI2.* Cancer Metastasis Rev, 2012. **31**(3-4): p. 519-28.

86. Wu, Y., et al., *Src phosphorylation of RhoGDI2 regulates its metastasis suppressor function.* Proc Natl Acad Sci U S A, 2009. **106**(14): p. 5807-12.

87. Choi, M.R., M. Groot, and H.C. Drexler, *Functional implications of caspase-mediated RhoGDI2 processing during apoptosis of HL60 and K562 leukemia cells.* Apoptosis, 2007. **12**(11): p. 2025-35.

88. Miersch, S. and J. LaBaer, *Nucleic Acid programmable protein arrays: versatile tools for array-based functional protein studies.* Curr Protoc Protein Sci, 2011. **Chapter 27**: p. Unit27 2.

89. Wang, Y., et al., *The complement C1qA enhances retinoic acid-inducible gene-I-mediated immune signalling.* Immunology, 2012. **136**(1): p. 78-85.

90. Zhang, B. and Y. Zheng, *Negative regulation of Rho family GTPases Cdc42 and Rac2 by homodimer formation.* J Biol Chem, 1998. **273**(40): p. 25728-33.

91. Ham, H., et al., *Unfolded Protein Response-regulated Drosophila Fic (dFic) Protein Reversibly AMPylates BiP Chaperone during Endoplasmic Reticulum Homeostasis.* J Biol Chem, 2014. **289**(52): p. 36059-69.

92. Han, J., et al., *ER-stress-induced transcriptional regulation increases protein synthesis leading to cell death.* Nat Cell Biol, 2013. **15**(5): p. 481-90.

93. Hollien, J., et al., *Regulated Ire1-dependent decay of messenger RNAs in mammalian cells.* J Cell Biol, 2009. **186**(3): p. 323-31.

94. Xu, H., et al., *Innate immune sensing of bacterial modifications of Rho GTPases by the Pyrin inflammasome.* Nature, 2014.

95. Chambers, J.E., et al., *ADP ribosylation adapts an ER chaperone response to short-term fluctuations in unfolded protein load.* J Cell Biol, 2012. **198**(3): p. 371-85.